

**Functional Characterization of
IGHMBP2, the Disease Gene Product of
Spinal Muscular Atrophy with
Respiratory Distress Type 1
(SMARD1)**

Dissertation zur Erlangung des
naturwissenschaftlichen Doktorgrades
der Julius-Maximilians-Universität Würzburg

vorgelegt von
Lusy Lusiana Handoko
aus Tuban, Indonesien

Würzburg 2007

Eingereicht am: 18.09.2007

bei der Fakultät für Chemie und Pharmazie

1. Gutachter: Prof. Dr. U. Fischer

2. Gutachter: Prof. Dr. F. Grummt

der Dissertation

1. Prüfer: Prof. Dr. U. Fischer

2. Prüfer: Prof. Dr. F. Grummt

3. Prüfer: Prof. Dr. M. Gessler

des Öffentlichen Promotionskolloquiums

Tag des Öffentlichen Promotionskolloquiums: 6.11.2007

Doktorurkunde ausgehändigt am:

Diese Doktorarbeit wurde in der Arbeitsgruppe von Prof. Dr. U. Fischer am Institute für Biochemie der Julius-Maximilians-Universität Würzburg angefertigt.

Teile dieser Arbeit gehen in folgende Veröffentlichung ein:

Handoko L*, Günther U*, Chari A, Sickmann A, Lagerbauer L, Fischer U, Von Au-Grohmann K. 2007. IGHMBP2 is a ribosome-associated RNA helicase that is inactive in spinal muscular atrophy with respiratory distress type 1. Submitted (*equally contributed)

CONTENTS	i-iii
1. SUMMARY	1
2. ZUSAMMENFASSUNG.....	3
3. INTRODUCTION.....	5
3.1 Spinal Muscular Atrophy with Respiratory Distress Type 1	5
3.1.1 Clinical Features of SMARD1	6
3.1.2 Genetic Analysis of SMARD1.....	8
3.1.3 Mouse Model of SMARD1.....	9
3.2 Immunoglobulin μ -Binding Protein 2.....	10
3.2.1 Domain Organization of the IGHMBP2	11
3.2.2 Proposed Cellular Functions of IGHMBP2	16
3.3 Aim of this Study	18
4. RESULTS	19
4.1 Characterization of Enzymatic Activities of Recombinant IGHMBP2 as a Member of the Helicase Superfamily 1	19
4.1.1 Expression and Purification of Recombinant IGHMBP2	19
4.1.2 ATPase Activity of Recombinant IGHMBP2.....	22
4.1.3 RNA Unwinding Activity of Recombinant IGHMBP2.....	25
4.2 Identification of Cellular Binding Partners of IGHMBP2.....	27
4.2.1 Biochemical Analysis of Endogenous IGHMBP2 in Cellular Extracts	27
4.2.2 Isolation and Characterization of the Cellular Components of IGHMBP2 Complexes	30
4.3 <i>In Vivo</i> Association of Endogenous IGHMBP2 with Ribosomes.....	36
4.4 Studies on the Cellular Function of IGHMBP2	39
4.4.1 Downregulation of Cellular IGHMBP2 by RNA Interference Had No Detectable Effect on Ribosomal Profiles	40
4.4.2 Reduced Expression of IGHMBP2 by RNA Interference Did Not Effect Global Protein Synthesis	41
4.4.3 Tethering IGHMBP2 to Reporter mRNA Increase the Abundance of the Reporter mRNA	43
4.5 Biochemical Analysis of Pathogenic IGHMBP2 Variants	46
4.5.1 ATPase and RNA Unwinding Activities of Pathogenic IGHMBP2 Variants	46
4.5.2 Association of Pathogenic IGHMBP2 Variants with Ribosomal Subunits.....	49
5. DISCUSSION	51
5.1 Enzymatic Properties of IGHMBP2.....	51
5.1.1 IGHMBP2 Is an ATP-Dependent 5'-3' RNA/DNA Helicase <i>in Vitro</i>	51
5.1.2 IGHMBP2 Might Function as RNA Helicase Rather than DNA Helicase in Living Cells.....	53

5.2	Characterization of the Cellular Function of IGHMBP2	54
5.2.1	IGHMBP2 Is a Ribosome-Associated Protein	54
5.2.2	IGHMBP2 Is Linked to Gene Regulation at the Level of Translation.....	55
5.3	Pathogenic IGHMBP2 Variants Lose their Enzymatic Activities but Still Associate with Ribosomes	58
5.4	The Pathomechanism of SMARD1: a Hypothesis	61
6.	MATERIALS	63
6.1	Chemicals	63
6.2	Antibodies	63
6.3	Cell Lines	63
6.4	Plasmid Vectors	63
6.5	Consumable Materials.....	65
6.6	Dye Solutions	65
6.7	Enzymes and Inhibitors	65
6.7.1	Enzymes	65
6.7.2	RNase and Protease Inhibitors	66
6.8	Oligonucleotides	66
6.9	Standard Buffers and Cell Culture Media	66
6.9.1	Standard Buffers.....	66
6.9.2	Cell Culture Media and Reagents	66
6.10	Standard Markers	66
7.	METHODS	67
7.1	Nucleic Acid Analysis.....	67
7.1.1	Purification and Isolation	67
7.1.2	Quantification of Nucleic Acids	67
7.1.3	Gel Electrophoresis of Nucleic Acids	68
7.2	DNA Analysis	70
7.2.1	Plasmid Isolation from <i>E. coli</i> Cells	70
7.2.2	Plasmid Linearization	70
7.2.3	Polymerase Chain Reaction	70
7.2.4	DNA Cloning in Plasmid Vectors.....	71
7.2.5	Transformation of <i>E. coli</i> Cells.....	72
7.3	RNA Analysis	72
7.3.1	RNA Isolation from Cell Extract	72
7.3.2	RNA Isolation from Cell Culture using Trizol	72
7.3.3	RNA purification using Size Exclusion Chromatography	72
7.3.4	<i>In vitro</i> Synthesis of RNA Molecules	72
7.3.5	Preparation of Double-Stranded RNA	73
7.3.6	RNA Unwinding Assay	73

7.3.7	Northern Blot Analysis	74
7.4	Protein Analysis	74
7.4.1	Quantification of Protein Concentration according to Bradford.....	74
7.4.2	Denaturing Discontinuous SDS PAGE (Sodium Dodecyl Sulfate Polyacrylamide Gel Electrophoresis).....	74
7.4.3	Protein Precipitation.....	76
7.4.4	Cell Extract Preparation.....	76
7.4.5	Covalent Coupling of Protein on Affinity Matrix	77
7.4.6	Protein Expression and Purification.....	78
7.4.7	Protein Separation using Centrifugation	79
7.4.8	Dialysis of Protein.....	80
7.4.9	Purification Using GST-Fusion Protein as Affinity Matrix (GST Pull-Down)	80
7.4.10	ATPase Assay	80
7.5	Immunological and Immunbiochemical Analysis	81
7.5.1	Production of Polyclonal Antibody.....	81
7.5.2	Antibody Purification using Affinity Chromatography	81
7.5.3	Immunoaffinity Purification	81
7.5.4	Western Blot Analysis	82
7.6	Methods in Cell Culture	82
7.6.1	Cell Cultivation.....	82
7.6.2	Determination of Cell Density	82
7.6.3	Cell Transfection.....	83
7.6.4	Metabolic Protein Labeling using ³⁵ S	83
7.6.5	β-globin mRNA Reporter-Based Tethering Assay	84
7.6.6	Immunofluorescence Microscopy.....	84
8.	ABBREVIATIONS.....	86
9.	REFERENCES.....	87
	Acknowledgements	iv
	Lebenslauf	v
	Erklärung	vi

1. SUMMARY

Spinal muscular atrophy with respiratory distress type 1 (SMARD1) is an autosomal recessive neuronal disorder in infants. The disease is marked by early onset of respiratory distress and predominantly distal muscle weakness, as consequences of diaphragmatic paralysis and progressive degeneration of α motor neurons in the spinal cord, respectively. Genetically, SMARD1 is caused by mutations in the single gene encoding Immunoglobulin μ -Binding Protein 2 (IGHMBP2). Despite the tissue specific degeneration observed in SMARD1 patients, the disease gene product IGHMBP2 is ubiquitously expressed in human and mouse tissues. Therefore, SMARD1 appears to be a motor neuron disease caused by the malfunction of a “housekeeping” protein, rather than a neuron specific factor. IGHMBP2 harbors an N-terminal DEXDc-type helicase/ATPase domain and has been classified as a member of the Superfamily 1 (SF1) of helicases. This protein has been assigned to various cellular activities such as DNA replication, pre-mRNA splicing and transcription. However its precise function in either process has remained elusive. The study presented here aimed at the enzymatic characterization of IGHMBP2, the identification of a specific cellular process to which IGHMBP2 is connected and the role of this factor in the pathophysiology of SMARD1.

As a first step toward this end, a two-step purification strategy was established, which enabled the large-scale purification of properly folded and enzymatically active IGHMBP2. *In vitro* enzymatic studies using this recombinant protein defined IGHMBP2 as an ATP-dependent helicase that catalyzes unwinding of duplexes composed of either DNA or RNA in a 5'→3' direction. In contrast to previous reports, indirect immunofluorescence studies revealed a predominantly cytoplasmic localization of IGHMBP2. Size-fractionation studies and affinity-purification experiments further showed that IGHMBP2 is part of an RNase-sensitive macromolecular complex, which was identified as the ribosome. Interestingly, IGHMBP2 was abundantly detected in both subunits as well as to 80S ribosomes but only in small amounts in actively translating polysomes. These data strongly point to a role of IGHMBP2 in ribosomes-associated gene

regulation control, such as in mRNA stabilization or mRNA translation. However, its precise function in those pathways remains to be identified.

The biochemical and enzymatic characterization of IGHMBP2 allowed for the first time insights into the pathomechanism of SMARD1. SMARD1-causing pathogenic IGHMBP2 variants were investigated for their enzymatic activities and interaction with ribosomal subunits. Interestingly, among all missense mutations that have been tested thus far, none obstructs association with ribosomal subunits. However, these mutants exhibit specific defects in either the ATPase or RNA helicase activity or both. The data suggest that defects in the enzymatic activity of IGHMBP2 directly correlate with the pathogenesis of SMARD1. Furthermore, these data also raise the possibility that the disease SMARD1 is caused by alterations in the cellular translation machinery.

2. ZUSAMMENFASSUNG

Spinale Muskelatrophie mit Atemnot Type 1 (SMARD1) ist eine autosomal rezessive, neurodegenerative Erkrankung, die sich häufig schon im Säuglings- und Kleinkindalter manifestiert. Pathologisches Merkmal von SMARD1 ist eine frühe und akut einsetzende Atemnot und eine progrediente, zunächst distal betonte Muskelschwäche, die durch eine Lähmung des Zwerchfells und der Skelettmuskulatur aufgrund des Absterbens der motorischen Vordernhornzellen des Rückenmarks eintritt. SMARD1 ist eine monogene Krankheit, die durch Mutationen im Gen für das Immunoglobulin μ -bindende Protein 2“ (IGHMBP2) hervorgerufen wird. Obwohl Mutationen in IGHMBP2 ausschließlich die Degeneration von Motoneuronen auslösen, ist das Gen bei Menschen und Mäusen ubiquitär exprimiert. Deshalb scheint SMARD1 durch den Defekt eines „Haushaltsproteins“ statt eines Neuron-spezifischen Faktors verursacht zu werden. IGHMBP2 verfügt über eine N-terminale DEXDc-Helicase/ATPase-Domäne und gehört zur Superfamily 1 Helicase. Bislang war lediglich bekannt, dass das Protein in verschiedenen zellulären Aktivitäten wie DNA Replikation, Transkription und prä-mRNA Splicing zugewiesen wurde. Die präzise Funktion von IGHMBP2 in den obengenannten Prozessen, und damit auch die molekulare Ursache von SMARD1 sind jedoch noch völlig unklar. Das Ziel der vorliegenden Arbeit war es daher, das IGHMBP2 Protein sowohl enzymatisch zu charakterisieren als auch den Prozess zu identifizieren, in dem dieses Protein *in vivo* agiert. Mit diesem Wissen sollten dann pathogene Mutanten von IGHMBP2 auf Defekte hin untersucht werden.

Ein Schlüssel für diese Arbeit war die Gewinnung von rekombinantem, biologisch aktivem IGHMBP2 durch eine zweistufige Aufreinigungsstrategie. Dieses hochreine Enzym zeigte eine ATP-abhängige Helikaseaktivität, die sowohl doppelsträngige DNA als auch RNA mit einer 5'→3' Direktionalität entwindet. Interessanterweise zeigte sich, dass dieses Enzym -im Gegensatz zu früheren Befunden- nahezu ausschließlich im Zytoplasma von Zellen lokalisiert ist. Darüber hinaus wiesen die Affinitätsaufreinigungsexperimente und Grossenfraktionierungsuntersuchungen daraufhin, dass IGHMBP2 ein Bestandteil des

RNase-empfindlichen Komplexes ist, der als Ribosomen identifiziert wurde. IGHMBP2 interagiert primär mit 80S Monosomen, wobei das Protein mit beiden Untereinheiten in Kontakt steht. Hingegen ist IGHMBP2 an Polysomen nur in geringen Mengen zu finden. Diese Befunde deuten stark auf eine Rolle von IGHMBP2 bei der mRNA Verarbeitung am Ribosom hin, wobei noch unklar ist, ob es sich um translationsrelevante Prozesse handelt oder die mRNA-Stabilität beeinflusst.

Die biochemische und enzymatische Charakterisierung von IGHMBP2 erlaubte erstmals Einblicke in den Pathomechanismus von SMARD1. In den folgenden Untersuchungen wurden die enzymatischen Aktivitäten der SMARD1-erregenden Ighmbp2 Mutante und ihre Assoziation mit ribosomalen Untereinheiten nachgeforscht. Interessanterweise konnten pathogene Missense-Mutanten von IGHMBP2 noch genauso gut wie das Wildtyp-Protein mit ribosomalen Untereinheiten wechselwirken. Jedoch inhibierten alle bisher getesteten Mutanten die RNA Helikaseaktivität, allerdings über unterschiedliche Mechanismen. Diese Daten weisen darauf hin, dass ein Defekt in den enzymatischen Aktivitäten des IGHMBP2 direkt mit der Pathogenese der SMARD1 korreliert. Des Weiteren lassen die im Rahmen dieser Arbeit erhaltenen Ergebnisse vermuten, dass SMARD1 durch Defekte in der zellularen Translationsmaschinerie entsteht.

3. INTRODUCTION

3.1 Spinal Muscular Atrophy with Respiratory Distress Type 1

In 1974, Mellins and colleagues described two infants exhibiting the clinical features similar to those of the most common and most-characterized motor neuron disease, spinal muscular atrophy (SMA1; MIM #253300). They suffered from neurogenic muscular atrophy with subsequent symmetrical muscle weakness of limb and trunk, resulting from loss and dysfunction of alpha motor neurons in the anterior horn of the spinal cord. Additionally, the affected infants displayed respiratory failure at the very early stage of the disease (at the age of one to three months). A more detailed investigation on the developing symptoms of this newly discovered disease also revealed defects which clearly differ from the classical SMA1. In contrast to SMA1, in which proximal limb muscles are primarily affected followed by respiratory failure due to paralysis of the intercostal muscle, this new disease is marked by the early onset of respiratory distress due to diaphragmatic paralysis and muscle weakness with predominantly distal muscle involvement (Wilmschurst *et al.*, 2001; Grohmann *et al.*, 2003). To date, more than 100 cases with similar characteristics have been reported (Grohmann *et al.*, 1999; Grohmann *et al.*, 2003; Giannini *et al.*, 2006; Guenther *et al.*, 2007, Maystadt *et al.*, 2004, Wilmschurst *et al.*, 2001; Mohan *et al.*, 2001). This “unusual variant” of SMA1 is now known as spinal muscular atrophy with respiratory distress type 1 (SMARD1; MIM #604302). The prevalence of this disease is still unclear. Patients with diaphragmatic paralysis constitute largely 1% of patients of those with the early onset of SMA (Rudnik-Schöneborn *et al.*, 1996). Genetically, SMARD1 is also divergent from SMA1 that is caused by deletion or mutation in the *SMN1* (survival motor neuron 1) gene on chromosome 5q13. SMARD1 results from recessive mutations in the single, immunoglobulin μ -binding protein 2 (*IGHMBP2*) gene at chromosome 11q13. The following parts describe detailed clinical features of SMARD1 patients and the phenotype of a mouse model of SMARD1, the so-called neuromuscular degeneration or *nmd* mouse.

3.1.1 Clinical Features of SMARD1

In almost all SMARD1-affected infants, prenatal features like intrauterine growth retardation (birth weigh below 10th percentile), decreased fetal movements or prematurity have been observed as the first symptoms (Grohmann *et al.*, 2003; Rudnik-Schönenborn *et al.*, 2004). Within the first 6 months, SMARD1 infants suffer from an acute irreversible respiratory distress due to diaphragmatic paralysis and develop progressive muscle weakness with the involvement of predominantly distal lower limb muscles (Wilmshurst *et al.*, 2001; Grohmann *et al.*, 2003; Gianinni *et al.*, 2006; Mohan *et al.*, 2001). These features clearly distinguish SMARD1 from SMA1, in which the symptoms manifest in reverse order. Due to weakness of proximal limb muscles, SMA1 patients become floppy and assume a frog leg position prior to respiratory failure by the age of two years. Some exceptions to the early onset of respiratory distress have recently been reported. Two SMARD1 patients exhibit respiratory distress and severe distal muscle weakness at the age of 4.3 and 10 years (designated as the juvenile type SMARD1), illustrating the clinical heterogeneity of this disease (Guenther *et al.*, 2004; Guenther *et al.*, 2007b).

Acute life-threatening respiratory distress is the most prominent sign of SMARD1. SMARD1 patients exhibit eventration of right or both hemi-diaphragms without any thorax deformity due to predominantly diaphragmatic paralysis (Fig. 1A). This respiratory failure can be initially recognized by inspiratory stridor and/or weak cry in SMARD1 infants. Due to the acute respiratory failure, SMARD1 patients require permanent mechanical ventilatory support to prolong their survival (4.5-11 years) (Fig. 1C). Some of them die early following acute respiratory events or withdrawal of mechanical ventilator. Weakness of distal muscles initially begins in the lower limbs, rapidly progresses to the upper limbs, causing a complete paralysis of limb and trunk muscles. Consequently, affected infants develop foot deformities before finger contractures. They also can not move their legs and arms against gravity. Marked distal muscle weakness and atrophy, fatty pads and no antigravity movement are characteristic phenotypes of fingers and hands in SMARD1 patients (Fig. 1B) (Grohmann *et al.*, 2003).

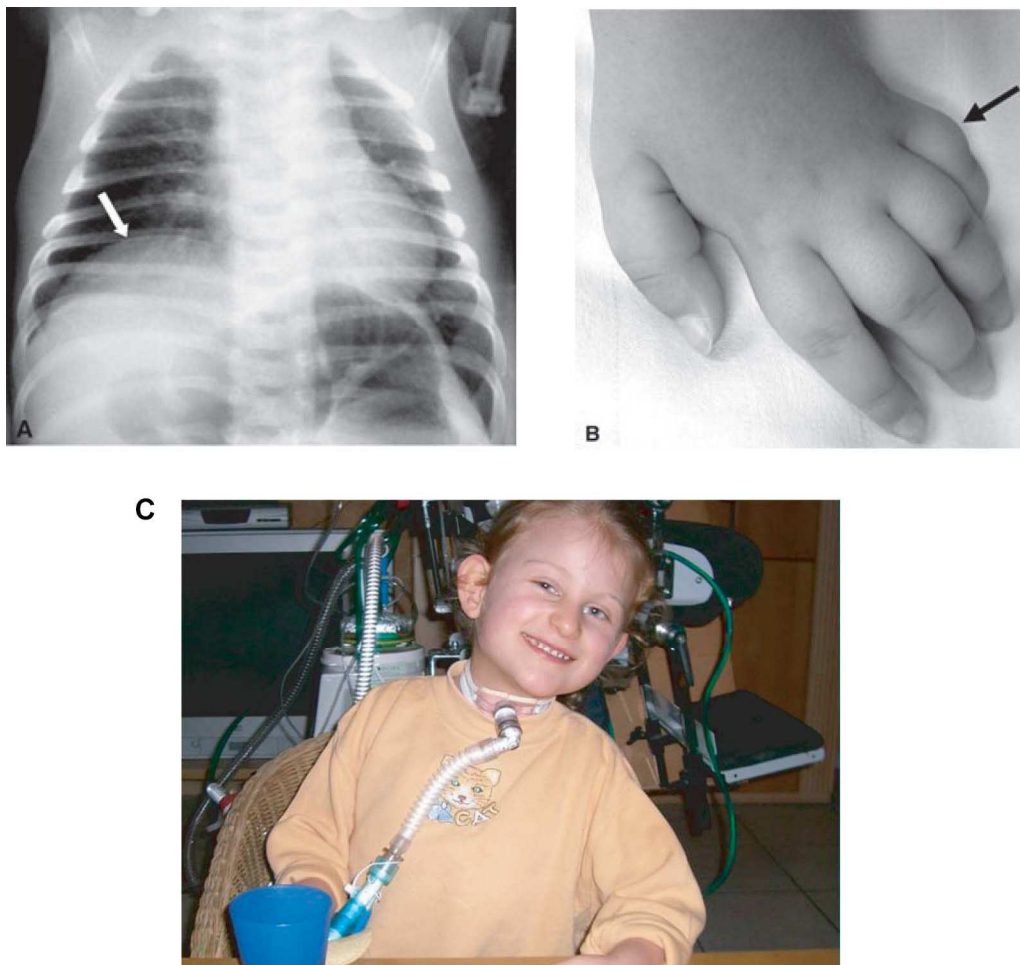


Figure 1. Clinical Features of SMARD1 Patients. **A.** Diaphragmatic paralysis in a 6-week old girl affected with SMARD I. Chest radiography shows an abnormal elevation of the right hemidiaphragm (the white arrow). **B.** No antigravity movement, marked muscle atrophy, and fatty pads (the black arrow) are characteristic for hands and fingers of SMARD I patients. **C.** A young girl affected by SMARD1 remains alert and tentative. Due to respiratory defect, SMARD1 patients require continuous ventilatory support through tracheostoma to prolong their life.

In addition to the symptoms described above, features similar to those observed in classical SMA1 patients have also been reported for SMARD1. At later stages of the disease, motor and sensory nervous systems are affected (Mohan *et al.*, 2001, Wilmhurst *et al.*, 2001 and Diers *et al.*, 2006). SMARD1 infants exhibit elevated body temperature, tachycardia, increased sweating and hypertension, suggesting also the involvement of autonomic nervous system (Mohan *et al.*, 2001 and Gianinni *et al.*, 2006). Histopathological analysis shows a severe loss of myelinated axons in sensory and motor nerves, late axonal

degeneration and high number of unmyelinated axons (Mohan *et al.*, 2001; Wilmshurst *et al.*, 2001; Grohmann *et al.*, 2003). Ultrastructural studies in peripheral nerves, skeletal muscles and neuromuscular junctions (NMJ) of SMARD1 patients have revealed the coexistence of Wallerian degeneration of nerve fibers without regeneration and marked axonal atrophy, similar to the defects observed in SMA1 (Diers *et al.*, 2005). Neurogenic atrophy and inactivity are observed in skeletal muscles and are more significantly in the older patients. In neuromuscular junctions of SMARD1 patients, all motor end-plates are defective and lack of the terminal axons indicating the impaired interaction of the skeletal muscles, motor neuron and Schwann cells. Moreover, this study also identified abnormalities in myelination such as hyper or hypomyelination which are characteristic in several types of hereditary neuropathy, but have not yet been described for SMAs so far. These ultrastructural findings indicate that SMARD1 is primarily caused by the impairment in maintenance and regeneration of skeletal muscles, axons and Schwann cells.

3.1.2 Genetic Analysis of SMARD1

Recessive mutations in *IGHMBP2* are known to be responsible for SMARD1 (Grohmann *et al.*, 2001; Biswas *et al.*, 2001). To date, 67 mutations of *IGHMBP2*, which include frame-shift deletion-, splice site donor, nonsense and missense mutations have been already identified in SMARD1 patients (Grohmann *et al.*, 2001; Maystadt *et al.*, Gianinni *et al.*, Guenther *et al.*, 2007a). The *IGHMBP2* gene is composed of 15 exons and the disease-causing mutations are spread over thirteen exons, one mutation was detected in an intron and no mutations are located in the 1st, 4th and 14th exons. Allelic heterogeneity of SMARD1 has been previously reported (Maystadt *et al.*, 2004, Guenther *et al.*, 2007b; Pitt *et al.*, 2003). SMARD1 patients carry homozygous or compound heterozygous mutations at the *IGHMBP2* locus. Moreover, in almost all SMARD1 patients with the infantile onset of respiratory distress and muscle weakness at least one *IGHMBP2* allele has a nonsense mutation. In the juvenile SMARD1 patient compound heterozygote for two different missense mutations has been identified (Guenther *et al.*, 2007b).

Most mutations target highly conserved amino acid residues found in the N-terminal part of *IGHMBP2* that is proposed to be an ATPase/Helicase domain (Guenther *et al.*, 2007a;

200b; Grohmann *et al.*, 2003). No mutations have been so far identified in the other structural domain of IGHMBP2, such as RH3 and zinc finger domains (the detailed domain composition of IGHMBP2 is described in 3.2.1). Mutations in *IGHMBP2* probably affect either its mRNA level or its protein products. In SMARD1 patients carrying splice site donor mutations in *IGHMBP2*, mRNA levels of *IGHMBP2* are significantly reduced, likely due to nonsense-mediated mRNA decay (Guenther *et al.*, 2007a). At the protein level, IGHMBP2 harboring a missense mutation within the putative helicase domain was reported to influence the stability of IGHMBP2 in SMARD1 patients (Guenther *et al.*, 2007b). These data indicate that reduced levels of functional IGHMBP2 and/or alterations in its enzymatic activities may contribute to the pathogenic events of SMARD1. Further studies would be needed to prove this hypothesis.

3.1.3 Mouse Model of SMARD1: *nmd* mouse

In 1995, Cook and colleagues from the Jackson Laboratory discovered a mutant mouse, whose phenotypes resemble those of SMARD1. The mouse, named *neuromuscular degeneration (nmd)* mouse, resulted from a spontaneous autosomal recessive mutation in the *Ighmbp2* gene on chromosome 19 (Cox *et al.*, 1998; Cook *et al.*, 1995) and has been used as a model to study SMARD1 and to investigate the role of *Ighmbp2* in motor neuron degeneration (Grohmann *et al.*, 2004; Maddatu *et al.*, 2004; Cox *et al.*, 1998).

Nmd mice resemble patients with a milder form of SMARD1 rather than the acute SMARD1. While paralysis of the diaphragm appears at early stages and becomes the most prominent symptoms in infantile SMARD1, *nmd* mice develop the respiratory failure at late stages of the disease. At an age of 3 weeks, *nmd* mice rapidly develop muscle weakness beginning in the hindlimbs that progress into generalized muscle weakness in limb and trunk muscles (Grohmann *et al.*, 2004; Maddatu *et al.*, 2004; Cox *et al.*, 1998; Cook *et al.*, 1995). Consequently, these mice can not spread their hindlimbs and pull themselves up from the ground when suspended by the tail. Before first clinical symptoms can be detected, a severe loss of motor neuron cell bodies in the lumbar spinal cord already appears, indicating that motor neuron cell death is an early event during the disease in mice. Like in SMARD1 patients, axonal degeneration and the loss of axon terminals at

motor end-plates occur following loss of motor neuron cell bodies in the lumbar spinal cord, which leads to neurogenic muscular atrophy (Grohmann *et al.*, 2004; Maddatu *et al.*, 2004; Cox *et al.*, 1998; Cook *et al.*, 1995). The progression of motor neuron degeneration in the spinal cord, axonal degeneration and clinical symptoms slows down until the mutant mice die at the age of 3-4 months. Respiratory failure becomes apparent at late stages (8 weeks of age) and seems to be caused by myopathic alterations in diaphragmatic muscle fibers, not by axonal loss (Grohmann *et al.*, 2004).

Genetic analysis of *Ighmbp2* in *nmd* mice reveals two mutations in two independent *nmd* mice (*nmd*^{1j} and *nmd*^{2j}), namely a single amino acid deletion in exon 8 of *nmd*^{1j} allele (this mouse is extinct) and a splice site donor mutation in intron 4 of *nmd*^{2j} allele (this mouse is referred to as *nmd*). Like in SMARD1 patients, *Ighmbp2* mutations in *nmd* mice may result in reduction of its mRNA level. Mutation in intron 4 creates a cryptic splice donor and reduces the amount of functional *Ighmbp2* mRNA by ~ 80% (Cox *et al.*, 1998). Since *nmd*^{1j} mice are extinct, the effect of the single amino acid deletion in exon 8 can not be assessed. It could be however possible that the mutation in exon 8, which encodes third and fourth helicase motifs, affects the helicase activity of *Ighmbp2* (Cox *et al.*, 1998), thus suggesting that like in SMARD1 patients, the helicase activity of *Ighmbp2* may be impaired in *nmd* mice.

3.2 Immunoglobulin μ -Binding Protein 2

The gene *IGHMBP2* has received several names in the literature: *S μ bp2* (Mizuta *et al.*, 1993; Fukita *et al.*, 1995), Glial factor 1 (GF-1, an incomplete version of *Ighmbp2*) (Kerr and Khalili 1991), rat insulin enhancer-binding protein 1 (RIP-1) (Shieh *et al.*, 1995) and cardiac transcription factor 1 (Catf1) (Sebastiani *et al.*, 1994). For the sake of clarity, from now on, the gene and the gene product are referred to as *IGHMBP2* and IGHMBP2, respectively throughout the text. *IGHMBP2* was originally isolated as a cDNA clone derived from a cDNA library of mRNA prepared from LPS/IL-4-stimulated spleen cells which specifically binds 5' phosphorylated single-stranded DNA containing 5'G and GGGG stretches similar to the immunoglobulin μ chain switch region (Mizuta *et al.*, 1993). The gene is conserved among vertebrates but is not present in yeast and fruit fly

Drosophila melanogaster (Mizuta *et al.*, 1993). Its mRNA and protein products have been identified in various mouse, rat and human tissues and cell lines, thus indicating the ubiquitous expression of *IGHMBP2* (Grohmann *et al.*, 2004; Uchiumi *et al.*, 2004; Mohan *et al.*, 1998; Cox *et al.*, 1998; Shieh *et al.*, 1995; Mizuta *et al.*, 1993; Fukita *et al.*, 1993; Kerr and Khalili 1991). In humans, mRNA of *IGHMBP2* is expressed in all tissues with highest levels in testis, followed by brain and spleen, and low to moderate in other tissues (Kerr and Khalili 1991). *IGHMBP2* protein is observed at various levels in a wide range of mouse tissues, with the highest level in brain, spinal cord and muscle and a lower level in lung during mouse embryonic and postnatal development (Grohmann *et al.*, 2004). To date, relatively little is known about the function of the *IGHMBP2* gene product and its link to SMARD1.

3.2.1 Domain Organization of the *IGHMBP2*

In mice and humans, the gene of immunoglobulin- μ binding protein 2 encodes a protein containing 993 amino acids and a size of approximately 110 kDa. The nucleic acid sequence of human *IGHMBP2* is 78.6% homologous to the mouse gene (Fukita *et al.*, 1993). At the protein level, human and mouse *IGHMBP2* share 76.5% identities and 84% similarities. Sequence analysis has revealed several sequence motifs and structural domains in *IGHMBP2*: (i) an N-terminal putative helicase domain, (ii) a R3H single stranded nucleic acid binding domain, (iii) two potential nuclear localization signals and (iv) a zinc-finger domain (Fig. 3).

3.2.1.1 *IGHMBP2* Is a Putative Member of Superfamily 1 Helicase

Sequence comparisons of the N-terminal helicase domain of *IGHMBP2* with other helicase strongly suggested that the N terminal domain of *IGHMBP2* is homologous to Upf1-like proteins that belong to the DEAD/H box-like DExDc helicase of Superfamily 1 (SF1) (Czaplinski *et al.*, 2000; Gorbalenya and Koonin 1993; Koonin 1992). The group of SF1 helicases is evolutionary conserved from prokaryotes to eukaryotes and includes some well known proteins such as Upf1, Sen1, yeast helicase A, yeast MTT1, and Dna2p (Koonin, 1992; Czaplinski *et al.*, 2000).

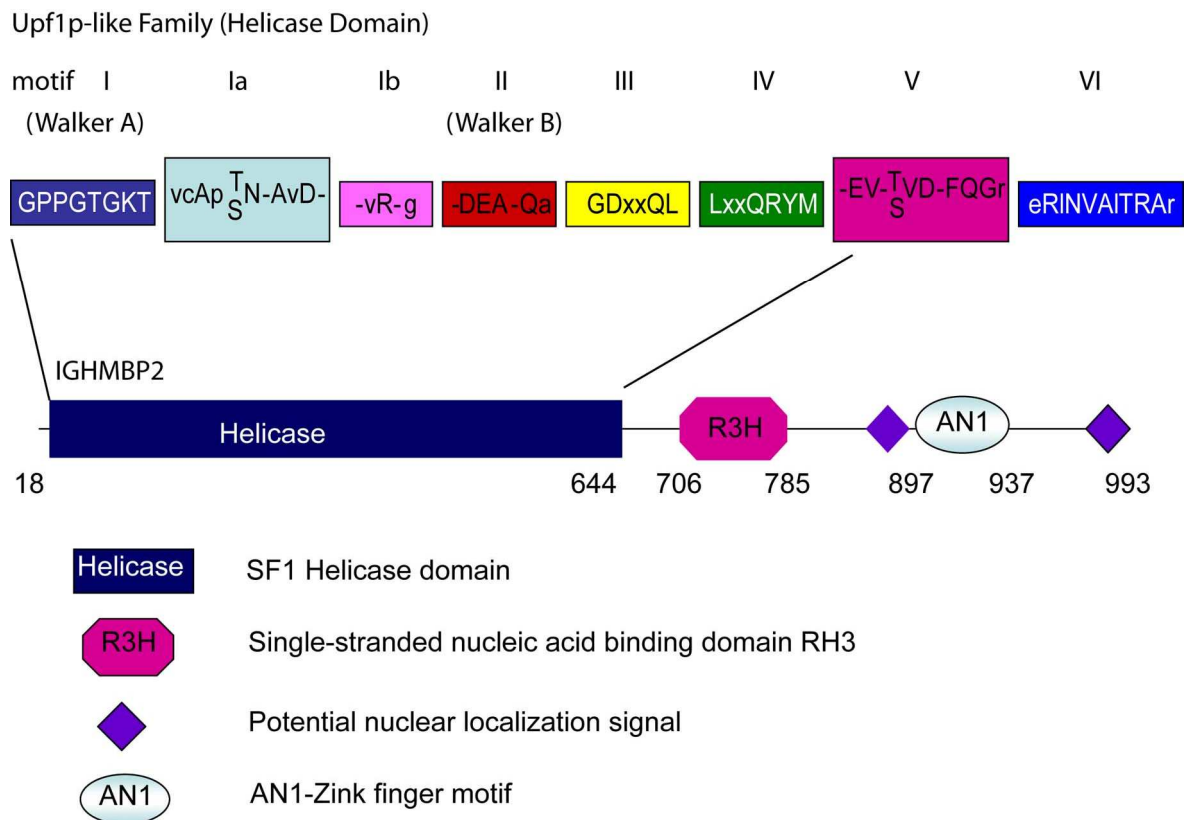


Figure 3. Domain Organization of the Human Immunoglobulin μ -Binding protein2. IGHMBP2 belongs to the Superfamily I helicase or Upf1-like proteins. Human and mouse IGHMBP2 are approximately 110 kDa in size harboring several structural domains as indicated above. The consensus sequence of each SF1- helicase motif is shown in the top panel (reviewed in de La Cruz *et al.*, 1999; Tanner and Linder, 2001). This figure is not drawn to scale.

RNA or DNA helicases are defined as enzymes that are able to unwind double-stranded polynucleotides or base-paired regions of single-stranded polynucleotide. This unwinding activity requires energy derived from the hydrolysis of a nucleoside triphosphate (NTP), preferentially ATP. The proteins of SF1 share 7-8 conserved helicase motifs including the well-known Walker A (phosphate-binding loop/P loop) and B (Mg^{2+} -binding asparagine) motifs implicated in purine NTP-binding that are also found in a wide variety of NTPases (Tanner and Linder 2001) (Fig.3 and Table 1). These 8 motifs are required for either NTP, or substrate binding and for coupling the energy of NTP hydrolysis to unwind double-stranded nucleic acids (see Table 1 for the detailed proposed functions of each motif). In addition to these 7-8 conserved motifs, a glutamine residue N-terminal of the motif I is present in ATP-specific SF1 helicases. In Dna2p (SF1), the role of the glutamine residue

seems not to be essential. In the DEAD box proteins (SF2), the similar motif (termed as Q motif) was discovered 17 residues N-terminal from the motif I or Walker A and consists of nine residues harboring a highly conserved glutamine residue (Cordin *et al.*, 2005). The Q- motif is specific for the DEAD-box proteins, found to be associated with motif I. In contrast to the glutamine residue in Dna2p, this motif is necessary for ATP hydrolysis and RNA binding in DEAD-box proteins. In addition to the helicase domain with the conserved motifs, helicases often contain variable amino- or carboxyl- terminal extensions that can be longer than 500 amino acids. These terminal extensions are considered to confer substrate specificity, protein and/or additional RNA binding motifs, and/or direct the protein to its subcellular localization (Wang and Guthrie, 1998).

The IGHMBP2 helicase domain harbors seven of eight putative helicase motifs common for SF1, namely motif I, Ia, Ib, II, III, IV, V and VI (Czaplinsky *et al.*, 2000; Mizuta *et al.*, 1993). Further analysis of the polypeptide sequence of IGHMBP2 has also revealed two additional conserved motifs (referred to as motif IIIa and motif IVa by Czaplinski *et al.*, 2000), which are also identified in some members of SF1 namely Upf1, Helicase A, MTT1 and Dna2p. Based on the occurrence of these motifs, Czaplinsky *et al.* (2000) subclassified these proteins into a subgroup of SF1, named Upf1-like subclass. Whether these proteins can be indeed categorized as one subgroup of SF1 remains unclear. Like other helicases, in addition to the helicase core domain, IGHMBP2 has a large extension at its C-terminal consisting of a R3H motif, two putative nuclear localization signals and a zinc finger domain.

Studies on *in vitro* enzymatic activities of some RNA helicases of SF1 have shown that these helicases possess RNA/DNA helicase and DNA or RNA-stimulated ATPase activities. *Saccharomyces cerevisiae* and human Upf1 proteins exhibit nucleic acid-stimulated ATP hydrolysis and 5'→3' RNA/DNA helicase activities (Bhattacharya *et al.*, 2000; Czaplinski *et al.* 1995). Yeast helicase A, another member of SF1 helicase has demonstrated strong DNA-dependent ATPase and 5'→3' DNA unwinding activities (Biswas *et al.*, 1995; 1997a). Moreover, MTT1 is known as a DNA/RNA-dependent ATPase and a 5'→3' DNA helicase which is dependent of DNA (Czaplinski *et al.*, 2000; Biswas *et al.*, 1997). Consistent with its classification as a member of SF1, *in vitro*, human IGHMBP2 has been previously characterized as an ATP- dependent DNA helicase as well

as DNA-dependent ATPase (Biswas *et al.*, 2000; Molnar *et al.*, 1997). In addition to ATPase activity, Molnar *et al.* 1997 have reported that IGHMBP2 is capable of GTP hydrolysis and this ATPase/GTPase activity is stimulated by RNA as well as DNA. The polarity of unwinding by IGHMBP2 on DNA substrates remains a matter of debate. According to Biswas *et al.* (2000), IGHMBP2 unwinds DNA substrates from the 5' end. By contrast, IGHMBP2 was assessed as a 3'→5' DNA helicase by Molnar and coworkers (Molnar *et al.*, 1997).

Motif	Proposed functions
I	The NTP-binding Walker motif A; NTPase and Helicase activities; interacts with the phosphate of the nucleotide, motif II, motif III and a highly conserved glutamine residue located 15-22 nucleotides upstream of motif I (the so-called Q motif in DEAD box).
Ia	Substrate binding; structural rearrangement upon NTP hydrolysis and binding.
Ib	Part of domain I; substrate binding, not highly conserved and is not always found.
II	The Walker motif B; crucial for NTP binding; the glutamine residue coordinates an Mg ion for the binding of NTP and is responsible for the hydrolysis of β - γ phosphoanhydride bond of a bound NTP.
III	Binds γ -phosphate and links the ATP binding and hydrolysis to the RNA binding motifs IV and V.
IV	Substrate binding through the ribose-phosphate backbone; known as motif IVa in SF1 DNA helicase.
V	An RNA binding motif; may regulate ATP hydrolysis upon substrate binding.
VI	Substrate binding and ATPase activities

Table 1. Eight Conserved Helicase Motifs in the Superfamily 1 (the proposed functional properties of each motif described here are established for Superfamily 1 and 2 helicases, including DEAD box RNA helicases; reviewed in Gorbalenya and Koonin, 1993; Cordin *et al.*, 2005; Tanner and Linder, 2001; de La Cruz *et al.* 1999).

3.2.1.2 The R3H Motif

The R3H motif of IGHMBP2 is located at amino acids 708-785 (Grishin, 1998). This motif consists of an invariant arginine (R) residue and a highly conserved histidine (H)

residue, separated by three amino acid residues (RxxxH, with x for any amino acid) (Grishin, 1998). R3H motifs are present in proteins from a wide range of organisms, including Eubacteria, green plants, fungi and metazoans. Although the precise function of this motif has not yet been defined, the fact that this motif is found in proteins associated with ATPase domains, SF1 and SF2 helicase domains, KH domains, Cys-rich repeats, and ring type zinc fingers indicates that R3H might be involved in polynucleotide binding, including DNA, RNA and single-stranded DNA. The secondary structure prediction also suggested that the R3H alone is not sufficient for high affinity binding to single-stranded DNA (Grishin, 1998).

Fukita *et al.*, 1993 have identified a region of the human IGHMBP2 consisting of 150 residues which specifically binds to 5' phosphorylated guanine-rich single-stranded DNA sequences *in vitro*. This region spanning amino acids 638-786 includes the C-terminal R3H domain of human IGHMBP2. The comparison of the 3D solution structure of the R3H domain of human IGHMBP2 and that of the C-terminal domain of the translational initiation factor IF3 suggests that the RH3 domain of human IGHMBP2 functions as a molecular surface not only for sequence specific nucleic acid recognition but also for protein-protein interaction (Liepinsh *et al.*, 2003). Whether IGHMBP2 indeed binds single-stranded nucleic acids and whether the RH3 domain is involved is, however, unclear.

3.2.1.3 The AN1-Like Zinc Finger Domain (AN1-ZnF)

Another structural motif found in the C-terminal part of IGHMBP2 is AN1-type zinc finger (ZnF). This motif was first identified in the protein from the *Xenopus laevis* AN1 maternal mRNA. The function of the AN1-type ZnF domain is still unclear; it is frequently found in association with domains linked to the ubiquitination pathway such as the A20-type ZnF and the ubiquitin-like domain. In general, ZnF domains are considered to function not only as sequence specific DNA binding motifs, but also as recognition motifs of RNA and other proteins (Gamsjaeger *et al.* 2007). It is therefore a possibility that the ZnF domain in IGHMBP2 serves as a binding site for proteins and/or nucleic acids.

3.2.1.4 The Putative Nuclear Localization Signal (NLS)

Further analysis of the peptide sequence of IGHMBP2 also reveals the presence of two potential nuclear localization signals (NLSs) (Fukita *et al.*, 1993). Generally, NLS is required for active and receptor-mediated nuclear import. However, it is still unknown whether these putative NLSs are functional in the context of IGHMBP2. The subcellular distribution of IGHMBP2 is still contradictory. IGHMBP2 was observed in the nucleus and in cytoplasmic discrete foci with some perinuclear accumulation in HeLa and epithelial cells 21PT (Molnar *et al.*, 1997). Its intracellular distribution in the nucleus and the cytoplasm seems not dependent of cell cycle. In contrast to the observations of Molnar and coworkers, Grohmann *et al.* (2004) detected IGHMBP2 at high levels in the cytoplasm of mouse motor neuron and cultured mouse motor neurons including axons and growth cones and only at low levels in the nucleus. Thus, further studies would be required to determine intracellular localization and trafficking of IGHMBP2.

3.2.2 Proposed Cellular Functions of IGHMBP2

Although attempts to unravel the function of IGHMBP2 have been independently made by several groups, the precise role of IGHMBP2 in living cells is still only poorly understood. Its widespread expression among various tissues and its nuclear and cytoplasmic distribution indicate that IGHMBP2 might be associated with “house keeping” functions in the nucleus and cytoplasm. *IGHMBP2* cDNA was initially cloned using a DNA probe corresponding to the immunoglobulin S μ region, but there is no evidence that supports the involvement of IGHMBP2 in immunoglobulin class switching (Fukita *et al.*, 1993). Biochemical characterization of recombinant human IGHMBP2 as an ATPase and DNA helicase (Biswas *et al.*, 2001; Molnar *et al.*, 1997) suggests a function in DNA metabolism, such as DNA replication, repair or recombination. But none of these proposed functions have been experimentally proven. Other studies however reported the function of IGHMBP2 as general transcription activator, repressor and non-snRNP splicing factor.

Early studies on cellular IGHMBP2 function showed that IGHMBP2 bound human virus JCV (JC virus, polyomavirus) early and late promoters and activated Glial cells-specific expression of JCV (Chen *et al.*, 1997; Kerr and Khalili, 1991). Further investigation found

that IGHMBP2 was also able to bind other promoter/enhancer sequences such as the ubiquitous rat insulin promoter element RIPE3b2 (Shieh *et al.*, 1995), human apoA-1 promoter in hepatoma cell line (Mohan *et al.*, 1998), tissue specific-rat antifreeze protein/AFP enhancer (Miao *et al.*, 2000), myocyte-specific element enhancer of the atrialnatriuretic factor (ANF) gene (Sebastiani *et al.*, 1994) and subsequently transactivate transcription of the genes carrying these sequence elements. Some other groups, in contrast, reported negative downstream effect of IGHMBP2 binding to promoter sequences. Transcription of genes containing adenovirus E1B BLZF1f promoter in EBV-negative B cell line (Zhang *et al.*, 1999) and mouse mammary tumor virus (MMTV) promoter (Uchiumi *et al.*, 2004;) was reduced by overexpression of IGHMBP2. All of these data indicated involvement of IGHMBP2 in transcription of several unrelated target genes. Nevertheless, until most recently, there is no further functional study that supports a potential role of IGHMBP2 in transcription.

As mentioned earlier, Czaplinsky *et al.* (2000) have sub-grouped several proteins of SF1 family into an Upf1-like subfamily of Superfamily 1. Since most members of this subclass display its cellular function in RNA metabolism, they hypothesized that the proteins of the Upf1-like subclass play a role in RNA- rather than in DNA-dependent processes and may constitute a new family of RNA helicases. Given that IGHMBP2 belongs to this subclass, it is likely that IGHMBP2 is likewise involved in RNA-dependent processes. In keeping with this notion, two groups reported a link of IGHMBP2 to the pre-mRNA splicing machinery. Interaction studies using the yeast two hybrid system identified IGHMBP2 as a binding protein of the U6 snRNP structural protein Lsm8 (Lehner and Sanderson, 2004). Furthermore, IGHMBP2 was found to colocalize with the splicing factor SC35 in nuclear speckles (Molnar *et al.*, 1997). IGHMBP2 also bound to spliceosomes assembled in nuclear extracts on a pre-mRNA substrate. These data suggested that IGHMBP2 might be involved in catalysis of pre-mRNA splicing in the nucleus (Molnar *et al.*, 1997), but its precise role *in vivo* remains to be elucidated.

3.3 Aim of this Study

Immunoglobulin μ -binding protein 2 (IGHMBP2) is the protein product of the spinal muscular atrophy with respiratory distress type 1 or SMARD1 disease gene. Despite of the remarkable cell specificity of the disease, the expression pattern of IGHMBP2 is ubiquitous rather than restricted to the affected tissues in SMARD1 patients. It is therefore likely that SMARD1 results from the malfunction of a “housekeeping” protein. Despite intensive studies on IGHMBP2 protein, presently only little is known about its cellular function and its contribution to the pathomechanism of SMARD1. The prime goal of this study was to link IGHMBP2 to a specific cellular pathway and to gain insights into the molecular basis of SMARD1.

As an initial step toward an understanding of the function of IGHMBP2, attempts were made to characterize its enzymatic activities *in vitro*. A prerequisite for these studies is the availability of recombinant functional protein in large amounts and an enzymatically-active state. To this end, an efficient bacterial expression and two-step purification strategy was established. Since IGHMBP2 contains an N-terminal helicase domain and belongs to the SF1 helicase, a major focus of these studies was put on the characterization of IGHMBP2’s putative ATPase and nucleic acid unwinding activities.

A second focus of this work was to connect IGHMBP2 to a specific cellular pathway. Two major questions were addressed in this context: apart from determining the precise subcellular distribution of IGHMBP2, these studies focused on the identification of cellular components that functionally interact with IGHMBP2. This technically challenging task was approached by affinity purification strategies making use of monospecific antibodies and functional recombinant IGHMBP2.

The biochemical characterization of IGHMBP2 and identification of its cellular function allow addressing the third focus of this study, namely the pathomechanism of SMARD1. For this purpose, pathogenic IGHMBP2 variants were expressed along the same lines as already established for the wild-type protein and compare their enzymatic activities with the wild-type protein. Lastly, the pathogenic IGHMBP2 variants were investigated for their interaction with its cellular partners

4. RESULTS

4.1 Characterization of Enzymatic Activities of Recombinant IGHMBP2 as a Member of the Helicase Superfamily 1

Based on sequence comparisons, IGHMBP2 has been classified as a member of the helicase Superfamily 1 (SF1). IGHMBP2 contains an amino-terminal helicase/ATPase domain and has previously been shown to display enzymatic activities similar to the best-characterized member of this family, the Upf1 protein (Biswas *et al.*, 2001; Molnar *et al.*, 1997). Human IGHMBP2 (IGHMBP2) displays nucleic acid-stimulated/dependent ATPase and DNA unwinding activities. However unlike Upf1, which was found to unwind not only DNA but also RNA substrates *in vitro* (Czaplinski *et al.*, 1995), no RNA unwinding activity of IGHMBP2 has been identified thus far (Molnar *et al.*, 1997). Taking into consideration that the helicase domains of Upf1 and IGHMBP2 are highly homologous, it is reasonable to speculate that in addition to DNA helicase activity, IGHMBP2 serves as RNA helicase *in vitro*. Until recently, attempts to demonstrate the RNA unwinding activity of IGHMBP2 have failed simply due to the difficulty to get hands on recombinant helicase. As an initial step toward the detailed functional studies on enzymatic activities of IGHMBP2, an expression and affinity purification strategy was developed to obtain recombinant full length IGHMBP2 from bacterial cells in a pure and catalytically active state. The recombinant IGHMBP2 obtained by this expression and purification protocol was used for the subsequent enzymatic studies of IGHMBP2 as a helicase, namely ATP hydrolysis activity and unwinding activity on RNA substrate.

4.1.1 Expression and Purification of Recombinant IGHMBP2

As a first step in expression and purification of recombinant IGHMBP2, a derivative of the pGex6p.1 expression plasmid vector containing the full length *IGHMBP2* was constructed, allowing for high level expression of the protein in *E. coli* Rosetta strains. A sequence encoding a hexahistidine tag (6His) was fused to the C-terminus of the full length coding

region of *IGHMBP2*. This fusion sequence was subsequently integrated into a downstream site of the glutathione S-transferase tag (GST tag) of the expression plasmid pGex6p1, resulting in IGHMBP2 preceded in-frame by an N-terminal GST tag and flanked by a C-terminal his tag (Fig 4). Taking advantage of both tags, bacterially-expressed IGHMBP2 was purified using a two-step affinity chromatography procedure (Fig. 4). In this purification protocol, the GST tag at the N terminus was used first for affinity purification on a glutathione Sepharose resin, followed by a second affinity chromatography on Ni-NTA resin. Prior to the second purification step, the fusion protein was cleaved by PreScission protease to remove the GST tag. The use of two separate purification steps allowed for removal of contaminating proteins and proteolytic degradation products of the fusion protein lacking either N- or C- terminal residues. Thus, after the final purification step, full length and apparently homogenous recombinant protein could be obtained.



pGex6p1-IGHMBP2-6His Expression in *E. coli*

Purification: GST-IGHMBP2-6His on Glutathione sepharose beads column

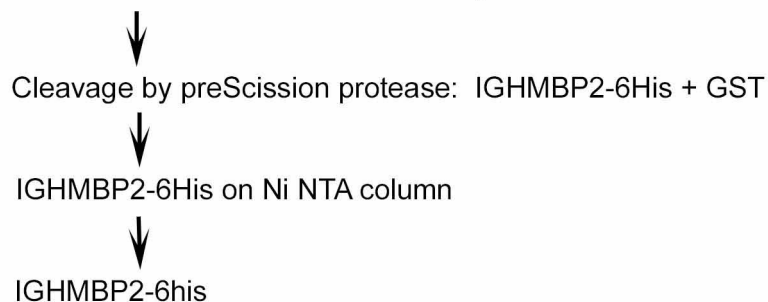


Figure 4. Strategy for Expression and Purification of Recombinant IGHMBP2. pGex6p1 containing the full length IGHMBP2 flanked by an N-terminal GST tag and a C-terminal 6xhis tag was transfected into *E. coli* strain Rosetta. Taking advantage of the GST and His tags, the bacterially-expressed GST-IGHMBP2-6xhis was subjected to a two-step purification protocol. The first purification was carried out using glutathione sepharose beads, followed by cleavage with PreScission protease to remove the GST tag, which was retained on the matrix. The cleavage products containing IGHMBP2-6his were loaded on to a Ni-NTA column. This second purification step produced his-tagged IGHMBP2.

As shown in Fig. 5, the full length IGHMBP2 in pGex6p1GST-IGHMBP2-6xhis, was expressed at high level in *E. coli* Rossetta cells upon induction with 1 mM IPTG at 10°C for 16 hours (Fig. 5 lanes 1 and 2, before and after induction, respectively). Following fractionation by high speed centrifugation, recombinant IGHMBP2 was largely retained in the soluble supernatant, only small amounts of IGHMBP2 was sedimented into the insoluble pellet (Fig. 5 lanes 3 and 4). The GST-IGHMBP2-6xhis was then purified from *E. coli* cells by glutathione Sepharose beads chromatography (see materials and methods for the detailed protocol). In order to remove the GST tag from the IGHMBP2-fusion, the purified protein was subsequently treated with preScission protease. This treatment led to cleavage of approximately 50% of IGHMBP2, producing the fusion protein harboring only His-tag at its C-terminal and the GST moiety, which was retained on the matrix (Fig. 5 lanes 5 and 6). The cleaved protein was further affinity purified by means of its C-terminal

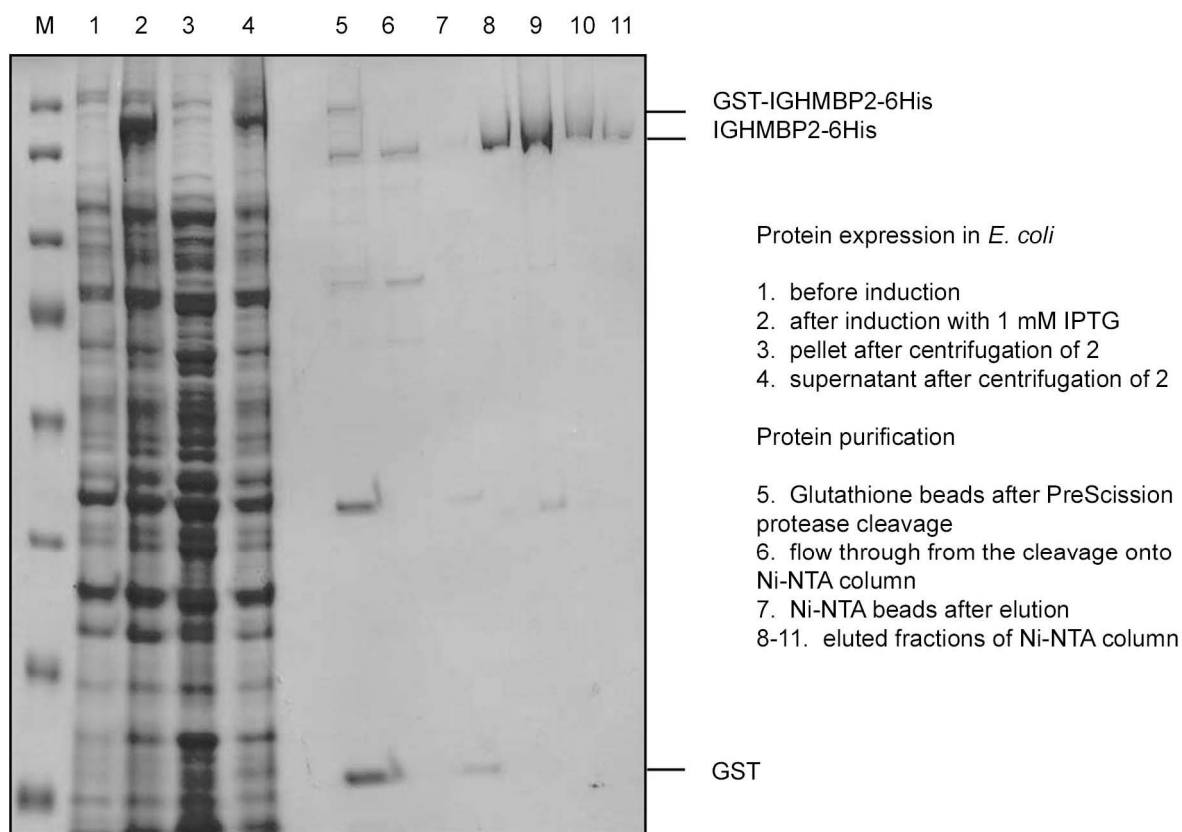


Figure 5. Expression and Purification of Recombinant IGHMBP2 in *E. coli* Strains Rossetta. Protein expression was achieved by induction with 1 mM IPTG at 10°C overnight (lane1-2). The protein was extracted from the bacterial cells and fractionated by high speed centrifugation (lane 3-4).

(Fig. 5 continued) The soluble fraction/supernatant (lane 4) was subject to protein purification by affinity chromatography through glutathione sepharose beads column. The bound IGHMBP2 was then cleaved with PreScission protease to remove the GST tag (lane 5-6) and the flow through containing IGHMBP2-6xhis was subsequently purified through Ni-NTA agarose beads. The bound proteins were eluted with imidazol (lane 8-11). Proteins were analyzed by 12% SDS PAGE and visualized by Coomassie blue staining. M: marker.

His-tag on a Ni-NTA column. In this step, the full length fusion protein as well as its N-terminal degradation products harboring 6His-tag was retained on the Ni-NTA resin. After extensive washing, the bound proteins were eluted with imidazole. As shown in Fig. 5 lanes 8-11, full-length IGHMBP2-6His was efficiently released from the resin by elution with imidazole and only a small fraction of IGHMBP2 remained bound on the Ni-NTA beads (Fig. 5 lane 7). Moreover, two faint bands of approximately 70 and 55 kDa in size were also observed in the eluted fractions, which were identified by Western blot analysis as the N-terminal degradation products of IGHMBP2 (data not shown). The purity of the recombinant protein was estimated to be greater than 95% by Coomassie blue staining and approximately 0.2 mg purified IGHMBP2-6His was obtained from 2L of *E. coli* culture (Fig 4. lanes 8-11). Taken together, using two constitutive steps of affinity chromatography, bacterially-expressed full length IGHMBP2 can be purified to a near homogeneity, thus facilitating enzymatic studies of IGHMBP2. Additionally, for these studies, expression plasmids containing IGHMBP2 with mutations either in the Walker A or B motifs (p.GKT219AAA and p.DE375AA, respectively) were also constructed, allowing for expression and purification of these mutant proteins as wild-type IGHMBP2. The experiments described in this section were performed by Ulf Günther, collaborator in this study.

4.1.2 ATPase Activity of Recombinant IGHMBP2

Having established an expression and purification procedure for IGHMBP2, an initial effort was made to investigate the capability of the recombinant protein to hydrolyze ATP. In the study performed by Ulf Günther (collaborator in this work), the recombinant protein was incubated with α -[P³²]-labeled ATP at 37°C for 60 minutes and the hydrolysis of α -[P³²]-ATP into α -[P³²]-ADP was then monitored by thin layer chromatography. ATP hydrolysis activity was evidenced by the appearance of labeled ADP and the simultaneous

disappearance of labeled ATP. As shown in Fig. 6, lane 1, the recombinant IGHMBP2 slowly catalyzed the hydrolysis of ATP when compared to the control reaction at 4°C (lane 14) and those in absence of protein (lanes 9-13). To exclude the possibility that the ATPase activity of the recombinant protein was due to contaminating factors in the protein preparation, IGHMBP2 harboring mutations in either Walker A or B motifs were also analyzed for ATP hydrolysis. Previous mutational studies on DEAD box helicases have suggested that both motifs are crucial for ATPase and helicase activities (reviewed in Cordin *et al.*, 2006). Indeed, in this assay both mutations reduced ATPase activity to background levels (Fig. 6A lane 7-8). These results indicate that recombinant IGHMBP2 obtained by using the two-step purification strategy exhibits intrinsic catalytic activity and therefore can be used for further functional studies.

Although ATP is commonly known as the most efficient cofactor in NTPase activity, many helicases are able to hydrolyze other nucleoside triphosphates. In order to determine whether IGHMBP2 acts as a general NTPase or has a preference for a certain type of nucleotide, a 50-fold molar excess of different unlabeled rNTPs and dNTPs was added as competitors to the ATPase reaction. The release of α -[P³²]-ADP was analyzed as described above. As shown in Fig. 6B, under these conditions, only ATP or dATP efficiently inhibited the hydrolysis of α -[P³²]-ATP, while the other nucleotides tested had no measurable effect (Fig. 6B). The cofactor requirement of IGHMBP2 is therefore identical to other known SF1 and SF2 helicases. Moreover, this competition assay also illustrates the specificity of IGHMBP2 for the cofactor ATP. The competition assay was performed by Ulf Günther as collaborator in this study.

Since the ATP turnover rates of many type I helicases are cooperatively coupled to substrate binding, the hydrolysis activity of IGHMBP2 was next analyzed in the presence of nucleic acids. For this purpose, recombinant IGHMBP2 was incubated with either double-stranded DNA or homopolymeric RNAs (poly (A), poly (C), poly (G) and poly (U)) and ATPase activity was measured as described above. Indeed, strong stimulation of the ATPase could be observed when either DNA or poly (A), (C) and (U) were added to the reaction mixture (Fig. 6A lanes 2, 3, 4 and 6, for quantitative analysis see Fig. 6C). Under the conditions applied here, the presence of DNA or poly A, C and U increased the release of hydrolysis product α -[P³²]-ADP by approximately 70%. Only poly (G) was

much less efficient in this assay and resulted only in a marginal increase of ATP hydrolysis (Fig. 6A lane 5). Moreover, only background levels of the hydrolysis product were observed in the absence of protein (Fig. 6A lanes 9-13), thus suggesting that the observed stimulation of ATP hydrolysis was due to binding of the nucleic acid to IGHMBP2. Together, these results indicate that IGHMBP2 is an ATPase that is stimulated by a variety of nucleic acids. The ATPase experiments in this part were performed by Ulf Günther, collaborator in this study.

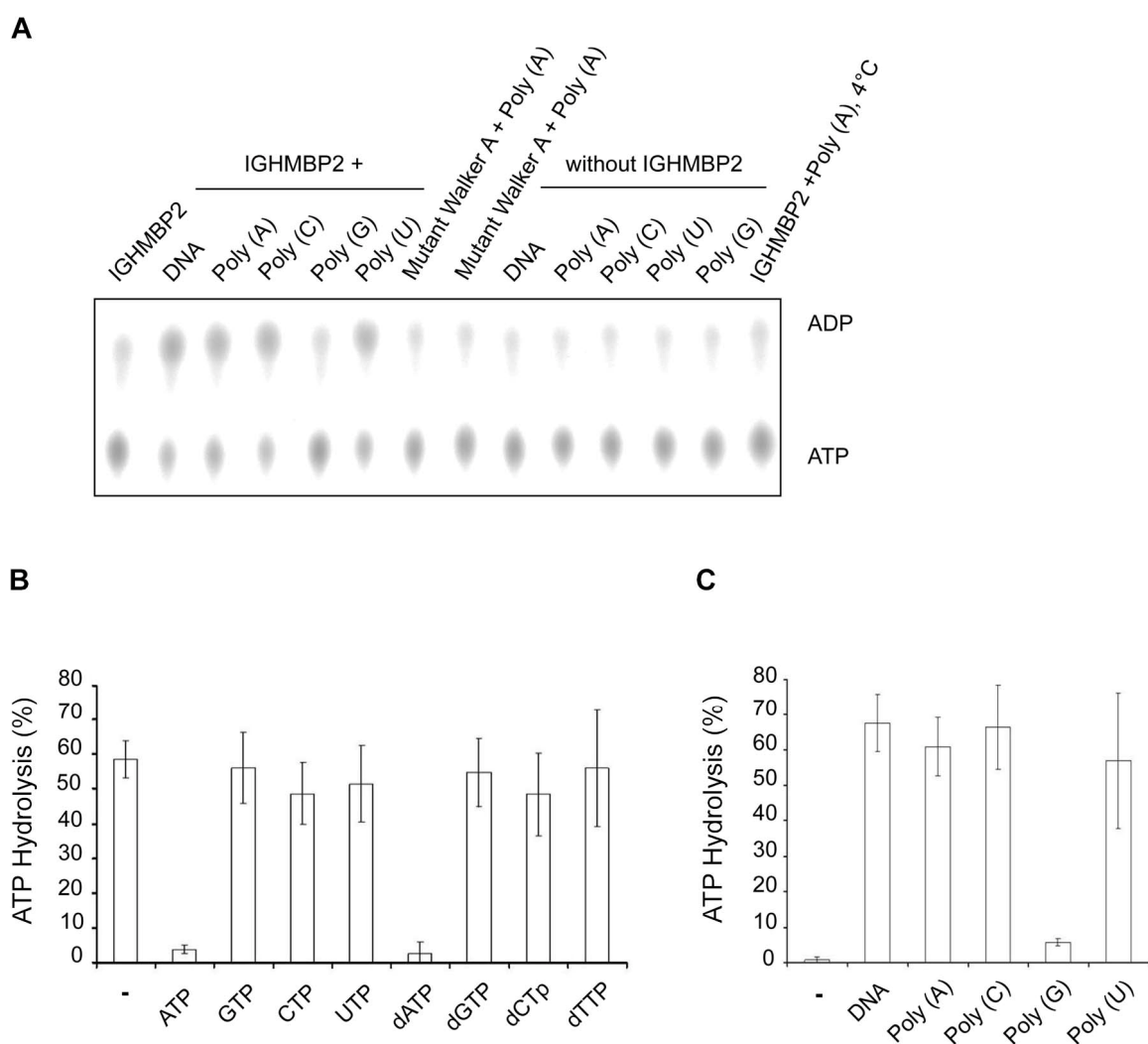


Figure 6. IGHMBP2 Has an ATPase Activity That Is Stimulated by a Variety of Nucleic Acids. **A.** ATP hydrolysis activity of IGHMBP2. Recombinant IGHMBP2 as well as Walker A and B mutants of IGHMBP2 was incubated with radioactively labeled α -[P^{32}]-ATP, in the presence or in the absence of nucleic acids and analyzed 60 minutes later by thin layer chromatography. **B.** ATPase competition experiment. A 50-fold molar excess of different unlabeled nucleotides was

(Fig. 6 continued) added into the ATPase assay; (-) no addition of unlabeled nucleotides. C. Quantitation of A. the ATP hydrolysis of recombinant IGHMBP2 was stimulated by nucleic acids. (-): no nucleic acids.

4.1.3 RNA Unwinding Activity of Recombinant IGHMBP2

The results above identify IGHMBP2 as a DNA/RNA-stimulated ATPase. Next, it was tested, whether this protein can also act as a helicase as predicted by sequence homology and by previous studies (Biswas *et al.*, 2001; Molnar *et al.*, 1997). In order to assess this possibility, an *in vitro* helicase assay was established, using partially double-stranded RNA substrates.

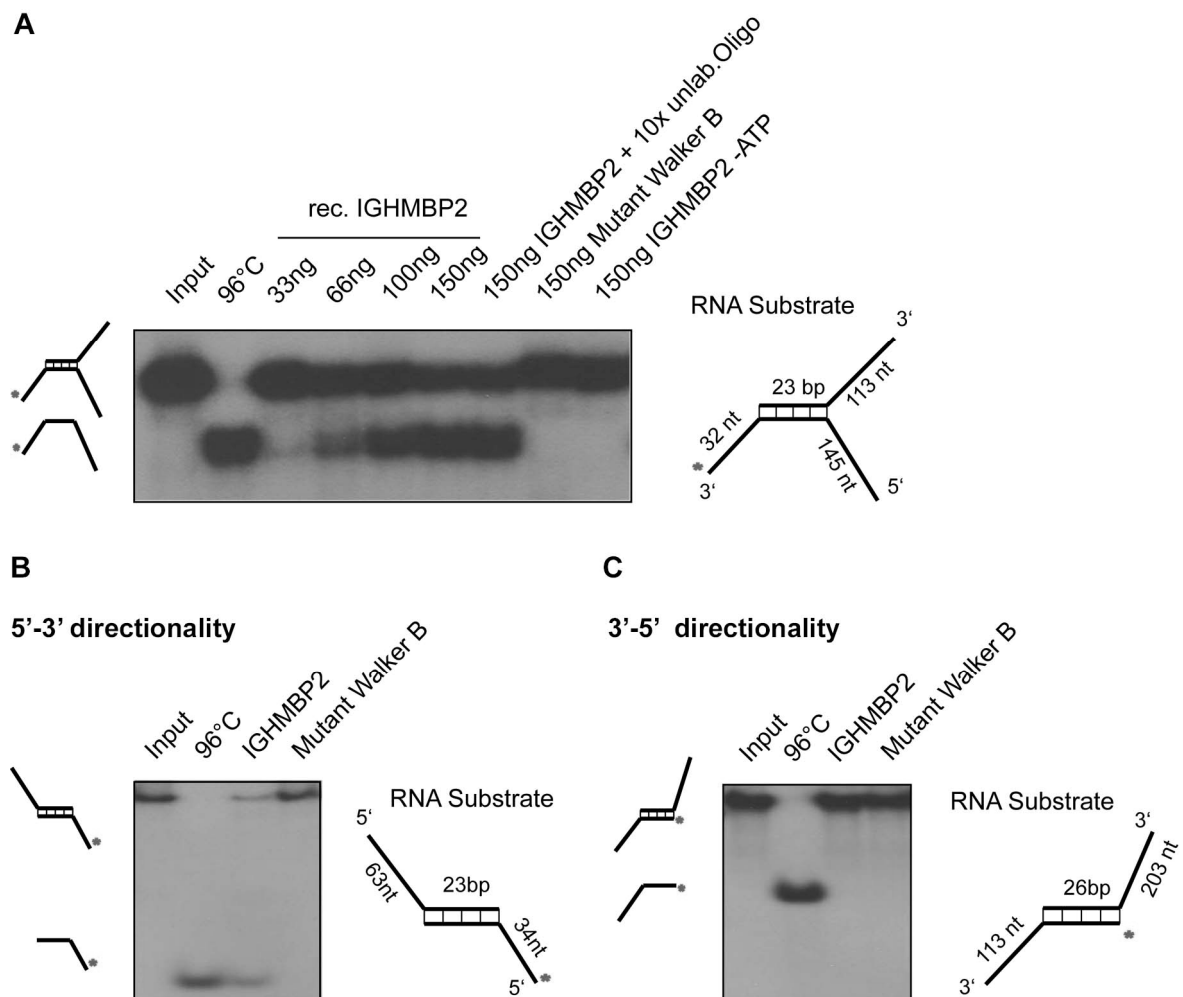


Figure 7. ATP-Dependent RNA Unwinding Activity of IGHMBP2. A. IGHMBP2 unwinds the RNA substrate in a dose dependent manner in the presence of ATP. The radioactively labeled

(Fig. 7 continued) partially complementary double-stranded RNA substrate/ [³²P]- RNA duplex (right) was incubated with increasing amounts of recombinant IGHMBP2 in the presence of ATP and subsequently analyzed by native RNA gel electrophoresis. The [³²P]- RNA duplex in the absence of protein is shown in lane 1 (input). The single-stranded RNA products are determined by comparison with those generated by denaturing the RNA duplex alone at 96°C. **B.** RNA unwinding assay was performed with RNA substrate containing 5' single stranded extension. **C.** as B, RNA substrate carries 3' single stranded extension.

In a first set of experiments, helicase assays were carried out with an RNA duplex, which contained single-stranded overhangs at the 3' and 5' ends (Fig. 7A). To generate this substrate, a radioactively-labeled 200 nt artificial RNA fragment was annealed to a 136 nt long partially complementary non labeled RNA (Fig. 7a RNA substrate). The RNA hybrid was then incubated with increasing amounts of recombinant IGHMBP2 in the presence or absence of ATP for 60 min and analyzed by native polyacrylamide gel electrophoresis. In this gel system, the radioactively-labeled double-stranded substrate is significantly more retarded than the single strand, thus allowing for monitoring the helicase reaction. The position of single-stranded RNA was determined by denaturing the RNA substrate at 95°C and loaded on the gel parallel with the helicase reactions (Fig. 6A lane 2). As shown in Fig. 6A lanes 3-7, recombinant IGHMBP2 unwound the RNA duplex in a dose dependent manner, as indicated by the appearance of the labeled single-stranded RNA and the concomitant decrease of the double-stranded RNA substrate. Approximately 100-150 ng IGHMBP2 were required to unwind 50% RNA duplex. Importantly, omission of ATP from the reaction or introduction of a single point mutation in the Walker B motif of the IGHMBP2 helicase domain virtually abolished the helicase activity of IGHMBP2. These controls show that the unwinding reaction was solely catalyzed by the protein and not due to any contaminating component in the reaction mixture. These experiments were done by Ulf Günther, collaborator in this study.

The above-mentioned findings indicate that IGHMBP2 is an ATP-dependent enzyme capable of unwinding RNA duplexes. In principle, IGHMBP2 could unwind the duplex either from the 5' end, the 3' end or from both sides. Whereas some helicases have the preference for unwinding the duplex only from one site, others more promiscuous toward directionality of unwinding. To determine the polarity of IGHMBP2-catalyzed unwinding activity, two different RNA substrates were generated, one containing only a 5' overhang and the other containing only a 3' overhang (Fig. 7B). Unwinding of the former substrate

would indicate helicase activity in 5'-3' direction, while the latter would suggest the opposite directionality. Strand displacement assays with these two RNA substrates were performed and analyzed as described above. These experiments were done by Ulf Günther, collaborator in this study. Fig. 7B shows that only the substrate containing 5' overhangs was unwound, as evidenced by the presence of the labeled-single-strand RNA product, whereas the substrate containing 3' overhangs remained stable over the entire period of the experiment. Very similar results were also obtained with DNA duplexes (data not shown). In conclusion, these data define IGHMBP2 as an enzyme that unwinds RNA or DNA duplexes with 5' overhangs in an ATP-dependent fashion.

4.2 Identification of Cellular Binding Partners of IGHMBP2

Functional enzymatic studies of recombinant IGHMBP2 described above characterize IGHMBP2 as an ATP-dependent 5'-3' RNA/DNA helicase *in vitro*. In living cells, IGHMBP2 has been implicated in DNA transcription as well as in the processing of pre-mRNAs (Mizuta 1993, Shieh *et al.* 1995, Zhang *et al.* 1999, Molnar *et al.* 1997 and Biswas *et al.* 2001). However, until most recently the precise function of IGHMBP2 in those processes is still unclear. The above-mentioned hypothesis about the cellular function of IGHMBP2 still awaits proof by functional assays or at least the identification of interacting proteins or cellular targets. The following study focused on isolation and characterization of proteins interacting with endogenous IGHMBP2. As initial steps toward this, studies were performed to investigate the precise subcellular localization of IGHMBP2 and the association of IGHMBP2 with other cellular components in cellular extracts.

4.2.1 Biochemical Analysis of Endogenous IGHMBP2 in Cellular Extracts

4.2.1.1 Subcellular Localization of IGHMBP2

According to Molnar *et al.* (1997) IGHMBP2 protein localizes in the nucleus as well as in discrete foci in the cytoplasm. In cultured mouse motor neuron cells and mouse motor neurons, by contrast, IGHMBP2 is found predominantly in the cytoplasm and only at the low levels in the nucleus (Grohmann *et al.*, 2004). Given that IGHMBP2 contains two

(Fig. 8 continued) examined by Western blotting against anti IGHMBP2 antibody. **B.** IGHMBP2 is present in salt sensitive ribonucleoprotein complexes. Cytoplasmic extract was prepared in a buffer containing 0.01% ionic detergent NP-40 (top panel), 0.5% NP-40 (second panel), 500 mM NaCl (third panel) or RNase A (bottom panel). **C.** IGHMBP2 complexes are DNase I-resistant. Prior to glycerol gradient centrifugation, cytoplasmic extract was incubated with 0.5U/ μ l DNase I at 37°C for 30 min.

The same findings were also obtained using different batches of purified anti IGHMBP2 antibodies. Furthermore, the predominantly cytoplasmic localization of IGHMBP2 was observed in other cell lines (rat PC12, monkey Cos7 and human 293), with other fixation methods such as methanol, methanol/formaldehyde, or when IGHMBP2 was expressed as GFP, HA, or Flag- tagged variants (data not shown). These observations are in agreement with the previous findings of Grohmann *et al.*, (2004), who demonstrated that IGHMBP2 predominantly localizes in the cytoplasm.

4.2.1.2 IGHMBP2 Is Part of Large Ribonucleoprotein Complexes

In a next step, the capability of IGHMBP2 to form stable complex with other components of the cellular extract was investigated. For this purpose, cytoplasmic extracts were prepared from mouse FM3A cells in a physiological buffer under mild ionic conditions. The extract was subsequently size-fractionated on a linear 5-30% (v/v) glycerol gradient by ultracentrifugation for 4 hours. 18 Fractions were collected from the gradient and proteins of each fraction were analyzed by Western blotting using anti IGHMBP2 antibody. As shown in Fig. 8B, IGHMBP2 could be detected under these experimental conditions in two major peaks with S-values larger than 30. The major fraction of endogenous IGHMBP2 (approx. 70%) was reproducibly found in the smaller one of both complexes. Both complexes seem to be detergent insensitive, since increasing the concentration of the non-ionic detergent NP-10 in cytoplasmic extract up to 0.5% had no effect on the stability of the complexes (Fig. 8C, first and second panels). Raising the salt concentrations above a critical level (500 mM NaCl), by contrast led to a quantitative disruption of these complexes and the floatation of IGHMBP2 on the top of the gradient (Fig. 8B third panel). A very similar sedimentation profile was observed in extracts derived from mouse brain tissue or from other cell lines (mouse and rat) (data not shown). These findings indicate that IGHMBP2 is associated with other cellular components in a salt-dependent manner.

The fact that IGHMBP2 not only contains a conserved sequence indicative for single-stranded nucleic acid binding (R3H) but also acts as a DNA/RNA helicase *in vitro* (see 4.2.3) raised the question whether these complexes contain nucleic acids. To address this question, FM3A cytoplasmic extract was treated either with RNase A (for 10 min at room temperature) or with DNase I (for 30 min at 37°C) prior to gradient centrifugation and subsequently analyzed as described above. Indeed, incubation of the cytoplasmic extract with RNase A completely disrupted both complexes and shifted IGHMBP2 to either the top of the gradient or into the insoluble pellet (Fig. 8B bottom panel). In contrast, both complexes were still observed upon treatment with RNase-free DNase I (Fig. 8C upper panel). Occasionally, a fraction of IGHMBP2 was also observed at the top of gradients under these conditions. This might be due to partial dissociation of IGHMBP2 from the complexes during incubation 37°C for 30 min rather than a specific effect upon DNase treatment, since the same profile was observed in the control extract incubated at 37°C for 30 min without DNase. In summary, these results suggest that the majority of soluble cellular IGHMBP2 forms cytosolic large ribonucleoprotein complexes (RNPs) *in vivo*.

4.2.2 Isolation and Characterization of the Cellular Components of IGHMBP2 Complexes

The previous results show that IGHMBP2 is a predominantly cytosolic protein and stably interacts with other proteins to form large RNPs. In an effort to elucidate the cellular function of IGHMBP2, biochemical approaches were developed to identify the cellular components of these RNPs. Initial attempts to isolate the IGHMBP2-RNP complexes were performed by an immunoaffinity chromatography approach. For this purpose, purified anti IGHMBP2 antibody was immobilized on protein A sepharose beads matrix and incubated with FM3A cytoplasmic extract. Following extensive washing, the bound IGHMBP2 and its interacting proteins were eluted from the beads by pH-shock and assayed by SDS PAGE and silver staining (data not shown). Unfortunately, affinity purification using anti IGHMBP2 antibody failed to isolate binding partners of IGHMBP2. Although IGHMBP2 was efficiently immunoprecipitated from cytoplasmic extracts using several anti IGHMBP2 antisera, the pattern of co-precipitated factors varied from experiment to experiment, suggesting that these proteins had bound non-specifically to either IGHMBP2

or the column matrix. A likely explanation for these results was that IGHMBP2 complexes were destabilized under the conditions of the immunoaffinity purification procedure.

The data described above suggest that immunaffinity purification seems to be unsuitable for purification of IGHMBP2 complexes. Therefore, an alternative strategy was then established to purify these complexes. The results summarized in Chapter 4.1 shows that recombinant IGHMBP2 is efficiently expressed in bacterial cells and purified to apparent homogeneity. Taking advantage of this recombinant GST-IGHMBP2-6his, affinity chromatography was performed using recombinant IGHMBP2 immobilized on beads as an affinity matrix.

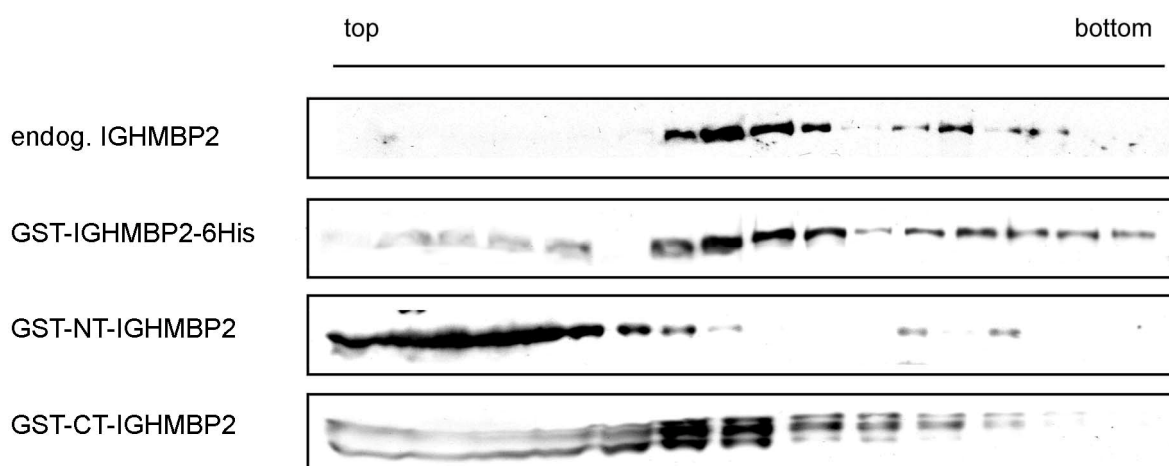


Figure 9. Sedimentation Profiles of the Recombinant IGHMBP2 in Cellular Extracts. Recombinant IGHMBP2 (full length IGHMBP2, C-terminal fragment of IGHMBP2 (amino acids 1-286) and N-terminal fragment of IGHMBP2 (amino acids 881-993)) was incubated with cytoplasmic extracts for 10 min on ice prior to 5-30% glycerol gradient centrifugation. Protein in each fraction was TCA-precipitated and analyzed by 10% SDS-PAGE followed by Western blot against anti GST antibody and anti IGHMBP2 antibody to detect GST fusion proteins and the endogenous IGHMBP2, respectively.

Recombinant proteins are commonly utilized as a molecular probe to purify protein complexes from cellular extracts. However, it is important to evaluate whether the recombinant protein engages in similar interactions in cellular extracts as the endogenous protein. To address this question, FM3A cytoplasmic extracts were incubated with

recombinant IGHMBP2 and then analyzed by a linear 5-30% (v/v) glycerol gradient ultracentrifugation in the similar manner as described in 4.2.1. As a control, recombinant IGHMBP2 was incubated with buffer only and then analyzed in parallel. Western blot analysis of the gradient fractions demonstrates that the recombinant full length IGHMBP2 co-sedimented with endogenous IGHMBP2 (Fig. 11 second panel), whereas IGHMBP2 alone accumulated on the top of the gradient (data not shown). Furthermore, neither GST-tagged C-terminal nor N-terminal fragment of IGHMBP2, which were expressed and purified as the full length IGHMBP2, was incorporated into the endogenous complexes (Fig. 11 lower panels). Considered together, these data indicate that endogenous and recombinant full length IGHMBP2 are efficiently incorporated into the same complex (Fig. 11). Therefore, immobilized recombinant full length IGHMBP2 was chosen as an affinity matrix to identify the components of the IGHMBP2-RNP complexes.

Recombinant IGHMBP2 was expressed in *E. coli* and purified similarly as described in 4.1.1. For preparation of the affinity matrix, GST-tagged recombinant IGHMBP2 was immobilized non-covalently on glutathione beads, thus allowing for the specific and native elution with glutathione at later stages. The affinity matrix was incubated with cytoplasmic extract prepared from mouse FM3A cells in a physiological buffer. After several wash steps under mild ionic conditions, the bound proteins were eluted from the beads with glutathione. The eluate was subsequently separated by SDS polyacrylamide gel electrophoresis and proteins were visualized by silver staining (Fig. 10A). To control for the specificity of this affinity chromatography, GST alone was immobilized on glutathione sepharose beads and treated identically as the recombinant IGHMBP2. As shown in Fig. 12A, lane 1, a series of predominantly small proteins (<50 kDa) specifically eluted from the IGHMBP2 column, but not from the control GST column (Fig. 10A lane 3). These bands were identified by mass spectrometry as ribosomal proteins of the large and small subunits, translation initiation and elongation factors and RNA binding proteins, such as general translation repressor Y-box binding protein (for details see Fig. 10 Table B). Furthermore, RNA analysis of the eluates shows that 18S as well as 28S rRNAs specifically co-eluted from the IGHMBP2 column (Fig. 10A bottom panel). These findings suggest that ribosomal subunits rather than individual proteins bound to IGHMBP2 affinity matrix.

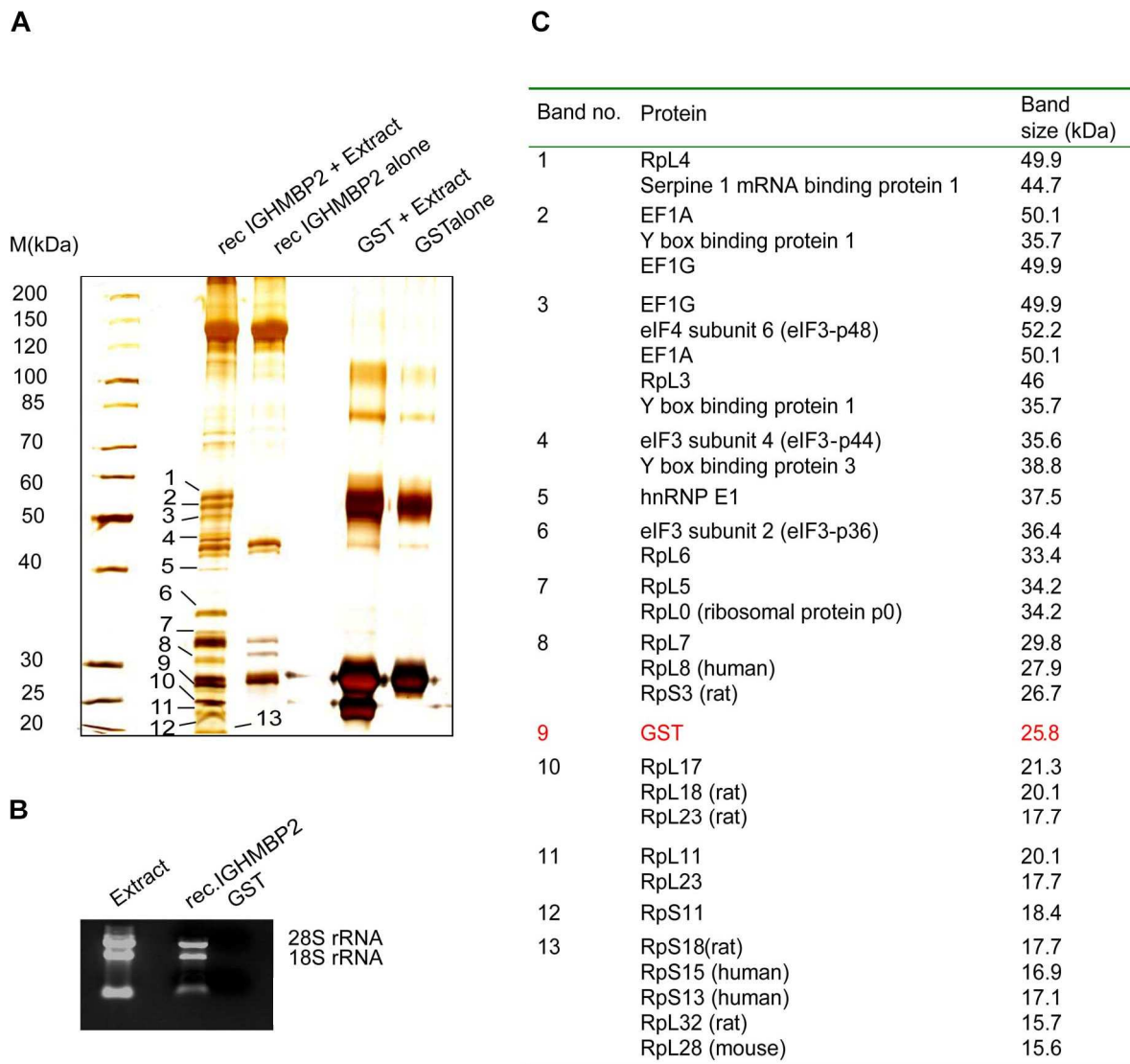


Figure 10. Purification of IGHMBP2 Complexes Using Recombinant IGHMBP2 as an Affinity Matrix. **A.** GST-IGHMBP2-6xHis or GST tag alone immobilized on glutathione sepharose beads was incubated with FM3A cytoplasmic extracts for one hour at 4°C. After washing, the bound proteins were eluted with reduced glutathione and analyzed by 10% SDS polyacrylamide gel electrophoresis followed by silver staining. The specific and prominent bands were excised and proteins were identified by mass spectrometry. **B.** RNAs were isolated from the eluates and analyzed by 1% agarose gel electrophoresis and ethidium bromide staining. **C.** Mass spectrometry analysis of the isolated bands indicated in A.

To exclude the possibility that the association of ribosomal subunits was unspecific due to the mild conditions of the purification strategy and the high abundance of ribosomes, the eluate of the IGHMBP2 column was further purified by sedimentation through a linear 5-

30% (v/v) glycerol gradient. The gradient analysis was carried out as described in 4.2.2. Proteins of individual fractions were separated by SDS PAGE and visualized by silver staining. As shown in Fig. 11A, the majority of proteins sedimented as part of two distinct, homogeneous complexes. Only few of the initially identified proteins did not withstand this treatment. Moreover, these complexes correspond to the small (40S) and large (60S) ribosomal subunits, as evidenced by the identification of 18S and 28S rRNAs, respectively in the same fractions (Fig. 11A bottom panel). Additionally, the sedimentation profiles of the isolated complexes perfectly correlate with those of the endogenous IGHMBP2 complexes in the cellular extracts analyzed parallel (Fig. 11A bottom panel).

5-30% glycerol gradient

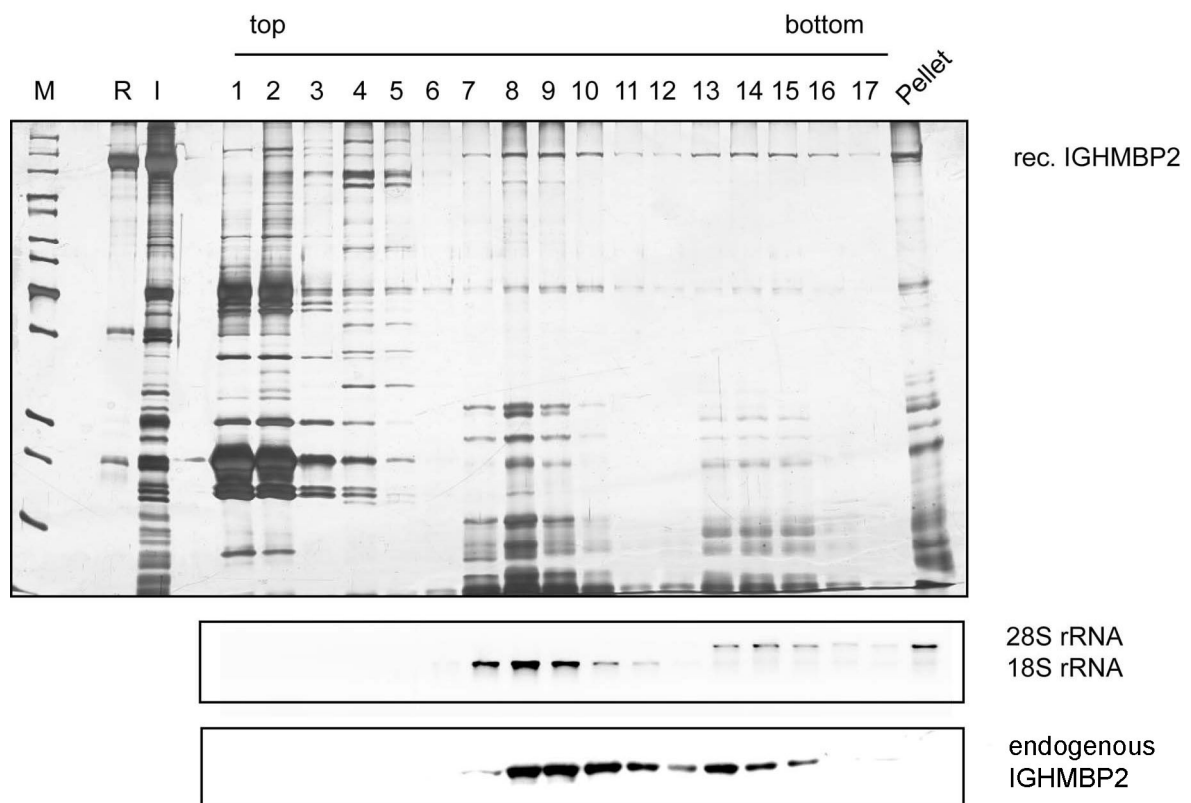


Figure 11. IGHMBP2 Binds 40S and 60S Ribosomal Subunits *In Vitro*. The eluate from the IGHMBP2-GST pull-down assay (Fig. 10) was analyzed by a 5-30% glycerol gradient sedimentation. 17 fractions and pellet were examined for RNA and protein. Proteins were analyzed by 10% SDS PAGE followed by silver staining. RNAs were separated on 1% agarose gel containing ethidium bromide (middle panel). The bottom panel: parallel to the eluate above, FM3A cytoplasmic extract was fractionated through a linear 5-30% glycerol gradient and the presence of

(Fig. 11 continued) IGHMBP2 in each fraction was determined by Western blot with purified anti IGHMBP2 antibody. M: Marker; R: recombinant IGHMBP2; I: input/the eluate.

The distribution of 18S and 28S rRNAs in the two different complexes indicated that 80S ribosomes might have dissociated into their subunits under these gradient conditions. To confirm this possibility, cytoplasmic extract was prepared in a low-salt buffer containing Mg^{2+} for ribosome stabilization. The affinity purification was performed as described above and the proteins eluted from the IGHMBP2 column were fractionated through a linear 7-47% (w/v) sucrose gradient. Fractions were collected from the gradient and analyzed by SDS PAGE and silver staining.

7-47% sucrose gradient

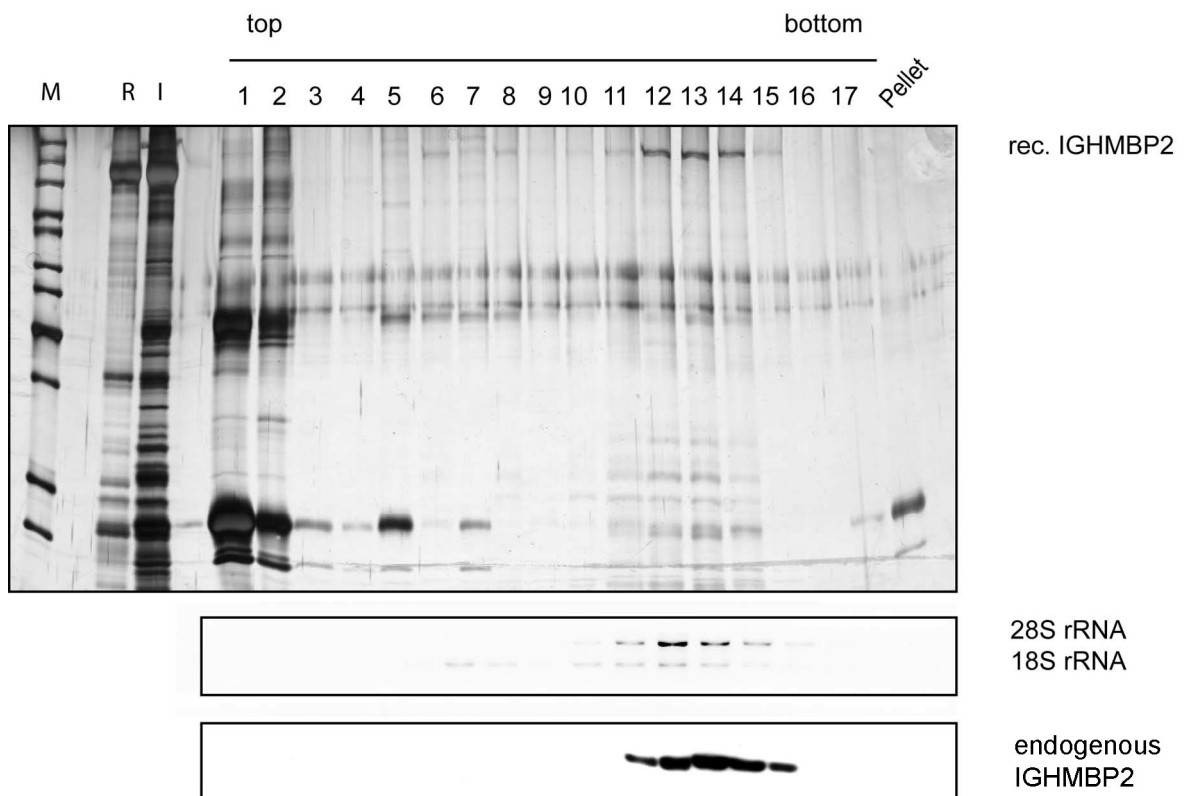


Figure 12. Recombinant IGHMBP2 Binds 80S Monosomes *In Vitro*. GST pull-down was done with FM3A cytoplasmic extract prepared in a Mg^{2+} -containing buffer. The eluate of the IGHMBP2 column was loaded onto a linear 7-47% (w/w) sucrose gradient. Protein of each fraction was TCA-precipitated, separated by 10% SDS PAGE and detected by silver staining. RNAs were isolated from each fraction, separated on 1% agarose gel and visualized by ethidium bromide (middle panel). FM3A cytoplasmic extract was fractionated through a linear 5-30%

(Fig. 12 continued) glycerol gradient parallel to the eluate and the presence of IGHMBP2 in each fraction was determined by Western blot with purified anti IGHMBP2 antibody. M: Marker; R: recombinant IGHMBP2; I: input/the eluate.

In fact, under these conditions, recombinant IGHMBP2 and its interacting proteins migrated as a single complex (Fig 12 fractions 11-15). RNA analysis of each fraction revealed the presence of both 18S and 28S rRNA in this complex, thus indicating that the isolated IGHMBP2 complex contains 80S ribosomes (Fig. 12). Of note, the sedimentation profiles of the purified, eluted complexes correspond to those of endogenous IGHMBP2 in cell extracts under the same conditions (Fig. 12 bottom panel). Collectively, these findings indicate that IGHMBP2 associates with 80S ribosomes. Moreover, under conditions that destabilize ribosomes, IGHMBP2 is still able to bind both 40S and 60S ribosomal subunits. This further also suggests that the complexes purified by this strategy recapitulate those into which endogenous IGHMBP2 is incorporated.

4.3 *In Vivo* Association of IGHMBP2 with Ribosomes

The findings that recombinant IGHMBP2 associates with ribosomes and ribosomal subunits *in vitro* raised the possibility that endogenous IGHMBP2 interacts with ribosomes *in vivo*. In order to prove this hypothesis, cytosolic extracts were prepared using a low-salt buffer containing Mg^{2+} , i.e. a condition known to stabilize 80 ribosomes. This extract was size-fractionated by centrifugation through a linear 5-30% sucrose gradient for 135 minutes. RNAs of each fraction were quantified by absorbance at 254 nm, isolated and separated by 1% agarose gel electrophoresis and was used as size markers for ribosomes and ribosomal subunits. Western blot analysis of each fraction shows that IGHMBP2 migrated to the positions corresponding to those of 80S ribosomes, as indicated by the sedimentation pattern of rRNAs (Fig. 13A).

Since formation and stability of ribosomes require Mg^{2+} , ribosomes can be dissociated into ribosomal subunits and release mRNAs particles in the presence of EDTA. If in fact, IGHMBP2 associates with ribosomes *in vivo*, treatment with EDTA should lead to dissociation of IGHMBP2 from ribosomes and as a consequence change its sedimentation pattern. To test this, 15 mM EDTA was added to the cell extract to chelate bivalent cations

required for 80S formation. Upon ribosomes dissociation with EDTA, a longer sedimentation (4 hours) through a 5-30% sucrose gradient was carried out to get a better resolution for ribosomal subunit separation. The assignment of 28S and 18S rRNAs in two different complexes confirmed the dissociation of ribosomes (Fig 13C bottom panel). Under these conditions, IGHMBP2 co-sedimented predominantly with 40S ribosomal subunits and to a lesser extent with 60S subunits (Fig. 13C upper panel). This result is consistent with the previous observation that IGHMBP2 was present in a complex with 40S and 60S ribosomal subunits *in vitro* (see Fig. 10A and 11). Furthermore, under these centrifugation conditions, endogenous IGHMBP2 from the EDTA-free cell extract co-sedimented with 80S monosomes (Fig. 13C bottom panel), thus suggesting an association of endogenous IGHMBP2 with ribosomes in cellular extracts.

Association of IGHMBP2 with ribosomes and its ribosomal subunits led to a question whether this protein interacts with actively-translating ribosomes or polysomes. To address this question, cytoplasmic extract was prepared from FM3A cells previously treated with cycloheximide for 10 minutes. Cycloheximide is a protein translation inhibitor, which blocks translocation of the ribosomes on mRNAs. As a consequence, ribosomes stall on their mRNAs, leading to the enriched formation of polysomes. The cycloheximide-treated cytoplasmic extract along with the control cytoplasmic extract was fractionated through 20-50% sucrose gradients for 135 minutes. The effectiveness of cycloheximide treatment was controlled by the detection of FMRP (fragile X mental retardation protein), a protein known to preferentially associate with polysomes (Feng *et al.*, 1997). In agreement with the previous findings, FMRP was found predominantly in the polysomal fractions (Fig. 13D mid panel). Likewise, a fraction of IGHMBP2 was clearly detected in the fraction beyond the monosome peak, illustrating polysome-association. However when compared to FMRP, polysome-association of IGHMBP2 was less pronounced (Fig. 13D). Additionally, no difference in the sedimentation pattern of IGHMBP2 was observed in the absence or in the presence of cycloheximide under these sedimentation conditions (Fig. 13D bottom panel). Together, these results indicate that IGHMBP2 preferentially associates with 80S ribosomes but also partially remains bound to actively-translating ribosomes.

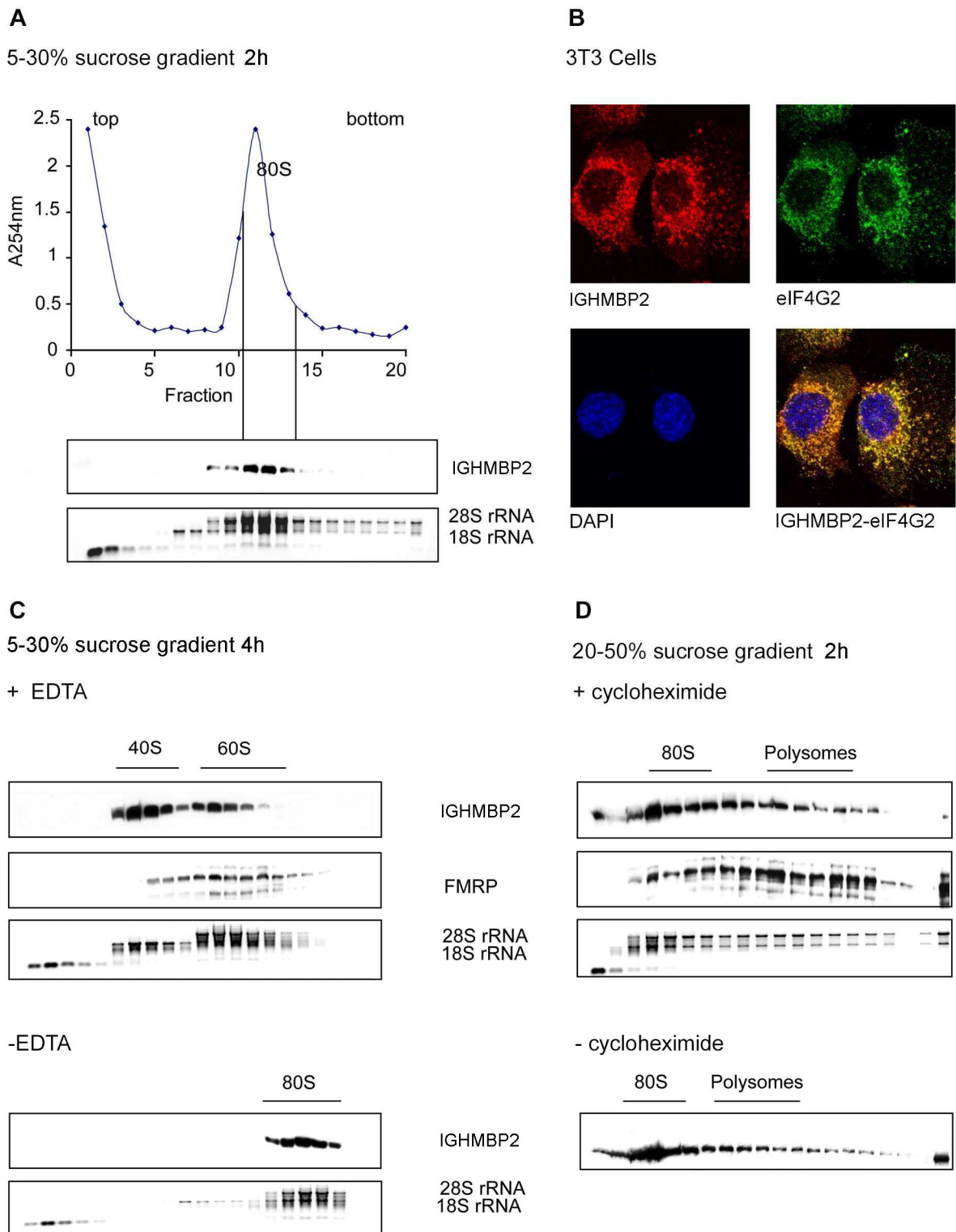


Figure 13. Association of Endogenous IGHMBP2 with Ribosomes. A. FM3A cytoplasmic extract was fractionated through a linear 5-30% (w/v) sucrose gradient for 135 min. 20 fractions were collected and analyzed for RNA and protein. Proteins from each fraction was TCA-precipitated and analyzed by SDS PAGE followed by Western blot with anti IGHMBP2 antibody.

(Fig. 13 continued) Total RNAs were isolated from each fraction and separated by a 1% agarose gel electrophoresis and visualized by ethidium bromide staining. A_{254} was measured from each fraction and the absorbance profile was shown at the top panel. The middle panel shows the sedimentation profile of IGHMBP2; the bottom panel shows the distribution of ribosomal RNAs in correlation to the sedimentation profile. **B.** Co-localization of endogenous IGHMBP2 with translation factor eIF4G2 in the cytoplasm. **C.** IGHMBP2 co-migrated with 40S and 60S ribosomal subunits. EDTA-treated cytoplasmic extract was fractionated through a 10-50% (w/v) linear sucrose gradient containing 15 mM EDTA for 4 hours. FMRP was used as a marker for 60S ribosomal subunits (middle panel). – EDTA (bottom panel): IGHMBP2 co-migrated with 80S ribosomes. **D.** IGHMBP2 is loosely associated with polysomes. Cytoplasmic extract was prepared from FM3A cells previously incubated with cycloheximide for 10 min and directed to a linear 20-50% (w/v) sucrose gradient sedimentation for 135 min along with the control extract (-cycloheximide, bottom panel). The third panel shows the distribution of 18S and 28S rRNA in correlation to the sedimentation profile.

Immunofluorescence studies shown in Fig. 8 (Chapter 4.2.1.1) revealed the cytoplasmic distribution of IGHMBP2 in granular structures, reminiscent to the distribution of the translational machinery. To test whether this pattern indeed reflects a co-localization of IGHMBP2 with components of translational machinery, indirect immunofluorescence studies were performed with anti IGHMBP2 antibody and anti eIF4G2 antibody in the similar manner as described in 3.2.1. Indeed, confocal microscopy analysis of the stained cells shows that IGHMBP2 co-localized with eIF4G2 in the cytoplasm, supporting the finding that IGHMBP2 is associated with protein synthesis machinery (Fig 13B).

4.4 Studies on the Cellular Function of IGHMBP2

Interaction of endogenous IGHMBP2 with ribosomes may reflect the cellular function of IGHMBP2 in cytoplasmic posttranscriptional gene regulation. In emerging views, such processes are exerted through mRNA localization (cytoplasmic compartmentalization and polysomal localization), mRNA turnover (stabilization and destabilization) and mRNA translation. Interestingly, some well-known SF1 helicases, such as Upf1p and yeast MTT1 have previously been shown to associate with polyribosomes and plays a role in mRNA turnover/nonsense-mediated mRNA decay and translation termination, respectively (Atkin *et al.*, 1995; Czaplinski *et al.*, 2000). Taking these data into consideration, in the following studies, pilot experiments were designed and performed to investigate possible roles of IGHMBP2 in mRNA translation and mRNA stability.

4.4.1 Downregulation of Cellular IGHMBP2 by RNA Interference Has No Detectable Effect on Ribosomal Profiles

Given the evidence that IGHMBP2 associates with 80S ribosomes at different functional states, i.e. at the initiation state (80S) and during translation (polysomes), IGHMBP2 may potentially have a role in the initiation step of translation, such as in 80S ribosome assembly. Therefore, a first set of experiments was performed in order to elucidate a role of IGHMBP2 in 80 ribosome assembly. It was suggested that if IGHMBP2 is in fact involved in assembly of 80S ribosomes, reduced cellular levels of IGHMBP2 may lead to alterations in the 80S monosome profile under conditions supporting stabilization of ribosomes. To address this point, cellular IGHMBP2 was down-regulated by RNA interference and the 80S monosome profile was analyzed by using sucrose gradient sedimentation.

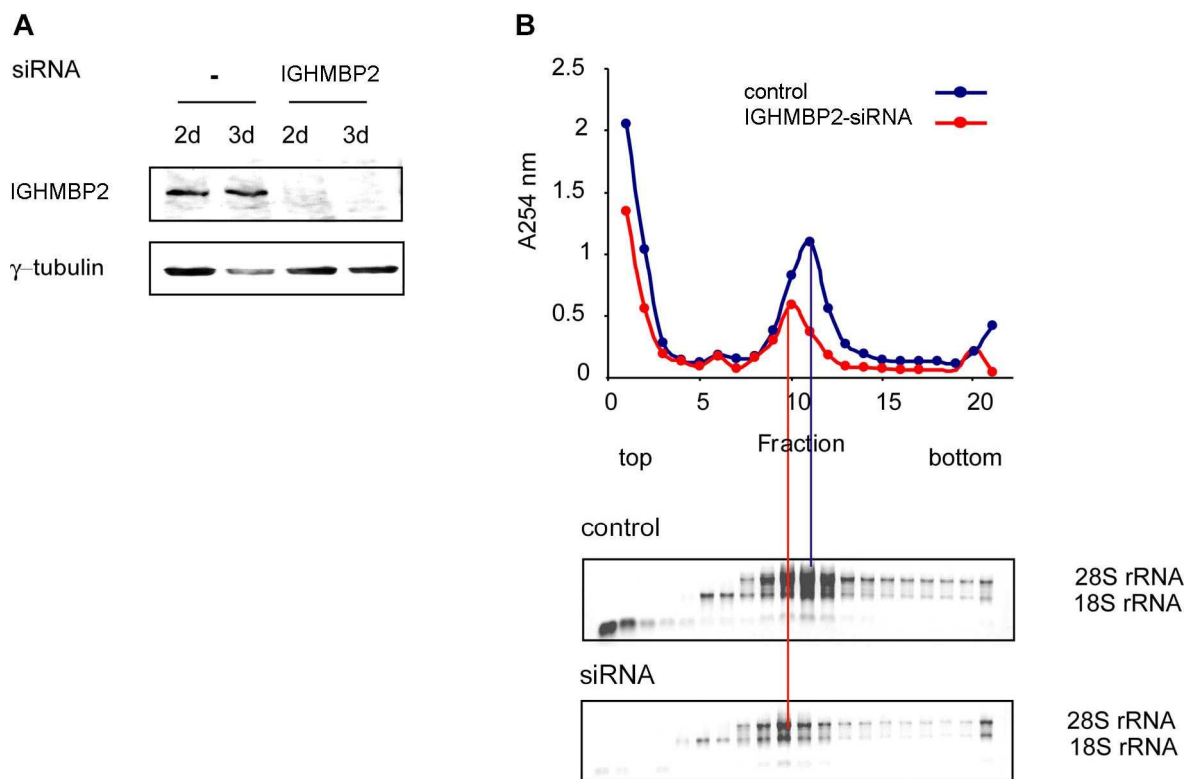


Figure 14. Down Regulation of Endogenous IGHMBP2 Levels by RNA Interference Did Not Affect Ribosomal Profile. IGHMBP2 siRNA was transfected into HeLa cells. At 72 hours after transfections, total lysates were prepared and used for subsequent analysis. **A.** The same amounts

(Fig. 14 continued) of the control and siRNA extracts were loaded on 10% SDS polyacrylamide gel and directed to immunoblotting analysis for IGHMBP2 (top) and γ tubulin for loading control (bottom). **B.** Total extract of the siRNA-treated cells as well as control cells was analyzed by size fractionation through linear 5-30% sucrose gradients for 2h. RNA was isolated from each fraction and separated on 1% agarose gel (bottom panel). Ribosomal profiles were obtained by plotting the absorbance A_{254} in each fraction against the fraction numbers (upper panel).

In this study, small interfering RNAs (siRNA) were designed against a sequence of the coding region of human IGHMBP2 and transfected into HeLa cells. Transfected cells were cultivated and harvested after 24 h, 48 h and 72 h. During these incubation periods, no remarkable changes were observed in the morphology and growth properties of the siRNA-treated cells in comparison to the non-transfected cells (data not shown). Total extracts were then prepared from the siRNA-transfected HeLa cells as well as from the control cells. The efficiency of siRNA treatment was evaluated by a Western blot analysis, which demonstrates that the protein level of IGHMBP2 was reduced by approximately 80% at 72 hours upon siRNA transfection (Fig. 14A). Extracts derived from these cells were subsequently size-fractionated on a linear 5-30% (w/v) sucrose gradient by ultracentrifugation, as described in Chapter 4.3. 20 fractions were collected and the absorbance at 254 nm was measured from each fraction and plotted against the fraction numbers (Fig 14B upper panel). Total RNAs were isolated from the gradient fractions and analyzed by agarose gel electrophoresis. As shown in Fig. 14C, although rRNAs levels were reduced in the siRNA-treated cells, the sedimentation profile of 80S ribosomes derived of the siRNA-treated cells appeared similar to the control cells. The basis of the observed difference in rRNAs level between siRNA-treated and control cells is not clear but might be due to slowed growth of the transfected cells. In conclusion, these results demonstrate that decrease in cellular level of IGHMBP2 has no effect on the 40S and 60S joining to form initiating 80S ribosomes.

4.4.2 Reduced Expression of IGHMBP2 by RNA Interference Did Not Effect Global Protein Synthesis

The previous experiment implies that IGHMBP2 may not play a major role in the 80S formation. Nevertheless roles in other aspects of translation cannot be excluded. Next it was investigated whether IGHMBP2 can affect the translational output of a cell and thus

behaves like a translation factor. To analyze this possibility, endogenous IGHMBP2 was down-regulated by RNA interference and its effect on protein synthesis was analyzed by radioactive pulse labeling of newly synthesized proteins.

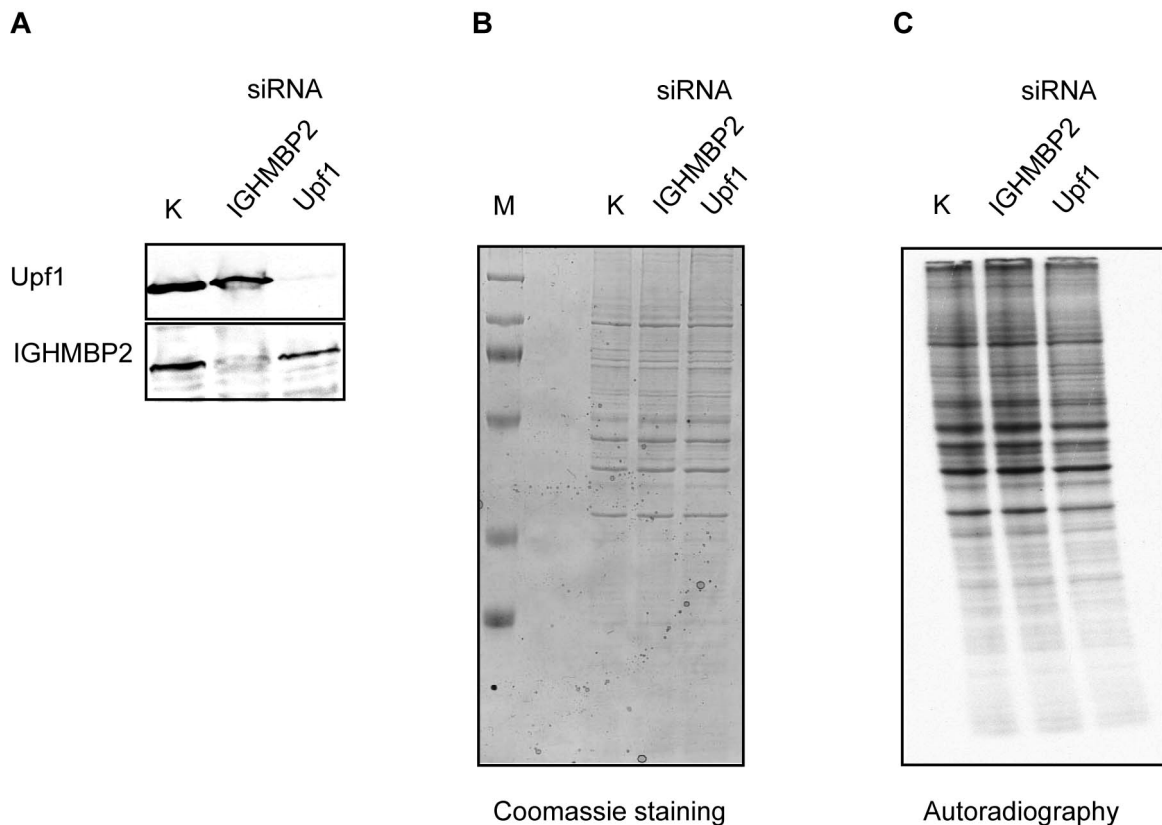


Figure 15. Reduction of Endogenous IGHMBP2 Levels Has No Effect on Global Protein Synthesis. HeLa cells were transfected with siRNA against IGHMBP2. 72 hours after transfection, cells were pulse-labeled with S^{35} methionine for 1 hour, and total extracts were prepared and separated by SDS PAGE. **A.** Equivalent amounts of each extract was separated and directed to Western blot analysis. **B.** The loading of total extract was visualized by Coomassie staining. **C.** The gel in B was dried and subjected to Autoradiography.

RNAi experiments were performed in the similar manner as mentioned in 4.4.1. At 72 h after siRNA transfection, cells were pulse-labeled with S^{35} -methionine for one hour and the synthesis of proteins was analyzed by SDS PAGE and visualized by autoradiography. Figure 15B shows that an equivalent amount of cell extracts were loaded on the gel. As shown in Fig. 15A, 72 hours after transfection, the siRNA against IGHMBP2 reduced the cellular protein by approximately 50%. However, under this condition, the overall cellular

translation output appeared not to be altered (Fig. 15C). Specifically, the intensity of ^{35}S -methionine labeled proteins was largely equivalent in the control lysates and the siRNA-treated lysates (Fig. 15C). Moreover, the same result was also obtained when the pulse of ^{35}S -methionine was extended to 3 hours (data not shown). These data suggest that IGHMBP2 has no effect on global protein synthesis.

4.4.3 Tethering IGHMBP2 to Reporter mRNA Increases the Abundance of the Reporter mRNA

In light of the studies described above, it seems unlikely that IGHMBP2 modulates the formation of 80S monosomes and global translation pathway. The next hypothesis to be tested was whether IGHMBP2 has a role in mRNA degradation or stabilization. This question was approached experimentally by a tethering system previously applied to identify factors involved in mRNA turnover. As shown in this study, tethering a fusion protein with the bacteriophage RNA-binding proteins, the MS2 coat protein or the lambda N (λN) peptide, to the 3' UTR of a reporter β -globin mRNA elicits degradation reporter mRNA via nonsense-mediated mRNA degradation (NMD) pathway, thus recapitulating NMD pathway (Lykke-Andersen *et al.*, 2000; Gehring *et al.*, 2003). Using this reliable system, the potential involvement of IGHMBP2 in NMD was investigated. For these experiments, a set of MS2- and λN -based tethering reporters was generated (Fig. 16). The coding sequence of IGHMBP2 was fused to the C-terminus of an MS2 coat polypeptide or to the C-terminus of λN peptide. The mRNA reporter plasmid contains the wild-type human β -globin mRNA with either 6MS2 binding sites or 4 λN peptide binding sites (termed as BoxB) in its 3' UTR at a position where an intron induces NMD of a transcript with a normal open reading frame (Fig. 16).

The expression plasmid containing MS2 or λN -tagged IGHMBP2 was co-transfected into HeLa cells with the corresponding β -globin mRNA reporter plasmid. Expression levels were controlled by inclusion of a third vector containing β -globin mRNA with extended 3' UTR without reporter binding site (wt300+e3). To evaluate the efficiency of the tethering systems applied in this study, the known NMD factors, namely Upf1, Upf2 and Upf3b were expressed as MS2 or λN fusion proteins and utilized as positive controls. At 48

hours after transfection, RNAs and proteins were extracted from transfected cells and subjected to Northern blot and Western blot analysis, respectively (Fig. 17 middle-and bottom panels).

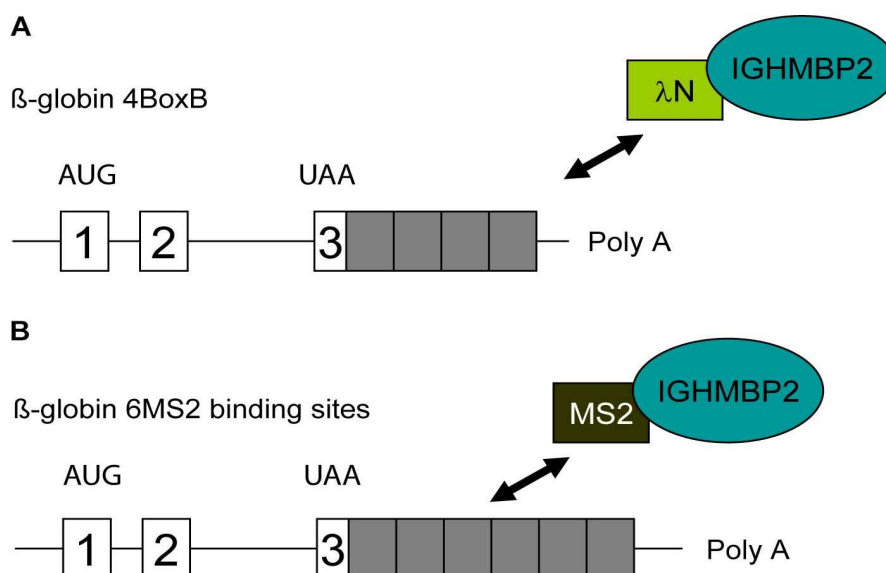


Figure 16. Schema of Basic MS2- and λ N Peptide-Based Tethering Systems. The β -globin gene contains either (A) 4 RNA binding sites for λ N (BoxB) or (B) 6 MS2 binding sites in its 3'UTR. The coding sequence IGHMBP2 was fused to the C-terminus of MS2 coat polypeptide or of λ N peptide. Position of start codon (AUG) and stop codon (UAA) was indicated above.

The mRNA expression level was determined by quantifying the signal intensity of mRNAs detected on Northern blot and is shown in a graphic representation. Consistent with previous reports, the co-expression of λ N-or MS2-tagged NMD proteins with the corresponding β -globin mRNA reporter induced a specific reduction of the mRNA reporter level (Fig. 17A and B top panel) (Gehring *et al.*, 2003). In contrast to the NMD-proteins, tethering IGHMBP2 to the reporter mRNA increased mRNA level by 1.4 and 1.3 fold in the λ N- and MS2-reporter system, respectively. These results show that IGHMBP2 does not induce a specific-degradation of mRNA in this assay. Rather, these suggest that IGHMBP2 has the opposite effect, namely the stabilization of bound mRNA. Further studies would be needed to elucidate, whether this is indeed a function of endogenous IGHMBP2 (see Chapter 5 Discussion, 5.2.2).

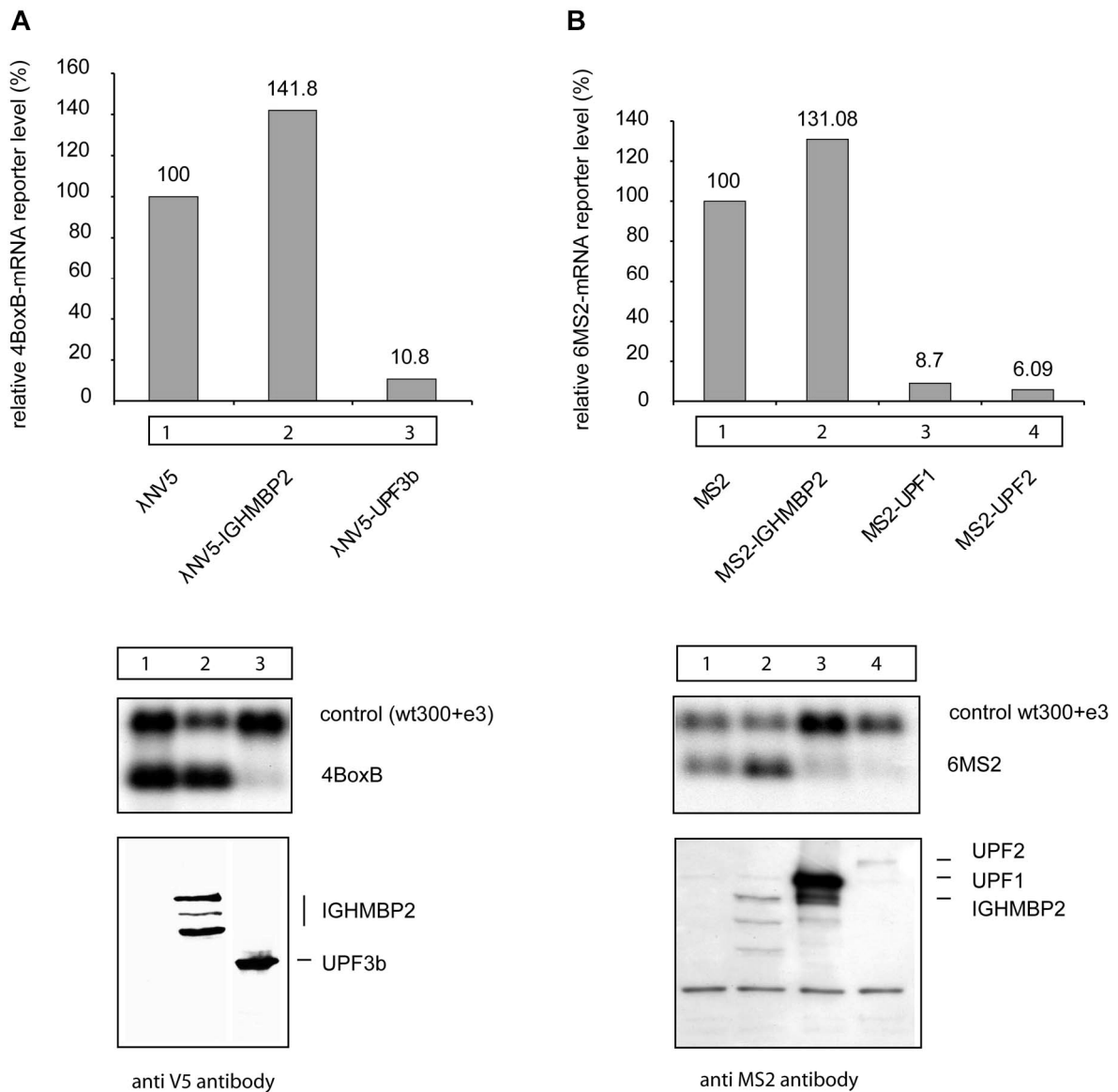


Figure 17. Tethering IGHMBP2 to the β -globin mRNA 3' UTR Increases the β -globin mRNA Level. **A.** λ N peptide-based tethering assay. HeLa cells were cotransfected with reporter plasmid containing β -globin MS2 and plasmids expressing λ N peptide-IGHMBP2 (lane 2), or λ N-UPF3b (lane 3) or plasmids producing λ peptide coat protein alone (lane 1). The third plasmid control plasmid (wt300+e3) was co-transfected to evaluate the efficiency of mRNA expression. Total HeLa cytoplasmic RNA was prepared 48 hr after transfection, fractionated in an 1.2% formaldehyde containing agarose gel, and probed with an antisense β -globin cRNA after transfer to a nylon membrane (middle panel). The radioactive signal intensities of RNA band were quantified by phosphorimager with the relative steady state level of the mRNA normalized to the internal control (wt300+e3) and to the corresponding control experiment (λ peptide coat protein alone), in which mRNA levels were set at 100% (shown as a graphic, top panel). The expression level of or λ N- tagged proteins was analyzed by Western blotting with anti V5 (bottom panel). **B.** MS2-based tethering assay, performed as A. HeLa cells were co-transfected with reporter plasmid containing

(Fig. 17 continued) β -globin MS2 peptide as well as plasmids expressing MS2-IGHMBP2 (lane 2) or MS2-UPF1 (lane 3) or MS2-UPF2 (lane 4) or plasmids producing λ peptide coat protein alone (lane 1). Proteins were analyzed by Western blotting with anti MS2 antibody.

4.5 Biochemical Analysis of Pathogenic IGHMBP2 Variants

Biochemical studies described in this study have characterized IGHMBP2 as a ribosome-associated helicase. As the disease gene product of neuromuscular disorder SMARD1, it was therefore of importance to investigate the link between the biochemical activities of IGHMBP2 and the pathophysiology of the disease. The fact that SMARD1-related mutations in IGHMBP2 are located within or adjacent to the putative helicase motifs and involve evolutionary conserved amino acid residues (Grohmann *et al.*, 2001; 2003; Guenther *et al.*, 2007a) suggests that the helicase/ATPase activity of IGHMBP2 may be affected in SMARD1. Prompted by the biochemical data described above and the genetic data of SMARD1 patients, the following studies were aimed to analyze the influence of pathogenic missense mutations on the enzymatic activities and functional association with ribosomes.

4.5.1 ATPase and RNA Unwinding Activities of Pathogenic IGHMBP2 Variants

As an initial step to gain insight into the link between the malfunction of IGHMBP2 and the disease, nine pathogenic IGHMBP2 variants carrying missense mutations were investigated for their enzymatic activities. These mutations were chosen based on their position in, or directly adjacent to, motifs described to be essential in distinct steps of catalysis by helicases (Fig. 18A). Eight IGHMBP2 mutant proteins contain a single point missense mutation which lies within or adjacent to the putative helicase motifs and target highly conserved residues (Q196R/a conserved glutamine residue upstream of motif I, T221A/motif I, C241R/motif Ia, E382K/motif II, H445P/motif III, D565N/motif V, N583I/motif V, R603H/motif VI). One mutation, namely T493I, is not located in close proximity to any helicase motif (between the motif IV and V), but was chosen because it was identified in two SMARD1 patients with a variable onset of the disease (Guenther *et al.*, 2007b). The pathogenic IGHMBP2 variants were bacterially-expressed as recombinant protein with an N-terminal GST and C-terminal 6His tags and purified in the same manner as described for wild-type IGHMBP2 (Fig. 18B, Fig. 4 and Chapter 4.1.2).

The purified proteins were analyzed by SDS PAGE and visualized by silver staining. As shown in Fig. 18B, using the expression and purification protocol described in 4.1.2, the recombinant mutant proteins were obtained in comparable purity to the wild-type protein. Expression and purification of IGHMBP2 was performed by Ulf Günther, collaborator in this study.

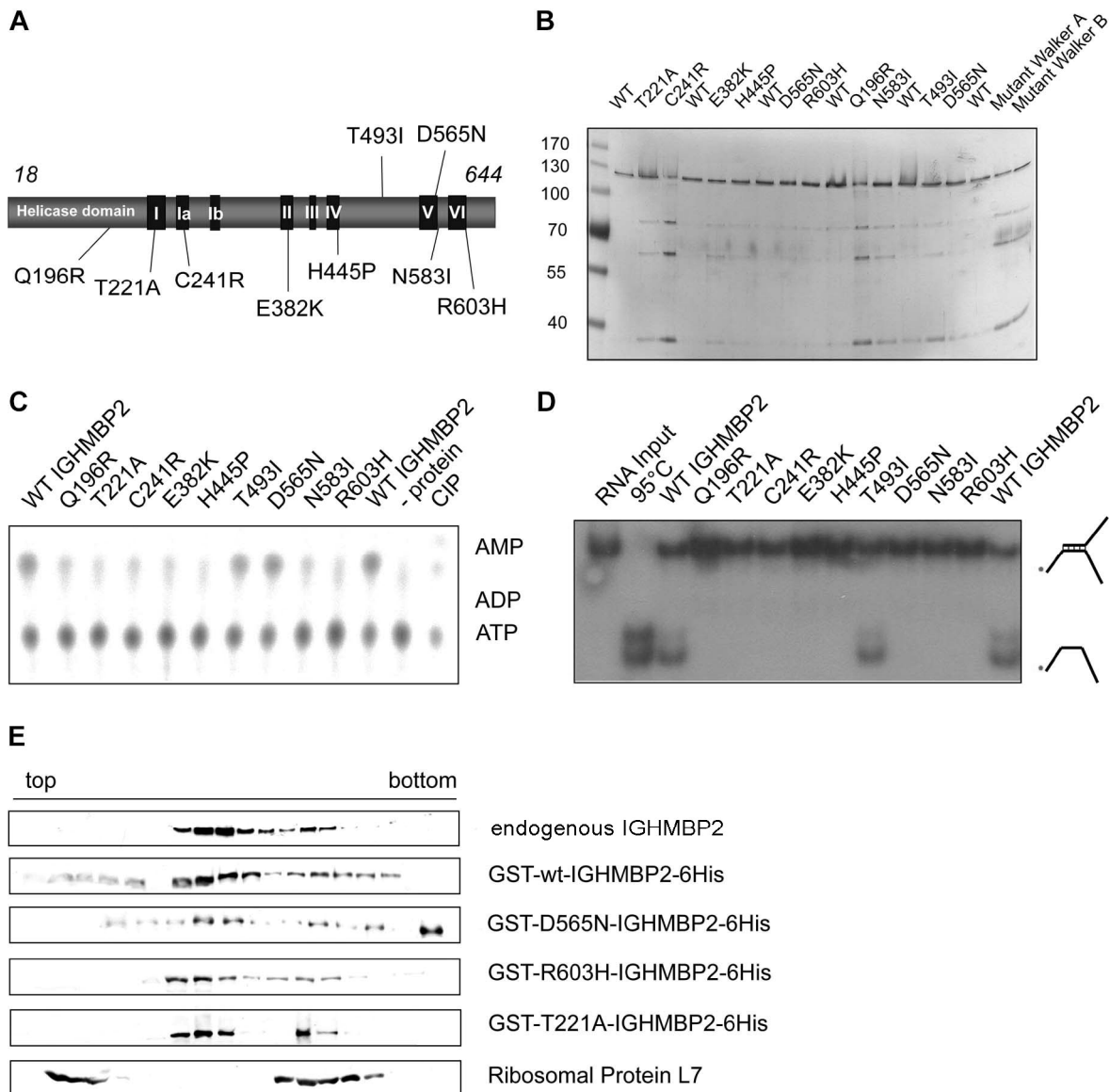


Figure 18. Biochemical Characterization of Pathogenic IGHMBP2 Variants. A. A schematic representation of nine SMARD1- related missense mutations used in this study. Eight missense mutations are located within or adjacent to the conserved helicase motifs of IGHMBP2.

(Fig. 18 continued) One mutation (T493I) is not in the close proximity to any helicase motif. **B.** Expression and purification of recombinant IGHMBP2 mutants. IGHMBP2 protein mutants were expressed and purified as described for wild-type IGHMBP2 (see Fig.4 and 5). **C.** Analysis of ATP hydrolysis activity of recombinant IGHMBP2 mutant. The ATPase assay was done in the presence of poly (A) as described in Fig.5. The products of ATP hydrolysis were identified by comparison with those generated by calf intestinal phosphatase (CIP, last lane). **D.** RNA unwinding activity of pathogenic IGHMBP2 variants. The RNA duplex containing 5' and 3' overhang was incubated with the recombinant mutant proteins and analyzed by native RNA gel electrophoresis, as described in Fig. 6. The [³²P]-RNA duplex in the absence of protein is shown in lane 1. The positions of duplex and single-stranded RNA are indicated. **E.** Sedimentation profile of pathogenic IGHMBP2 in cellular extracts. Three pathogenic IGHMBP2 mutants were incubated with cytoplasmic extracts and assayed by linear 5-30% glycerol gradient sedimentations as described previously in Fig 11. Protein of each fraction was TCA-precipitated and analyzed by Western blot analysis. Recombinant protein was detected by purified anti GST antibody.

The recombinant mutant proteins were initially tested for their ability to hydrolyze ATP in comparison to wild-type IGHMBP2. In the experiments performed by Ulf Günther (collaborator in this study), the proteins were incubated with α - [³²P]-ATP in the presence of poly (A) and subsequently analyzed by thin layer chromatography as described in 4.1.2. ATP hydrolysis activity of the proteins was indicated by the appearance of α -[³²P]-ADP as the product of hydrolysis. As shown in Fig. 18 lane 12 (-/without protein), incubation of radioactively labeled ATP with poly (A) alone produced background level of α -[³²P]-ADP. The previous result shows that ATPase activity of IGHMBP2 is stimulated in the presence of poly (A) (Fig. 6C). Consistently, in this assay, the wild-type protein displayed poly (A)-stimulated ATPase activity (Fig. 18C lane 1 and 11). By contrast, seven out of nine mutants (Q196R, T221A, C241R, E382K, H445P, N583I and R603H) exhibited only background level activity (Fig. 16C). Two mutants, namely D565N and T493I, still hydrolyzed ATP as efficiently as the wild-type protein (Fig. 18C).

Having investigated the ATPase activity of the recombinant mutant proteins, the next question was whether defect in ATPase activity of some mutants protein consequently affect RNA unwinding activity of the mutants. To address this question, the radioactively-labeled synthetic partial complementary RNA duplex containing 5' and 3' overhangs was incubated with the mutants in the presence of ATP. The single-stranded RNA unwinding product was examined by native RNA gel electrophoresis in the similar manner as mentioned in 4.1.3. Strikingly, all mutants deficient in ATPase activity were also defective in RNA unwinding (Fig. 18D). Mutant T493I which was still able to hydrolyze ATP could

also unwind the RNA substrate in this experiment. These findings are consistent with the fact, that helicase activity requires energy produced by hydrolysis of an ATP to unwind substrate. Nevertheless, one mutant namely D565N was completely inactive in the helicase activity, while it displayed an ATPase activity. Taken together, these data indicate that SMARD1-related missense mutations in or adjacent to critical catalytic motifs of IGHMBP2 reduce its enzymatic activity. Moreover, these observations support the hypothesis that the helicase activity of IGHMBP2 may be impaired in SMARD1 patients. Surprisingly, one pathogenic variant harboring T493I mutation seems to display enzymatic activity comparable to the wild-type protein. The T493I mutation is not located in the close proximity to any conserved helicase motif (Fig. 18A) and consequently exhibited neither defect in ATPase nor helicase activities. However, this mutation has been recently shown to affect the stability of IGHMBP2, hence providing an explanation for its pathogenicity (Guenther *et al.*, 2007b). The above mentioned experiments were performed by Ulf Günther, collaborator in this study.

4.5.2 Association of Pathogenic IGHMBP2 Variants with Ribosomal Subunits

The enzymatic characterization of pathogenic IGHMBP2 variants shows that missense mutations located adjacent to, or in conserved helicase motifs lead to loss of helicase/ATPase activities. In a continuing effort to better understand the biological behavior of pathogenic IGHMBP2 variants in living cells, effect of missense mutations on association of IGHMBP2 with ribosomes was biochemically explored by sedimentation through a glycerol gradient. Three variants, namely D565N (no helicase activity but ATPase activity, T221A (no helicase and no ATPase activities) and R603H (no helicase and no ATPase activities) were chosen for this study and expressed as described above. In this case, the GST tag was not cleaved from the recombinant protein, thus allowing for protein detection by anti GST antibody to differentiate the recombinant from the endogenous protein on Western blot. The mutant proteins along with the wild-type protein were incubated with FM3A cytoplasmic extract and their incorporation into ribosomes was analyzed by linear 5-30% (v/v) glycerol gradient ultra centrifugations as mentioned in 4.2.2. Western blot analysis of the gradients shows no significant differences in the sedimentation profile of the wild-type and mutant IGHMBP2 proteins (Fig. 18E). Hence,

mutations in the helicase domain of IGHMBP2 and loss of its enzymatic activities appear not to have effect on association of the protein with ribosomal subunits. Furthermore, these results suggest that the pathogenic missense-mutations do not cause an overall misfolding of IGHMBP2 but rather specifically affect its catalytic activity.

5. DISCUSSION

Mutations in the gene encoding IGHMBP2 are responsible for the infantile motor neuronal disorder “SMARD1” (Grohmann *et al.*, 2001). Despite intensive studies in the past years, only little was known about the enzymatic properties of this protein, its cellular function and the affected cellular pathway in the disease. Hence, it was a major goal of this study to link IGHMBP2 to a specific cellular pathway and to unravel a connection between its malfunction and SMARD1. The studies presented here describe the enzymatic properties of IGHMBP2 as an ATP-dependent helicase capable of unwinding RNA and DNA helices in 5'→3' polarity. Furthermore, the identification of IGHMBP2 as a ribosome-associated factor provides insights into potential roles of IGHMBP2 in mRNA translation or turnover. Lastly, biochemical studies on SMARD1-causing IGHMBP2 variants were conducted, which have revealed defects in their enzymatic properties. Based on these data, a model of how mutations in IGHMBP2 cause SMARD1 will be put forward.

5.1 Enzymatic Properties of IGHMBP2

5.1.1 IGHMBP2 Is an ATP-dependent 5'-3' DNA/RNA Helicase *in Vitro*

Based on protein sequence homology analysis, IGHMBP2 has been classified as a member of the helicase Superfamily 1 (SF1). This protein contains an N-terminal helicase domain with 7 conserved helicase motifs commonly found in this class (Czaplinski *et al.*, 2001; Koonin 1992). Unlike other well-known members of this family, such as Upf1 and Sen1p, which display DNA/RNA helicase activity *in vitro* (Czaplinski *et al.*, 1995; Kim *et al.*, 1999; Biswas *et al.*, 1995), previous studies by Biswas *et al.* (2001) and Molnar *et al.* (1997) have demonstrated exclusive DNA unwinding activity for IGHMBP2.

In this study, a two-step purification strategy was established, which allowed for the production of bacterially-expressed recombinant IGHMBP2 to near homogeneity and in an enzymatically-active state (Fig. 5 and below). Two lines of evidence suggest that wild-type IGHMBP2 purified in this manner is correctly folded and biologically active. First,

recombinant IGHMBP2 is incorporated into the same complexes as the endogenous protein in cellular extracts (Fig. 11 and 16E, data not shown). Second, the recombinant protein is able to hydrolyze ATP, indicating its intrinsic catalytic activity, as has been described for the endogenous protein previously. Purification of recombinant IGHMBP2 in its active state has supplied ample material for detailed investigations on its enzymatic activities as a helicase. To control for the specificity of the enzymatic characterization, all studies were evaluated by investigating the IGHMBP2 mutants of Walker A and B. Indeed, in contrast to the wild-type protein, these mutant proteins have no intrinsic enzymatic activities, confirming the specificity of the enzymatic studies here.

Helicases are generally thought to couple the energy of NTP binding and hydrolysis to promote displacement of duplex nucleic acids (reviewed in Tanner and Linder, 2001). Consistent with this view, IGHMBP2 can specifically hydrolyze ATP and unwind both RNA and DNA duplexes in an ATP-dependent manner (Fig. 6 and 7). Further analysis of the helicase polarity showed that IGHMBP2 unwinds nucleic acid duplexes in a 5'→3' direction (Fig. 7). Similar to other members of the SF1, namely Sen1p and Upf1p (Czaplinski *et al.*, 1995; Bhattacharya *et al.*, 2000), IGHMBP2 possesses very low intrinsic ATPase activity but the presence of various homo- and hetero polymers of DNA or RNA (poly (A), poly (C), poly (U)) can enhance this activity to a great extent. This result suggests that ATP hydrolysis of IGHMBP2 is highly cooperative with its nucleic acid binding activity. Interestingly, not all RNAs tested in this assay had the same stimulatory effect. In fact, poly (G) completely failed to increase the ATPase activity of IGHMBP2. The basis for this is not yet clear. However, assuming that binding of the nucleic acid to IGHMBP2 may provoke a conformational change required for stimulation of its ATPase activity; it is tempting to speculate that poly (G) is not able to bind IGHMBP2 and therefore could not elicit stimulation. Nevertheless, the hypothesis remains to be clarified, whether poly (G) in fact has no or less binding affinity to IGHMBP2 than other homopolymeric RNAs.

It is important to note that other groups obtained data that are in part in conflict with those of this study. According to Molnar and coworkers, IGHMBP2 unwinds the DNA duplex in a 3'→5' direction and is capable to hydrolysis not only ATP but also GTP. It is reasonable to speculate that two major reasons account for these differences. First, these

authors used markedly different conditions for their studies, including buffer composition, source and concentration of the protein and substrate. In fact, it has been shown previously for helicases such as eIF4A that their enzymatic activity can be dramatically influenced by buffer conditions. Furthermore, the helicase activity of eIF4A is also affected by the substrate stability and minimally dependent of the length of the single-stranded region adjacent to the duplex region of the substrate (Lorsch and Herschlag, 1998, Rogers *et al.*, 1999; 2001). Second, it is also noteworthy that IGHMBP2 analyzed by Molnar and coworkers was isolated from cell extracts using anti IGHMBP2 antibodies. It is likely that several other cellular components were co-purified with this approach, which might have influenced the enzymatic studies performed by this group. Such potential “contamination artifacts” can be excluded in the study presented here, as two enzymatically-inactive mutants of IGHMBP2 have been used as controls.

5.1.2 IGHMBP2 Might Function as RNA Helicase Rather than DNA Helicase in Living Cells

The enzymatic studies of recombinant IGHMBP2 have shown that IGHMBP2 can function as an RNA helicase as well as a DNA helicase *in vitro*. Generally, helicases exhibit very little substrate specificity when analyzed *in vitro* and their specificity might be conferred by the presence of additional domains and/or interactions with cofactors (Wang and Guthrie 1998). Other members of SF1, such as Upf1p and Sen1p have been characterized as DNA and RNA helicase *in vitro*, but it is now believed that they act solely in RNA metabolic processes *in vivo* (Ursic *et al.*, 2004; Gehring *et al.*, 2003). Several lines of evidence obtained in this study argued for a role of IGHMBP2 as an RNA-specific helicase *in vivo*. First, the cytoplasmic localization of IGHMBP2 (Fig. 8A) gives an indication that IGHMBP2 may favor RNA rather than DNA in living cells. Second, endogenous IGHMBP2 is associated with other cellular components in large RNPs (Fig. 8B and see below), indicating that IGHMBP2 may interact with cellular RNAs either directly or via other proteins.

Since cellular RNAs are commonly associated with proteins, RNA helicases are most likely to encounter RNA-protein complexes (RNPs) rather than RNA duplex. Consistent

with this view, some DExH RNA helicases have recently been reported to displace protein from RNA-protein complex *in vitro* as well as *in vivo* and this activity does not necessarily require RNA unwinding (reviewed in Jankowsky and Bowers, 2006; Fairman *et al.*, 2004). It would be thus of interest to examine whether IGHMBP2 is likewise able to displace protein from RNA-protein complex. This could provide further insight into the action of IGHMBP2 as an RNA helicase in a physiological context.

5.2 Characterization of the Cellular Function of IGHMBP2

5.2.1 IGHMBP2 is a Ribosome-Associated Protein

Despite intense studies in the past few years, the precise role of IGHMBP2 was only poorly understood. Previous studies have demonstrated that IGHMBP2 is ubiquitously expressed and highly conserved among vertebrates (Grohmann *et al.*, 2004; Uchiumi *et al.*, 2004; Mohan *et al.*, 1998; Cox *et al.*, 1998; Shieh *et al.*, 1995; Mizuta *et al.*, 1993; Fukita *et al.*, 1993; Kerr and Khalili 1991), thus suggesting that IGHMBP2 fulfills “house keeping” functions. In accordance with this notion, IGHMBP2 was found in the cytoplasm in various mouse and human cell lines in this study (Fig. 8A, data not shown). In a continuing effort to elucidate the cellular pathway, to which IGHMBP2 is linked, experiments were designed to identify the interacting partners of endogenous IGHMBP2. These studies indicate that IGHMBP2 associates with ribosomes in various cell types, of neuronal origin (mouse embryo brain tissue) or non-neuronal origin (mouse 3T3 and FM3A cells, rat PC12 cells) (Fig. 8B and C, data not shown).

The specific interaction of IGHMBP2 with ribosomes is supported by a series of *in vivo* and *in vitro* experiments. First, IGHMBP2 co-localizes with one of the components of the translation machinery, the initiation factor IF4G2, in the cytoplasm (Fig. 13B). Second, glycerol gradient analysis of endogenous IGHMBP2 in cytoplasmic extracts revealed the presence of IGHMBP2 in two RNase-sensitive peaks, corresponding to the 40S and 60S ribosomal subunits (Fig. 8). Third, investigation using three different sets of conditions that alter the polyribosomal profile in sucrose gradients also lends support to the notion that IGHMBP2 preferentially interacts with 80S ribosomes and only loosely with polysomes. In the presence of cycloheximide, cellular IGHMBP2 was found at a high

level in the 80S ribosome fractions and only at low level in the polysomal fractions (Fig. 13D). When cycloheximide was omitted, most of IGHMBP2 accumulated in fractions coincident with 80S monosomes (Fig. 13A). Furthermore, when polyribosomes were dissociated to monomers and ribosomal subunits in the presence of EDTA, IGHMBP2 co-migrated with 40S and 60S ribosomal subunits (Fig. 13C). Fourth, *in vitro* binding assays using GST-tagged IGHMBP2 in cell extracts demonstrated that cellular ribosomal proteins and ribosomal RNAs were specifically bound by recombinant IGHMBP2 (Fig. 10). Fifth, size-fractionation of the purified IGHMBP2-ribosome complex showed that IGHMBP2 was associated with 80S monosomes under conditions stabilizing ribosomes and with 40S and 60S ribosomal subunits under conditions promoting ribosome dissociation (Fig. 11 and 12). Taken together, these findings strongly suggest that IGHMBP2 associates with the cellular protein synthesis machinery.

These data are in obvious conflict to studies performed by others. Specifically, IGHMBP2 had previously been implicated in DNA transcription (Shieh *et al.*, 1995) and pre-mRNA splicing (Molnar *et al.*, 1997), two cellular processes that occur exclusively in the nucleus. While this work was in progress, several experimental findings by others raised serious doubt about the role of IGHMBP2 in these nuclear functions. First, IGHMBP2 could not be detected in proteomic profiles of spliceosomes, although their isolation has made a major leap in the past years, (Zhou *et al.*, 2002; Rappsilber *et al.*, 2002). Second, IGHMBP2 is primarily located in the cytoplasm including cell bodies, axons and growth cones of mouse spinal motor neurons and was detected at low levels in the nucleus, thus suggesting its cytoplasmic function (Grohmann *et al.*, 2004). Furthermore, immunofluorescence studies in differentiated rat PC12 cells revealed the co-localization of IGHMBP2 with rRNAs in the cytoplasm (data not shown). It is therefore currently unclear whether IGHMBP2 is involved in any other cellular pathway except for the one described here.

5.2.2 IGHMBP2 Is Linked to Gene Regulation at the Level of Translation

The specific association of IGHMBP2 with ribosomes raises the interesting possibility that this protein has a role in cytoplasmic post-transcriptional gene regulation. This could occur

at several levels and in different pathways, including assembly of the translation machinery or translation, stability and localization of mRNA. In fact, a large number of cytoplasmic RNA helicases, including members of the SF1 and SF2/DEAD box helicases, are known to be involved in initiation, termination of translation and in RNA decay pathways, (i.e. as nonsense-mediated mRNA decay, 5' mRNA degradation by 5'-3' exonuclease and 3' mRNA decay by exosome complex) (reviewed in de La Cruz *et al.*, 1999). Therefore, potential roles of IGHMBP2 in those processes have been considered.

5.2.2.1 IGHMBP2 Might Not Be Involved in General Translation Pathway

The process of translation can be divided into the three phases, initiation, elongation and termination. Several RNA helicases have been implicated in the initiation and termination of translation, such as the DEAD box helicases, eIF4A and Dbp5, respectively (Rogers *et al.*, 2001; Gross *et al.*, 2007). By contrast, no helicase described so far is required for the elongation of translation. Translation initiation represents all processes involving assembly of 80S ribosomes at the start codon on the mRNA template (reviewed in Preiss and Hentze 2001). Given the fact that IGHMBP2 preferentially associates with 80S ribosomes and it co-sediments with 40S and 60S ribosomal subunits when polyribosomes are disaggregated, it was likely that IGHMBP2 participates in the assembly of 80S ribosomes. However, upon reduction of the cellular level of IGHMBP2 by RNA interference, normal levels of 80S ribosomes could still be observed (Fig. 14), thus making the hypothesis unlikely that IGHMBP2 contributes to the assembly of 80S ribosomes.

The biochemical data obtained here also gave rise to the idea that IGHMBP2 might function as a general translation factor and this was addressed experimentally. Downregulation of IGHMBP2 by RNA interference, however, had no significant effect on global translation (Fig. 15). It is nevertheless possible that only a subset of cellular mRNAs requires IGHMBP2 for efficient translation and that these mRNAs have eluded detection in the assays applied here. Potential “substrates” for IGHMBP2 in translation may be mRNAs with very strong tendencies to form secondary and tertiary structures and/or to interact with mRNA binding proteins in a tight manner. Such mRNAs can only

be detected by a proteomic approach which has already been initiated to identify candidate targets.

5.2.2.2 A Potential Role of IGHMBP2 in mRNA Stability

In context of this work, it was also considered that IGHMBP2 could have a role in mRNA turnover/degradation rather than translation itself. Two general mRNA degradation pathways have been described so far in yeast and mammals, namely deadenylation/decapping-dependent 5' mRNA decay by Xrn1 (5'-3' exonuclease) and 3' degradation by the exosome complex (Mitchell and Tollervey, 2000; Anderson and Parker, 1998). Some RNA helicases have previously been reported to function as key players in mRNA degradation mechanisms, for example the DEVH box RNA helicase Ski2 as a component of the exosome and the DEAD box helicase Dhh1 for decapping (reviewed in Long and McNally, 2004; Anderson and Parker, 1998). RNA can also be degraded in the nonsense-mediated mRNA decay (NMD) pathway that selectively targets mRNAs containing premature termination codons (PTCs) (reviewed in Chang *et al.*, 2007). Interestingly, a member of the SF1 helicase, Upf1, together with other RNA-binding proteins Upf2 and Upf3 appears to constitute the core NMD machinery.

A potential role of IGHMBP2 in mRNA turnover was initially examined using a reporter λ - or MS2-based tethering assay, which is widely used to test whether a protein plays a role in nonsense-mediated mRNA pathway (Lykke-Andersen *et al.*, 2000). This assay is based on the fact that binding of a NMD factor to the MS2 or λ -peptide sequence in the 3' UTR of the reporter β -globin mRNA triggers the degradation of the reporter mRNA. Quite unexpectedly, a stabilization rather than destabilization of the reporter mRNA tethered to IGHMBP2 was observed (Fig. 17), indicating the contribution of IGHMBP2 to the stabilization of mRNA. This finding also ruled out the possibility that IGHMBP2 is involved in general mRNA degradation pathways. However, it is not clear whether the stabilization of the bound mRNAs observed in this assay subsequently influenced their translation. It has been recently reported that mRNA stabilization is functionally linked to translation in a fairly complex interplay. While in most cases stabilized mRNAs are preferentially subject to translational repression (Kawai *et al.*, 2004), in some cases

translationally-active mRNAs, also exhibit enhanced stability (Antic *et al.*, 1999; Audic *et al.*, 2002). According to this view, IGHMBP2 probably participates in translational control via mRNA stabilization. Alternatively, IGHMBP2 could stabilize mRNAs without changing the translation efficiency of the stabilized mRNA. This idea is supported by studies of polysomes-associated FMRP and Y box-binding protein1 (YB-1). FMRP controls mRNA abundance independently of its function as a translation factor (Zalfa *et al.*, 2007). YB-1, the predominant protein component of translationally inactive mRNPs, is considered to play two independent roles as a general stabilisator of capped-mRNA (Evdokimova *et al.*, 2001) and as a global translation repressor (Daydova *et al.*, 1997; Minich *et al.*, 1993). Interestingly, YB-1 has been identified in the purified IGHMBP2 complex which raises the possibility that both proteins function together in mRNA stabilization.

Although these data clearly point to a role in ribosome-associated processes, a definitive function of IGHMBP2 in mRNA metabolism has not yet been discovered. In this context, it is worth to note that IGHMBP2 is not an essential protein, which makes its analysis even more difficult. Thus, more elaborate experimental systems such as analysis of global protein synthesis in IGHMBP2-deficient cells will be of most importance to elucidate IGHMBP2's function.

5.3 Pathogenic IGHMBP2 Variants Loose their Enzymatic Activities *In Vitro*, but Still Associate with Ribosomes

Although the clinical feature of SMARD1 patients and its variation have been well described in the past few years, the contribution of IGHMBP2 to the pathomechanism of SMARD1 remains unknown. The fact that most SMARD1-causing missense mutations in IGHMBP2 are found within or adjacent to the highly conserved helicase motifs, led to the hypothesis that the helicase activity may be impaired in SMARD1 patients. Indeed, the enzymatic studies performed with SMARD1-causing missense mutations indicate that these mutations cause a net loss of RNA unwinding and ATPase activities of IGHMBP2 (Fig. 18), thus confirming the hypothesis above.

Seven of nine mutations analyzed (T221A, E382K, H445P, N583I, R603H, Q196R and C241R) abolished the ATPase and unwinding activities of IGHMBP2 (Fig. 18C and D). In human and yeast Upf1, the mutation in the corresponding residue of IGHMBP2-R603, namely R865 (hUpf1) and R809 (yUpf1) caused a defect in ATP binding and hydrolysis activity (Cheng *et al.*, 2007; Weng *et al.*, 1996). Recently, Cheng *et al.* (2007) have successfully solved the crystal structure of the helicase core of hUpf1. Accordingly, the residues R865 and T499 of hUpf1, which correspond to R603 and T221 of IGHMBP2 respectively, have been identified to be structurally located in the nucleotide binding cleft, thereby suggesting a direct role of these residues to facilitate ATP binding and hydrolysis (Cheng *et al.*, 2007). Given the assumption that the ATP binding cleft of IGHMBP2 is analogous to that of hUpf1, mutations in IGHMBP2 (E382K, H445P and N583I) alter residues close to the catalytically active residues in the ATP binding cleft, and as a consequence, the loss of ATPase activity is the primary defect in these protein mutants. In addition to conserved helicase motifs, ATP-specific SF1 helicases contain a highly conserved glutamine residue N-terminal from the motif I. In Dna2p, a member of SF1 helicase, this residue is apparently not essential (reviewed in Tanner and Linder, 2001). By contrast, like in DEAD box helicases, mutation of this residue (Q196R) completely abolished ATP hydrolysis and RNA unwinding activities of IGHMBP2.

Enzymatic studies of IGHMBP2 suggest that the energy derived from the hydrolysis of ATP is used for the helicase activity of IGHMBP2. However, an exception has been found in the D565N mutation of the helicase motif V, which led to the inhibition in the ATPase but not to the unwinding activity of IGHMBP2 (Fig. 18C and D). Uncoupling of the ATPase and helicase activities has also been reported for other SF1 helicases, namely UL5 and PcrA. In contrast to studies of the IGHMBP2 mutant, the ATPase of UL5 mutant was only moderately reduced to 30-39% (Graves-Woodward *et al.*, 1997) and the mutations in PcrA do not occur within the classical helicase motifs (Soulтанas *et al.*, 2000). Further structural studies of the IGHMBP2 protein would be necessary to address how a mutation within the classical helicase motif V uncouples full ATPase from helicase activity.

Taken together, these results provide direct correlation of the enzymatic activity of IGHMBP2 and the pathomechanism of SMARD1. Nevertheless, one exception has been observed among the missense mutations: the IGHMBP2 variant containing a substitution

of a threonine in position 493 to isoleucine (T493I) exhibited neither ATPase defects nor reduced helicase activity and hence behaved differentially as compared to other tested mutants. Studies on IGHMBP2 levels in the SMARD1 patients and heterozygotic carriers of the T493I (1478T>C) mutation could, however, provide an explanation why this mutant is pathogenic. In SMARD1 patients carrying this mutation, steady state levels of cellular IGHMBP2 is reduced to 50%, most probably due to impaired stability of this variant (Guenther *et al.* 2007b). As a consequence, the overall IGHMBP2 activity would be reduced in these patients. These observations suggest that SMARD1 may result from IGHMBP2 concentrations below a critical threshold. This hypothesis is further supported by the recent finding that IGHMBP2 protein levels in one SMARD1 patient with a late onset of the disease is higher than those in patients with early onset of SMARD1. Residual levels of IGHMBP2 may attenuate the disease progression in the juvenile SMARD1 patient (Guenther *et al.*, 2007b).

Although SMARD1-related missense mutations efficiently inhibit the unwinding activity of IGHMBP2, the association of IGHMBP2 with ribosomal subunits is not influenced by these mutations. All IGHMBP2 variants analyzed (one with impaired ATPase activity, two with impaired both ATPase and helicase activities) were incorporated into the 40S and 60S ribosomal subunits in a manner similar to the wild-type protein (Fig. 18E). Similarly, in the fragile X mental retardation syndrome, a FMRP mutant I304N, which causes an unusually severe phenotype, is still able to bind its cytoplasmic mRNA targets and large ribosomal subunits *in vivo* as the wild-type FMRP. However, this mutant is present in the “nonfunctional mRNPs”, which are not associated with translating ribosomes (Schier *et al.*, 2004; Feng *et al.*, 1997; Brown *et al.*, 1998). In the case of SMARD1, mutant proteins are still capable to bind ribosomal subunits but can not perform their function as RNA helicases. Considered together, the results strongly indicate that loss of IGHMBP2 helicase activity, but not its association with ribosomal subunits is the major cause of SMARD1 at the biochemical level.

5.4 The Pathomechanism of SMARD1: a Hypothesis

The data presented in this work suggest that defects in mRNA metabolism may be responsible for motor neuron degeneration in SMARD1. Several motor neuron diseases, including the well-known spinal muscular atrophy type 1 (SMA1), the amyotrophic lateral sclerosis type 4 (ALS4) and Ataxia-ocular apraxia 2 (AOA2), have also been linked to dysfunction in RNA metabolism (Chen *et al.*, 2006; Morreira *et al.*, 2004). In SMA1, the protein product of the disease gene, SMN is known to play roles in UsnRNPs assembly, mRNA splicing, mRNA localization and transcription (reviewed in Kolb *et al.*, 2007). Interestingly, ALS4 and AOA2 diseases result from mutations in the helicase domain of *Senataxin*, the human homolog of yeast Sen1p, a member of SF1 helicase, which has been implicated in tRNA termination and splicing (Chen *et al.*, 2006; Ursic *et al.*, 2004).

All the above-mentioned diseases have in common, that they are caused by defects in housekeeping genes. Hence the key question is, why only specific cell types are affected in these diseases while others survive unaffected. Given the role of IGHMBP2 in mRNA stabilization and/or translation, it is tempting to speculate that IGHMBP2 may modulate stabilization and translation of neuronal specific mRNAs necessary for the survival or maintenance of motor neurons. Hence, the loss of IGHMBP2 activity may result in inefficient translation of those mRNAs and in turn elicit a series of steps that ultimately lead to loss of motor neurons. The idea of proteins involved in stabilization and translation of neuronal specific mRNAs comes from FMRP in fragile X mental retardation syndrome. This protein is functionally involved in translation repression, stabilization or degradation of a subset of neuronal mRNAs in highly selective mechanism with regards to neuronal cell type and mRNA target (Zalfa *et al.*, 2007; Zang *et al.*, 2007; Feng *et al.*, 1997).

The speculation about the molecular pathogenesis of SMARD1 requires further investigations on the precise cellular role of IGHMBP2 within mRNA stabilization and/or translation. In the near future, it is thus of major importance to identify and to characterize “mRNA substrates” or “cellular targets” of IGHMBP2. This can be performed by proteomic studies using IGHMBP2-deficient cells and control cells. The identification of cellular mRNA targets would then allow studies to assess whether mishandling of these mRNAs can be directly linked to the disease. These studies would pave the way to explore

the function of IGHMBP2 in motor neurons, i.e. the cell type that is most severely affected in SMARD1.

6. MATERIALS

6.1 Chemicals

All laboratory chemicals were obtained from Roth, Sigma, and Merck KGa at least in p.a quality.

6.2 Antibodies

Primary Antibodies for immunolocalization studies, immunopurification, Western blot analysis

Antibody	Antigene	Antibody Type	References
481	Fl-Ighmbp2	Rabbit polyclonal	In this work
482	Fl-Ighmbp2	Rabbit polyclonal	In this work
483	N-terminal mIghmbp2	Rabbit polyclonal	In this work
484	N-terminal mIghmbp2	Rabbit polyclonal	In this work
eIF4G2	human eIF4G2	Goat polyclonal	Santa Cruz Biotechnology
rpL7	rpL7	Goat polyclonal	Santa Cruz Biotechnology
GST	Human GST	Rabbit polyclonal	In this work

Fl: full length

Secondary antibodies

Antibody	References
Cy2-conjugated goat anti mouse IgG	Dianova GmbH
Cy3-conjugated mouse anti rabbit IgG	Dianova GmbH
Cy2-conjugated anti goat IgG	Dianova GmbH
Peroxide-conjugated anti-mouse IgG	Sigma
Peroxide-conjugated anti-rabbit IgG	Sigma

6.3 Cell Lines

Bacterial Cell Lines : *E. coli* DH5, *E. coli* Rosetta, *E. coli* BL21

Eukaryotic Cell Lines: HeLa (human negroid cervix epitheloid carcinoma)
 HEK 293 (human embryonic kidney)
 3T3 (Swiss albino mouse fibroblast)
 FM3A (mouse C3H mammary carcinoma)
 COS7 (African Green Monkey SV40-transfected kidney fibroblast)
 PC12 (rat pheochromocytoma)

6.4 Plasmid Vectors

Plasmid Vector:	pBluescript KSII(-)	(Stratagene, La Jolla USA)
	pCDNA3	(Invitrogen)
	pCMV4B	(Stratagene, La Jolla USA)
	pCMV5B	(Stratagene, La Jolla USA)
	pCI-Neo	(Promega)
	pET28a	(Novagen)

pGem-Mol (Promega)
 pGem-C4 (Promega)
 pGex6p1 (Amersham Biosciences)

Plasmid constructs for IGHMBP2 expression

Protein	AA	Construct N/C terminal	Plasmid	5'/3' RE	Amino acid Mutation
IGHMBP2	1-993	-	pBluescript KSII(-)	Sall/HindIII	WT
IGHMBP2	1-993	GST/6His	pGex6p1	Sall/HindIII	WT
IGHMBP2	1-993	GST/6His	pGex6p1	Sall/HindIII	Q196R
IGHMBP2	1-993	GST/6His	pGex6p1	Sall/HindIII	T221A
IGHMBP2	1-993	GST/6His	pGex6p1	Sall/HindIII	C241R
IGHMBP2	1-993	GST/6His	pGex6p1	Sall/HindIII	E382K
IGHMBP2	1-993	GST/6His	pGex6p1	Sall/HindIII	H445P
IGHMBP2	1-993	GST/6His	pGex6p1	Sall/HindIII	T483I
IGHMBP2	1-993	GST/6His	pGex6p1	Sall/HindIII	D565N
IGHMBP2	1-993	GST/6His	pGex6p1	Sall/HindIII	N583I
IGHMBP2	1-993	GST/6His	pGex6p1	Sall/HindIII	R603H
IGHMBP2	1-993	GST/6His	pGex6p1	Sall/HindIII	GKT219AAA
IGHMBP2	1-993	GST/6His	pGex6p1	Sall/HindIII	DE375AA
Ighmbp2	1-993	His/-	pET28a	Sall/HindIII	WT
Ighmbp2	881-993	GST/-	pGex6p1	Sall/HindIII	WT
Ighmbp2	1-296	GST/-	pGex6p1	Sall/HindIII	WT
IGHMBP2	1-993	-/Flag	pCMV4B	Sall/HindIII	WT
IGHMBP2	1-993	-/myc	pCMV5B	Sall/HindIII	WT

AA: amino acid

Plasmid constructs for tethering assay

Protein/mRNA	Construct (N/C Terminal)	Plasmid	References
WT IGHMBP2	V5-λN/-	pCINeo	In this work
WT IGHMBP2	MS2/-	pCINeo	In this work
WT hUpf1	MS2/-	pCINeo	Gehring <i>et al.</i> 2003
WT hUpf2	MS2/-	pCINeo	Gehring <i>et al.</i> 2003
WT hUpf3b	V5-λN/-	pCINeo	Gehring <i>et al.</i> 2003
MS2 coat protein	-	pCINeo	Gehring <i>et al.</i> 2003

λ N peptide	V5/-	pCINeo	Gehring <i>et al.</i> 2003
WT β globin+e300 mRNA	-	pCINeo	Gehring <i>et al.</i> 2003
WT β -globin mRNA	-/3' UTR 6xMS2 binding sites	pCINeo	Gehring <i>et al.</i> 2003
WT β -globin mRNA	-/3' UTR 4BoxB	pCINeo	Gehring <i>et al.</i> 2003

h: human

Plasmid constructs for preparation of dsRNA substrates for RNA unwinding assay

dsRNA	plasmid	Promoter	RE
C4/Mol	pGem-C4	SP6 Polymerase	Pvu II
	pGem-Mol	T7 Polymerase	HindIII
RNA-A1/RNA-A2	pCDNA3	T7 Polymerase	Not I
	pCDNA3	SP6 Polymerase	Eco RI
RNA-A3/RNA-A4	pBluescript IIKS(-) Δ Sac/KpnI	T3 Polymerase	Pvu II
	pBluescript IIKS(-) Δ Sac/KpnI	T7 Polymerase	Pvu II

RE: Restriction enzyme for plasmid linearization

6.5 Consumable Materials

Glutathione sepharose beads	Amersham Bioscience
Ni-NTA agarose beads	Amersham Bioscience
Protein A sepharose beads	Amersham Bioscience
Protein G sepharose beads	Amersham Bioscience
Dialysis membrane MWCO 1000Da	Spectra/Por Biotech
Microspun – chromatography	Biorad
Whatman paper	E. Merck AG
Nitrocellulose Membrane (Western Blot)	PAL
Nitrocellulose Membrane (Northern Blot)	Nytran N, 0.45 μ M, Schleicher & Schluell
X-Ray film	Kodak

6.6 Dye Solutions

Coomassie Brilliant Blue G250	Serva
Ponceau S	Roth
Bromphenol blue	Serva

6.7 Enzymes and Inhibitors

6.7.1 Enzymes

Alkaline phosphatase	Promega
RNase-free DNase I	Promega
Restriction enzymes	MBI Fermentas
T4 DNA ligase	MBI Fermentas
T4 RNA ligase	MBI Fermentas
Taq Polymerase	Promega

RNase Promega

6.7.2 RNase and Protease Inhibitors

Aprotenin (AP)	Sigma
4-(2-Aminoethyl)benzenesulfonyl (AEBSF)	Sigma
Leupeptin	Sigma
Pepstatin	Sigma
Phenyl methyl sulfonyl flourid (PMSF)	Sigma
RNase inhibitor (RNasin)	Promega

6.8 Oligonucleotides

[α - ³² P]-ATP	Amersham Biosciences
[γ - ³² P]-ATP	Amersham Biosciences
dNTPs (dATP, dCTP, dTTP, dGTP)	MBI Fermentas
NTP (ATP, UTP, CTP, GTP)	MBI Fermentas
SiRNA against IGHMBP2	IBA GmbH Göttingen
5' AA GAG CUC CAG AGC CGA GGC G TT 3'	
3' TT CUC GAG GUC UCG GCU CCG C AA 5'	

6.9 Standard Buffers/Solutions and Cell Culture Media

6.9.1 Buffers/Solutions

1XPBS (phosphate buffer saline): 130mM NaCl, 77.4ml 1M Na₂HPO₄, 22.6 ml 1M NaH₂PO₄, ad 1LddH₂O
 TBE (Tris/Borat/EDTA): 89mM Tris/HCl pH 8.3, 89mM Boric acid, 2 mM EDTA
 10TBT : 87.6g/l NaCl, 7.25g/l Tris-base, 30g/l Tris-HCl, 50ml/l Tween 20
 10x Net-Gelatin blocking buffer: 1.5 M NaCl, 0.05 M EDTA, 0.5 M Tris-Cl pH 7.5, 0.5% (w/v) triton X-100, 25 g/L gelatin, adjust to pH 7.5

6.9.2 Cell Culture Media and Reagents

Media for bacterial culture

LB: 1% (w/v) Bactotrypton, 0.5% (w/v) yeast extract, 1% (w/v) NaCl
 Superbroth: 3.5% (w/v) Bactotrypton, 2% (w/v) yeast extract, 0.5% (w/v) NaCl

Media for mammalian culture

DMEM (Dulbecco's Modified Eagles Medium)	PAA
Methionine-free DMEM	PAA
RPMI	PAA
Transfection agents: Nanofectin	PAA
Oligofectamin	Invitrogen

6.10 Standard Markers

Protein standard (unstained and prestained)	MBI Fermentas
DNA standard (DNA Ladder mix)	MBI Fermentas

7. METHODS

7.1 Nucleic Acids Analysis

7.1.1 Purification and Isolation

7.1.1.1 Purification of Nucleic Acids Using Phenol/Chloroform extraction

Proteins are removed from nucleic acid preparation by extraction with PCI (Phenol/Chloroform/Isoamyl alcohol). An equal volume of equilibrated phenol/chloroform/isoamyl-alcohol was added into a nucleic acid preparation. The mixture was mixed vigorously using vortex and centrifuged at 13,000 rpm for 5 min. The aqueous phase was transferred in a new tube. The extraction was repeated with an equal volume of chloroform/isoamylalcohol (24:1) in the same manner as described above. The aqueous phase containing nucleic acids was removed into a new tube and directed to precipitation (7.1.1.2).

PCI: Phenol/Chloroform/Isoamyl alcohol: 50% (v/v) Phenol (equilibrated in TE pH 7.5); 48% (v/v) Chloroform; 2% (v/v) Isoamyl alcohol.

7.1.1.2 Nucleic Acids Precipitation from Aqueous Phase

Nucleic acids are recovered from aqueous solutions by ethanol precipitation in the presence of cations. Nucleic acid solution was mixed with 0.1x volume of 3 M Sodium acetate pH 4.8 as cation donor and 2.5-3x volume of ice-cold absolute ethanol. After incubation at -20°C for at least 1 hour, the mixture was centrifuged at 13,000 rpm at 4°C for at least 30 min. The pellet was then washed with ice-cold 80% ethanol. Following centrifugation at 13,000 rpm at 4°C for 10 min, the pellet was air-dried and dissolved in ddH₂O. If a small quantity of nucleic acid will be precipitated, carrier or co-precipitate, such as glycogen that can trap nucleic acid and generates a visible pellet, was added to the nucleic acid preparation.

7.1.2 Quantification of Nucleic Acids

Concentration of nucleic acid was determined using UV spectrophotometer. This method is based on average absorption maximum of bases at 260 nm and Lambert Beer Law.

$$A = \epsilon \times c \times d, \text{ where } \epsilon \text{ is molar extinction coefficient.}$$

Absorbance (A) is proportional to molar concentration of the absorbing substance (c) and length of the light path in cm (d). When d is equal to 1 cm, an absorption of 1 corresponds to concentration of 50 µg/ml for double-stranded DNA, and 40 µg/ml for single-stranded RNA. To verify the purity of a nucleic acid solution, absorption spectrum between 210 – 340 nm was determined and ratio of OD₂₆₀/OD₂₈₀ was calculated. Ratio OD₂₆₀/OD₂₈₀ less than 1.8 or 2.0 indicates the presence of contaminants in the DNA or RNA sample respectively.

7.1.3 Gel Electrophoresis of Nucleic Acids

7.1.3.1 Agarose Gel Electrophoresis

Native Agarose Gel Electrophoresis

0.8%- 1% (w/v) agarose gel was used to verify the PCR products, plasmid DNA and rRNAs.

Gel preparation: a desired amount of agarose was melted in 1x TBE buffer. Ethidium bromide was subsequently added into the warm agarose gel at the end concentration of 0.5µg/ml.

Sample preparation: DNA samples were mixed with 0.2x volume of 6x DNA loading buffer. RNA samples were mixed with 0.5x volume of 2x denaturing RNA loading buffer.

Gel running: nucleic acid separation was carried out by electrophoresis in running buffer/1x TBE at 120 V.

5x DNA loading buffer: 60% glycerin, 60 mM Tris, 0.2 mM EDTA, Bromphenol blue, xylen cyanol, pH 6.8.

Denaturing RNA loading buffer: 90% formamide, 0.025% (w/v) xylen cyanol, 0.025 % bromphenolblue

Denaturing Agarose Gel Electrophoresis

Denaturing agarose gel with formaldehyde as the denaturant was used to separate RNAs for subsequent Northern blot analysis (7.3.7).

Gel preparation: an appropriate amount of agarose was melted in ddH₂O and cooled to 60°C. 10x MOPS buffer and formaldehyde were then added into the agarose solution. The gel was allowed to set at RT.

RNA sample preparation: RNA sample was mixed with the following solutions: 10µl formamide, 3.5 µl formaldehyde, 2 µl 10x MOPS buffer, 2-5 µg RNA, and ddH₂O to 19 µl. The mixture was incubated at 65° C for 15 min and put on ice. One µl ethidium bromide (10 mg/ml) and 2 µl RNA loading buffer was added to the RNA sample.

Gel running: the gel was run in 1x MOPS running buffer at 50-110 Volts for 8-16 hours for Northern blot analysis. The gel was visualized on UV transilluminator.

1.4% formaldehyde agarose gel (150 ml): 2.1 g agarose in 100 ml ddH₂O, 15 ml 10x MOPS-buffer, 30 ml 37% formaldehyde pH >4.

RNA loading buffer: 50% glycerol, 1 mM EDTA, 0.25% Bromphenol blue.

10x MOPS: 0.4 M MOPS (3-(N-morpholino) propanesulfonic acid), 0.1 M Sodium acetate, 0.01 M EDTA.

7.1.3.2 Polyacrylamide Gel Electrophoresis

Polyacrylamide gel electrophoresis was used to separate RNAs under native or denaturing condition. To achieve denaturing condition, denaturing agent, 8M Urea and formamide was added to PAA gel solution and RNA samples, respectively.

Denaturing Polyacrylamide Gel Electrophoresis

Gel preparation:

8% (w/v) denaturing polyacrylamide gel (50 ml): 26 g Urea (8 M), 8% polyacrylamide 40 (19:1), 10 ml 5x TBE, 500 µl APS, 50µl TEMED, ad 50 ml ddH₂O.

10% (w/v) denaturing polyacrylamide gel (50 ml): 24 g Urea (8 M), 10% polyacrylamide 40 (19:1), 10 ml 5x TBE, 500 µl APS, 50µl TEMED, ad 50 ml ddH₂O.

Sample preparation: RNA solution was mixed with 1x volume of 2x RNA gel loading buffer containing formamide (7.1.3.1). The mixture was heated at 95°C for 2-5 min, put on ice for 30 sec to keep RNA strands separated and loaded into wells.

Gel running: prior to sample loading, PAA gel was pre-run at 39 Watt for at least 15 min and the wells were rinsed with 1x TBE to remove the remaining urea. The gel was then run in 1xTBE at 39 W.

Native Polyacrylamide Gel Electrophoresis

Gel preparation:

8% (w/v) polyacrylamide gel (50 ml): 8% polyacrylamide 40 (19:1), 10 ml 5xTBE, 500 µl APS, 50µl TEMED, ad 50 µl ddH₂O.

Sample preparation: RNA solution was mixed with native RNA sample buffer.

Gel running (in the cold room): prior to sample loading, PAA gel was pre-run at 30 Watt for at least 15 min and the wells were rinsed with 1x TBE to remove the remaining urea. The gel was then run in 1xTBE at 30 W.

Native RNA-loading buffer: 16% (v/v) Glycerin, 10 mg/ml Heparin, 0,025% (w/v) Xylen cyanol, 0,025% (w/v) Bromphenol blue.

7.1.3.3 Detection of Nucleic Acids

Ethidium Bromide

Ethidium bromide stained nucleic acids (RNA/DNA) on gels were detected under UV light at the wave length of 254 nm. Ethidium bromide molecules intercalate into nucleic acid strands and subsequently exhibit fluorescence which is visualized under illumination by UV light.

Autoradiography

Radioactively labeled RNA on gels was detected by autoradiography. The gel was wrapped with plastic membrane, and exposed on X-ray film (Kodak) for about 3 min in the dark room. Then the film is developed, fixed and dried.

Phosphorimaging

Phosphorimaging is a quantitative imaging that uses phosphor storage screen to localize radioactively-labeled RNAs. In this technique, radioactively labeled RNAs in a gel are exposed to the image recording plate/phosphor storage screen which in turn accumulates energy radiation. The radiation image is then scanned by laser beam and read as a digital image that can be quantified.

RNA gel transferred to a filter paper (Whatman) or a northern blot membrane was covered with a plastic membrane and exposed to an imaging plate (IP) for 2-8 h in the cassette. The IP was scanned by phosphoimager (FLA-5000 Image Reader, Fuji film, Version 1.0) at laser wave length of 635 nm. Images were analyzed using Image Gauge 3.41.

7.2 DNA Analysis

7.2.1 Plasmid Isolation from *E. coli* Cells

Plasmid isolation from bacterial cultures was performed according to manufacture's protocols (Promega, Qiagen and Macherey-Nagel). This technique is based on the alkaline and SDS/Sodium dodecyl sulfate treatment (Birnboim and Doly, 1979). Plasmid-transformed *E. coli* cells were grown in 5 ml LB medium containing 50µg/µl appropriate antibiotics overnight at 37°C. The cells were pelleted by centrifugation at 14.000 rpm for 30 seconds. The addition of SDS and Sodium hydroxide led to lysis of bacterial cell wall and denaturation of chromosomal DNA, plasmid DNA and protein. After neutralization with potassium acetate, protein, chromosomal DNA as well as bacterial cell debris formed a non-soluble complex in the presence of less soluble-potassium dodecyl sulfate. This complex was then precipitated under high salt concentration, while plasmid DNA remains in solution. The plasmid DNA was purified from other cellular components and chromosomal DNA on an anion exchange chromatography column. Following washing with ethanol-containing wash buffer, the Plasmid DNA was eluted and precipitated using isopropanol and ethanol. The pellet was dissolved in sterile ddH₂O and plasmid concentration was measured using spectrophotometer (7.1.2), the isolated plasmid was examined by digestion with restriction enzymes and analyzed on 1% (w/v) agarose gel (7.1.3.1).

7.2.2 Plasmid Linearization

Plasmid DNA was used as template for *in vitro* RNA synthesis (see 7.3.4). For this purpose, plasmid DNA was previously linearized by an appropriate endonuclease restriction enzyme. In a total volume of 50 µl, 5 µg Plasmid DNA were incubated with 15U restriction enzyme and 1x corresponding restriction buffer at 37°C overnight. Upon incubation, phenol-chloroform extraction (7.1.1.1) was done to purify the digestion products from the enzyme. The linearized plasmid DNA was recovered by ethanol precipitation (7.1.1.2). DNA concentration was measured using spectrophotometer (7.1.2). Two hundred ng of each digestion product were analyzed on 1% (w/v) agarose gel (7.1.3.1).

7.2.3 Polymerase Chain Reaction

Polymerase chain reaction allows the DNA from a selected region to be amplified *in vitro*. A set of a PCR is shown in the following table:

Components	Stock Concentration	End Concentration
dNTPs	10 mM	0.3 mM
PCR Buffer	10x	1x
Primer 1	25 µM	0.5 µM
Primer 2	25 µM	0.5 µM
DNA Polymerase	2.5U/µl	2.5 U
DNA Template	variable	10 ng
ddH ₂ O	ad 50 µl	

PCR program: Denaturation	95 °C	5 min
Denaturation	95 °C	1 min
Annealing*		1 min
Polymerization**	72°C	1 min
Polymerization	72°C	10 min

PCR was also used to check whether bacterial clones contain the correct plasmid. In this PCR, instead of purified DNA, single colony was directly used as source of DNA template. A reaction of colony PCR is described following:

Components	Stock concentration	End concentration
dNTP	10 mM	0.2 mM
PCR Buffer	10x	1x
Primer 1	25 μ M	0.5 μ M
Primer 2	25 μ M	0.5 μ M
DNA Template	-	Bacterial colony
DNA Polymerase	1U/ μ l	0.4 U
ddH ₂ O	ad 20 μ l	

PCR program: Denaturation	95 °C	5 min
Denaturation	95 °C	1 min
Annealing*		1 min
Polymerization**	72°C	1 min
Polymerization	72°C	10 min

* annealing temperature depends on the melting temperature of primers used (annealing temperature: $T_m - 5$ °C).

** Polymerization is variable, dependent of the length of DNA template to be amplified and DNA polymerase used.

7.2.4 DNA Cloning in Plasmid Vectors

DNA cloning is used to reproduce DNA fragment in bacterial cells. In principle, DNA fragment to be cloned is inserted into a corresponding plasmid vector using enzyme ligase and the ligation product is cloned in bacterial cells. Plasmid DNA as well as DNA fragment to be cloned must be previously cleaved with appropriate restriction enzymes to generate the complementary ends. To avoid the recirculation and self-ligation of DNA, alkaline phosphatase is used to remove 5' phosphate end of DNA. The dephosphorylated Plasmid DNA is then ligated with the DNA insert to generate an open circular DNA molecule. This reaction is catalyzed by bacteriophage T4 DNA ligase. The ligation product is in turn transformed to *E. coli* cells.

Enzymatic Digestion of Double-Stranded DNA and Dephosphorylation of Nucleic Acids

Reaction mix: 10 μ g DNA (PCR product or plasmid vector), 20U DNA restriction enzyme, 1x restriction buffer.

The mixture was incubated at 37°C overnight. One U/ μ l Calf intestine phosphatase (CIAP) per 20 μ l mix was added to the reaction and incubation was continued for an additional one hour. The cleavage products were separated by agarose gel electrophoresis, and purified from the gel.

Recombination of DNA

20 μ l reaction mix: 1x ligase buffer, 100 ng vector, DNA insert (= 2.5x [vector]), 5U T4 DNA ligase, ad 20 μ l ddH₂O.

Ligation was performed at RT for 2 hours. 10 μ l of the reaction mix was used for transformation in *E. coli* (5.2.6).

Cloning of *IGHMBP2* (see Materials): A linker sequence containing a 6xHis-tag was introduced at the C-terminus of the *IGHMBP2* open reading frame in pBluescript KSII(-) vector by dual

asymmetric PCR (Young and Dong, 2004). This open reading frame was subcloned into pGex6p1 vector, resulting in pGex6p1-*IGHMBP2*-6His.

Cloning of *IGHMBP2* mutants (see Materials): pBluescript KSII(-) containing *IGHMBP2*-6His was used as template for *in vitro* mutagenesis according to the protocol of the QuickChange® Site-Directed Mutagenesis Kit (Stratagene). All open reading frames were then subcloned into pGex6p1 vector, as described above.

7.2.5 Transformation of *E. coli* Cells

100-150 ng Plasmid DNAs were incubated with 100 μ l competence cells for 30 min on ice. After 90 second heat shock at 43°C, the cells were incubated on ice for 2 min and grown in 500 μ l LB medium without antibiotic at 37°C for 30 min. The bacterial culture was plated on LB agar medium containing corresponding antibiotic(s) and cultivated overnight at 37°C.

7.3 RNA Analysis

7.3.1 RNA Isolation from Cell Extract

1x volume of PK buffer and 2x volume of phenol were added to cell extract or gradient fraction and mixed vigorously under shaking for 5 min at RT. The mixture was then centrifuged at 13,000 rpm at RT for 5 min. The aqueous phase was transferred to a new tube and directed to PCI extraction followed by ethanol precipitation (7.1.1).

PK buffer: 150mM NaCl, 100 mM Tris pH 7.0, 12.5 mM EDTA pH 8.0, 1% SDS

7.3.2 RNA Isolation from Cell Culture Using Trizol

3x volume of TRizol reagent was added to cytoplasmic extract. The sample was incubated for 5 min at 15-30°C and mixed with 0.2 ml chloroform per 750 μ l trizol vigorously by hand for 15 sec. The mixture was centrifuged at 12,000xg for 15 min at 4°C. The colorless aqueous phase was transferred to a new tube. To precipitate RNA, 0.5 ml Isopropyl-alcohol was added to the aqueous phase and mixed vigorously by vortex. The sample was subsequently incubated for 10 min at 2-8°C. The pellet was washed once with 80% ethanol (1 ml ethanol per 750 μ l Trizol). After vigorously mixing using vortex, the sample was centrifuged at 7500xg for 5 min at 4°C. The pellet was air-dried and dissolved in ddH₂O and stored at -20°C or was stored at -80°C for one year.

7.3.3 RNA Purification Using Size Exclusion Chromatography

Gel filtration chromatography was used to separate DNA/RNA molecules according to their shape and size. In this work, spin column chromatography was performed to separate radioactively labeled RNAs from unincorporated radioactive precursor.

Spin column chromatography was done by using the ready used-Micro-Bio-Spin chromatography column of Biorad: Bio-Gel P-6 and Bio-Gel P-30 with exclusion limit of 5 bp and 20 bp respectively.

7.3.4 *In Vitro* Synthesis of RNA Molecules

Bacteriophage T7 RNA Polymerase has a high activity for *in vitro* transcription due to its property that it has only a single polypeptide and does not require initiation site (Milligan and Uhlenbeck

1989). This enzyme is known to recognize only the T7 promoter sequence and catalyzes RNA synthesis from nucleotide with dsDNA as a template in the presence of cation. A set of transcription condition with a total volume of 20 μ l contains the following components:

Components	Stock concentration	End concentration
Transcription buffer	5x	1x
NTP mix	25 mM	5 mM
RNasin	40 U/ μ l	40 U
DNA template	-	2 μ g
T7 RNA polymerase	2U/ μ l	4U
dH ₂ O	add 50 μ l	

All components were brought to RT except for RNasin and T7 RNA polymerase. Enzyme was added after all other components were mixed. After one hour incubation, 1 μ l T7 Polymerase was added in the reaction and the mixture was incubated for an additional 1 hour at 37°C, followed by DNaseI digestion to remove DNA template. DNase I degrades dsRNA and produces a mixture of 5' phosphorylated nucleotides in the presence of dication such as Mg²⁺. 10 U DNase I and 10 mM MgCl₂ were added into the reaction and incubated at 37° C for 30 min. Then the mixture was brought up to 200 μ l by adding RNase-free ddH₂O. After phenol/chloroform extraction and ethanol precipitation (7.1.1), the pellet was dissolved in 30 μ l RNase-free ddH₂O. 1 μ l transcription products was analyzed by 1% agarose gel electrophoresis or polyacrylamide gel electrophoresis.

7.3.5 Preparation of Double-Stranded RNA

Double-stranded RNA was produced by annealing two partially/fully complementary RNAs in hybridization buffer. In this study, one RNA strand was radioactively labeled during transcription (7.3.4) and the other strand was unlabeled. The mixture was denatured at 95°C for 5 min and slowly cooled at RT.

Hybridization buffer: 25 mM Hepes-KOH pH. 7.4, 500 mM NaCl, 1 mM EDTA, 0.1% (w/v) SDS)

7.3.6 RNA Unwinding Assay

25 fmol RNA duplex was incubated with 33-150 ng protein in 50 μ l of a reaction mixture containing unwinding buffer at 30°C for 1h. The reaction was stopped by the addition of 150 mM Na₂EDTA pH 8.0, 50% (v/v) glycerol, 2% (w/v) SDS and 0.25% (w/v) xylene cyanol. The reaction was subjected to non-denaturing 8% polyacrylamide gel electrophoresis (7.1.3.2). Visualization was achieved by autoradiography (7.1.3.3).

dsRNA substrate used in this work: C4/mol (5' and 3' single-stranded extensions); RNA-A1/RNA-A2 (a 5' single stranded extension); RNA-A3/RNA-A2 (a 3' single-stranded extension).

Unwinding buffer: 200 μ M ATP, 50 mM NaCl, 30 mM Tris-HCl pH 7.0, 1.2 mM MgCl₂, 1.5 mM DTT, 0.5 mM EDTA, 20U RNasin, 15% glycerol (DTT, ATP, RNasin were freshly added).

7.3.7 Northern Blot Analysis

Gel preparation: see 7.1.3.1 (denaturing agarose gel)

Northern transfer of RNA: the formamide agarose gel was gently soaked in sterile ddH₂O for 2x10 min and was incubated in 50 mM NaOH for 20 min. Subsequently, the gel was rinsed with ddH₂O and equilibrated in 20XSSC for at least 40 min. The capillary blot (baking dish) was filled with 20XSSC and set up as following: 1 Whatman 3MM paper-gel-wet transfer membrane (a nylon membrane)-two wet Whatman 3MM papers-two dry Whatman- paper towels- glass plate-weight. Transfer was allowed for 18 hours. RNA on the nylon membrane was UV-crosslink in a UV cross linker (1200 mJ in a Stratalink).

Hybridization with cRNA probes (Church): the northern membrane was pre-hybridized in Church buffer at 65°C for 2 hours. The pre-hybridized membrane was then incubated with the radioactively-labeled RNA probe in prewarmed church buffer overnight at 65° C. The membrane was washed 2x 15 min with wash buffer 1 at 65°C followed by washing with wash buffer 2 for an additional 2x15 min. The membrane was dried, wrapped in saran and exposed to x-ray film at 80°C.

20xSSC: 3 M NaCl, 0.3 M TriSodium-citrate, pH 7.0

Church buffer: 0.5 M Na₂HPO₄, 1 mM EDTA, 7% SDS, pH 7.2

Wash buffer 1: 2x SSC, 0.1% SDS

Wash buffer 2: 0.2x SSC, 0.1% SDS

7.4 Protein Analysis

7.4.1 Quantification of Protein Concentration According to Bradford

Protein concentration was estimated using Coomassie blue (Bradford) assay. This method takes advantage of the fact that the absorbance maximum of the dye in acidic solution will shift from 465 to 595 nm after adding protein. Protein sample was diluted in 800 µl ddH₂O, mixed with 200 µl Bradford reagents, incubated at RT for 5 min and absorbance of this mixture was measured at 595 nm. As a reference: instead of protein sample to be measured, an appropriate buffer used in the protein sample was added into the ddH₂O-Bradford reagent mixture.

7.4.2 Denaturing Discontinuous SDS PAGE (Sodium Dodecyl Sulfate Polyacrylamide Gel Electrophoresis)

Proteins are separated on polyacrylamide gel in the presence of negatively-charged detergent, SDS according to their molecular weight (Laemlli, 1970).

Gel preparation and composition:

Separating gel:

Components	8%	10%	12%
Acrylamide/Bis (39:1)	6.4 ml	8 ml	9.6 ml
1 M Tris pH 8.8	12 ml	12 ml	12 ml
10% SDS	320 µl	320 µl	320 µl
APS	400 µl	400 µl	400 µl
TEMED	20 µl	20 µl	20 µl
ddH ₂ O	12.8 ml	11.26 ml	9.66 ml
Total Volume	32 ml	32 ml	32 ml

Stacking gel:

Components	Volume
Acrylamide/Bis (39:1)	0.81 ml
0.5 M Tris pH 6.8	1 ml
10% SDS	80 μ l
APS	40 μ l
TEMED	10 μ l
ddH ₂ O	3.09 ml
Total Volume	4.5 ml

Sample preparation: a protein sample was diluted with 0.2x volume of 6x SDS loading buffer. The mixture was then heated at 95°C for 3-5 min to completely denature proteins.

Gel running: the gel was run in 1x SDS/Laemlli running buffer at 80 volt until the samples reached the top of the separating gel, and the current was increased to 120 Volt.

Following electrophoresis, proteins were visualized by methods described in 5.4.2.2

Gel running buffer: 10x SDS/Laemlli buffer: 250 mM Tris pH 6.8, 1.92 M glycine, 1% SDS
 6x SDS-loading buffer: 100 mM Tris/HCl pH 6.8, 2.5 mM EDTA, 0.1% Bromophenol blue
 50% Glycerin, 100 mM DTT (Dithioerythrol)

7.4.2.1 Detection of Proteins on Gel

Visualization of electrophoretically separated proteins requires use of dyes or stains. Organic stain such as Coomassie blue and metal-based stain, silver stain, has been adapted for protein detection on gels.

Dye staining with Coomassie Brilliant Blue

In the Coomassie blue staining, an acidic medium is required for generation of an electrostatic attraction between dye molecules and amino groups of protein. This electrostatic attraction, together with van der Waals forces, binds the dye-protein complex together. Proteins are visualized as discrete blue bands. Gel was soaked immediately after electrophoresis in a Coomassie blue fixative solution for 15 minutes and then washed with a large excess of a destaining solution. The destaining solution was changed several times, until the background has been satisfactorily removed.

Coomassie blue fixative solution: 1,25g Coomassie Brilliant Blue, 225ml Methanol, 225ml H₂O, 50ml Essigsäure (100%)

Destaining solution: 30% acetic acid, 10% methanol

Silver staining

Silver staining offers the highest sensitivity and provides more than a 100 fold increase in sensitivity over the commonly used organic protein stain, Coomassie blue. As little as 0.1 – 1 ng protein/band can be detected by silver stain that is based on the differential reduction of silver ion bound to side chain of amino acids. Reactive groups of polypeptides involved in the silver-staining reaction are the free amines and the sulfur groups. In this work, silver staining was done according to Merrill-system. The gel was briefly washed twice with ddH₂O. Proteins in the gel were fixed with fixative solution at RT for at least 1 hour. The gel was then washed 3x20 min with wash buffer. After incubation with fresh oxidizer solution (thiosulfate buffer) for 1 min, the gel was briefly washed 3x 20 sec with ddH₂O. Following soaking the gel in fresh silver reagent for 25 min, the gel was then rinsed briefly with ddH₂O for 2x 20 sec and immersed in the freshly-prepared

developer solution until satisfactory staining was achieved. Image development was stopped with stop buffer and the gel was stored in 50% methanol.

Fixative solution: 50% methanol, 12% acetic acid + 0.5 ml/L formaldehyde (added freshly)

Wash solution: 50% ethanol (gel thickness: 1 mm) or 30% ethanol (gel thickness < 1mm)

Oxidizer solution (thiosulfate buffer): 0.2 g/L $\text{Na}_2\text{S}_2\text{O}_3 \cdot 5\text{H}_2\text{O}$

Silver stain solution: 2g/L AgNO_3 , 0.75 ml/L formaldehyde (added freshly)

Developer solution: 60 g/l Na_2CO_3 0.5 ml/L formaldehyde (added freshly)

Stop solution: 50% ethanol, 12% acetic acid

7.4.3 Protein Precipitation

Protein precipitation using trichloroacetic acid (TCA)

TCA is used to concentrate protein with concentration > 5 $\mu\text{g/ml}$. 0.1-0.2x volume of TCA was added to protein solution, followed by incubation on ice at least for 30 min. The mixture was then centrifuged at 13,000 rpm at 4°C for 30 minutes. The pellet was washed with wash buffer by centrifugation at 13,000 rpm at 4°C for 10 min. This step was repeated until the pellet didn't show yellow color. The pellet was air-dried and dissolved in 2x protein loading buffer under vigorous shaking.

Protein precipitation using acetone

Precipitation technique using acetone is used if protein concentration is very low (< 1 $\mu\text{g/ml}$). Protein solution was mixed with 5x volume of ice-cold acetone and incubated on ice for at least 30 min. After centrifugation at 13,000 rpm at 4°C for 30 min, pellet was washed twice with 80% ethanol. The pellet was air-dried and dissolved in 2x protein loading buffer.

TCA Wash buffer: 70% Acetone, 20% Ethanol, 7.5% H_2O , 2.5% 2M Tris-HCl 8.0, bromphenol blue.

2x protein loading buffer: 125 mM Tris-HCl pH 6.8, 17% (v/v) glycerin, 4.1% (w/v) SDS, 0.001% (w/v) bromphenol blue, 17% (v/v) β -mercaptoethanol.

2x urea-protein loading buffer: 8M Urea, 5% SDS, 200 mM Tris-HCl pH 6.8, 1 mM EDTA, Bromphenolblue, 1.5 % DTT (freshly added).

7.4.4 Cell Extract Preparation

7.4.4.1 Preparation of Cytoplasmic Extract

FM3A cells were harvested at a cell density of 10^7 cells/ml. All steps of the cell extract preparation were carried out on ice. Cells suspension was transferred into centrifuge beakers and cells were collected by centrifugation at 500xg for 10 min at 4°C. The cell pellet was washed twice with ice cold 1xPBS pH 7.4 by centrifugation at 200xg for 10 min at 4°C and quelled on ice in lysis buffer for 15 minutes. The cell suspension was transferred into a Brown dounce homogenizer and lysed with 18 strokes. Cell breakage was evaluated under a phase-contrast microscope. To remove cell debris, organelles and unbroken cells, the lysate was spun at 3500 rpm for 15 min (Heraus centrifuge). The supernatant was centrifuged at 25,000xg for 30 min at 4°C. Protein concentrations were measured according to Bradford (7.4.1). The cell extracts were frozen in liquid N_2 and stored at -80°C.

Lysis buffer:

-1xPBS, Protease inhibitor (0.1 mM AEBSF, 0.5 mg/L leupeptin-pepstatin, 2 mg/L aprotinin), 1 mM DTT, 0.01 % NP-40.

-Hepes-buffer: 10 mM Hepes pH 7.4-7.5, Protease inhibitor (0.1 mM AEBSF, 0.5 mg/L leupeptin-pepstatin, 2 mg/L aprotinin), 150 mM NaCl, 1 mM DTT, 0.01 % NP-40.

-polysomal buffer1: 5 mM MgCl₂, 100 mM KCl, 10 mM Hepes-KOH pH 7.4, protease inhibitors (0.1 mM AEBSF, 0.5 mg/L leupeptin-pepstatin, 2mg/L aprotinin), 1 mM DTT, 0.3% NP-40.

-polysomal buffer2: 15 mM MgCl₂, 100 mM KCl, 10 mM Acetate, 10 mM Hepes-KOH pH 7.4, protease inhibitors (0.1 mM AEBSF, 0.5 mg/L leupeptin-pepstatin, 2mg/L aprotinin), 1 mM DTT, 0.3% NP-40.

7.4.4.2 Preparation of Total Cell Extract

Cells derived from suspension or adherent cultures were collected by centrifugation at 100xg for 5 min at 4°C. Following washing the cell pellet with ice-cold 1x PBS, cells were resuspended in a lysis buffer and incubated on ice for 10 min. Cell lysis was done by passing the cell suspension in a gauge 26-needle for 30 times. The lysate was centrifuged at 13,000 rpm for 10 min at 4°C. Protein concentration of the extract was determined by Bradford assay (7.4.1). The total extract was frozen in liquid N₂ and stored at -80°C.

Lysis buffer: 5 mM MgCl₂, 100 mM KCl, 10 mM Hepes-KOH pH 7.4, protease inhibitors (0.1 mM AEBSF, 0.5 mg/L leupeptin/Pepstatin, 2mg/L aprotinin), 1 mM DTT, 0.3% NP-40.

7.4.5 Covalent Coupling of Protein on Affinity Matrix

There are several techniques used for covalent binding of proteins to solid phase matrices. In this study, covalent coupling mediated by a bifunctional reagent dimethylpimelidate (DMP) and cyanogen bromide activated sepharose were applied to crosslink antigens to an appropriate matrix for subsequent antibody purification (7.5.2) and to crosslink antibody to protein A-sepharose beads for Immunopurification (7.5.3).

Covalent coupling protein by Dimethylpimelidate (DMP)

Following binding of protein to appropriate beads, the beads were washed twice with 10xV of 0.2 M Sodium borate (pH 9.0) by centrifugation at 1000xg for 5 min at RT. The beads were then resuspended in 20 mM DMP in 0.2 M Sodium borate (pH 9.0) and incubated for 30 min at RT on a rocker. The reaction was then stopped by washing the beads once in 0.2 M ethanolamine pH 8.0. The beads were then incubated with 0.2 M ethanolamine pH 8.0 for 2 hours at RT to block active groups. After incubation, the beads were washed with 1xPBS and could be stored at 4°C in 1x PBS + 0.01% NaN₃. To evaluate the efficiency of covalent coupling, a 10µl-aliquot of beads was collected before addition of DMP and after the final wash and then analyzed by SDS PAGE.

Covalent coupling protein to cyanogen bromide activated sepharose beads

Proteins to be covalently coupled to cyanogen bromide (CNBr)-activated sepharose beads were previously dialyzed against coupling buffer for 2x 8 hours. The protein solution was added to an appropriate amount of cyanogen bromide activated sepharose beads and incubated for 1 hour at RT or overnight at 4°C. Excess proteins were washed three times, each with at least 5x volumes of coupling buffer. Unused active groups were blocked by incubating the beads with 0.1 M Tris-Cl buffer pH 8.0 for 2 hours at RT. The cross linking products were washed with at least three cycles of alternating pH (wash buffer 1 and wash buffer 2). The beads were then washed with 1x PBS and can be stored in 1x PBS + 0.01% NaN₃ at 4°C prior to use.

Coupling buffer: 0.1 M NaHCO₃ pH 8.3, 0.5 M NaCl

Wash buffer 1: 0.1 Acetate buffer pH 4.0, 0.5 M NaCl

Wash buffer 2: 0.1 M Tris-Cl buffer pH 8.0, 0.5 M NaCl

7.4.6 Protein Expression and Purification

7.4.6.1 Protein Expression in Bacterial Cells

One single colony was inoculated into 50 ml superbrot medium in the presence of appropriate antibiotics at 37° C overnight under vigorous shaking. The 50 ml-bacterial pre-culture were transferred into a 5 L flask containing 1 L superbrot medium and incubated for 5 hours at 37°C under shaking followed by addition of 1 L superbrot medium. Temperature was then set to 10°C and protein expression was induced by adding IPTG at the final concentration of 1 mM. The cells were grown at 10°C overnight.

7.4.6.2 Protein Purification

7.4.6.2.1 Purification of GST Fusion Proteins by Affinity Chromatography on Glutathione Sepharose Beads

GST-fusion proteins expressed in *E. coli* cells were purified to a near homogeneity by affinity chromatography on glutathione sepharose bead matrix.

Preparation of glutathione sepharose beads: an appropriate amount of glutathione sepharose beads was washed three times with at least 10x volume of ice-cold lysis buffer by centrifugation at 200xg for 5 min. The suspension was kept on ice until it was ready to use.

Preparation of bacterial cell extract: bacterial cells containing GST fusion proteins of 2 L culture were collected by centrifugation at 500xg at 4°C for 10 min. The cell pellet was resuspended in 50 ml ice-cold lysis buffer and incubated for 10 min on ice. The cells were lysed by sonification at 50% input for 4x30 sec. To remove insoluble debris, the cell suspension was centrifuged at 35,000 rpm for 30 min at 4°C in a 45Ti Beckmann rotor. The supernatant was directed to the purification step.

Purification of fusion proteins: the cell lysate was incubated with prepared affinity matrix for 3 hours at 4°C. Bound matrix was washed by at least three cycle of alternating washing with high salt and low salt buffers. The fusion protein was eluted from the resin by adding an appropriate volume of glutathione elution buffer and followed by incubation for 10 min at 4°C. The eluted protein was analyzed by SDS polyacrylamide gel electrophoresis. If required, the eluate was directed to dialyses. Protein concentration was determined according to Bradford (7.4.1).

Lysis buffer: 20 mM Hepes-KOH pH 7.5; 200 mM NaCl; Protease inhibitors (0.1 mM AEBSF, 0.5 mg/L leupeptin/pepstatin A, 2 mg/L aprotinin); 0.01% NP-40; 1 mM DTT (DTT and protease inhibitors were freshly added).

Wash buffer: High salt: 20 mM Hepes-KOH pH 7.5; 1 M NaCl

Low salt: 20 mM Hepes-KOH pH 7.5; 200 mM NaCl

Elution buffer: 30 mM reduced glutathione; 20 mM Hepes-KOH pH 8.0; 200 mM NaCl

7.4.6.2.2 Purification of Histidine-Tagged Proteins By Immobilized Ni²⁺ Affinity Chromatography

Recombinant proteins containing polyhistidine tracts or 6-his were purified through a resin charged with divalent nickel ions, Ni-NTA agarose (Qiagen).

Preparation of Ni-NTA agarose: done as described in 7.4.6.2.1

Preparation of bacterial cell lysate: done as described in 7.4.6.2.1

Purification of 6xHis-tagged proteins: The cell lysate was transferred to a tube containing previously washed Ni-NTA agarose and incubated for 3 hours at 4°C. The beads were washed

with at least three cycles of alternating salt concentrations (high salt and low salt wash buffers). Elution was performed by incubating the beads with imidazole elution buffer for 10 min at 4°C. Each fraction was analyzed by SDS PAGE followed by Coomassie staining, and if necessary, the eluted protein was subjected to dialysis. Protein concentration was determined using Bradford assay (7.4.1).

Lysis buffer: 50 mM Na⁺PO₄⁻ pH 8; 200 mM NaCl; 10 mM imidazole pH 8.0; protease inhibitors (0.1 mM AEBSF, 0.5 mg/L leupeptin-pepstatin A, 2 mg/L aprotinin); 5 mM β-mercaptoethanol; 0.01% NP-40 (protease inhibitors and β-mercaptoethanol were freshly added)

Wash buffer: High salt: 50 mM Na⁺PO₄⁻ pH 8; 1M NaCl; 20 mM imidazole pH 8.0

Low salt: 50 mM Na⁺PO₄⁻ pH 8; 200 mM NaCl; 20 mM imidazole pH 8.0

Elution buffer: 50 mM Na⁺PO₄⁻ pH 8; 200 mM NaCl; 300 mM imidazole pH 8.0.

7.4.6.2.3 Purification of GST-His Recombinant Proteins (Two-Step Purification)

Recombinant proteins containing two different tags, namely GST and His tags (see Materials), were purified by combining two purification protocols previously described (7.4.6.2.1 and 7.4.6.2.2). First, the recombinant protein was purified through a glutathione sepharose matrix column (7.4.6.2.1). The beads were washed and subject to PreScission protease. The cleavage product, namely the recombinant protein containing a 6His tag, was released in the flow through, while the GST cleavage product remained bound on the beads. The flow through was incubated with Ni-NTA agarose as described in 7.4.6.2.2.

Site-specific proteolytic cleavage of fusion proteins: the appropriate site-specific protease solution (PreScission Protease) was added to the purified fusion protein and incubated at 4°C for 2-16 hours.

7.4.7 Protein Separation using Centrifugation

Linear Continuous 5-30% Glycerol Gradient

5%-30% (v/v) glycerol gradient in an appropriate buffer (PBS or Hepes buffer) was prepared by using Gradient mixer. The gradient was allowed to stand at least 30 minutes at 4°C prior loading. Approximately 0.5 ml cell extract containing 5-10 mg protein was carefully layered on the top of the gradient. Proteins then were sedimented at 38,000 rpm 4°C for 5 h in a SW41Ti Beckmann rotor. 17 700 μl-fractions were collected and the protein was precipitated using TCA (see). For RNA analysis, 100 μl of each fraction was mixed with 100 μl PK buffer and 200 μl Phenol (7.3.1).

Analysis of Polysomal and Ribosomal Profiles using Linear Sucrose Gradient

Linear gradients of 20%- 50% and 7%-47% sucrose were prepared in 10 mM Hepes KOH pH 7.4, 100 mM KCl, 5 mM MgCl₂. 300-500μl total cell extract were gently layered onto the gradient and centrifuged for 2h 15 min at 40,000 rpm in a Beckmann SW 41 Ti rotor.

Linear 5-30% sucrose gradients were prepared in buffer containing 15 mM MgCl₂, 100 mM KCl, 10 mM acetate, 10 mM Hepes-KOH pH 7.4. Extracts were separated by centrifugation at 40,000 rpm in a Beckmann SW41Ti rotor.

To analyze ribosome dissociation, instead of MgCl₂, 15 mM EDTA was added into lysis buffer and gradient buffer. Linear sucrose gradients containing EDTA were run at 40,000 rpm for 4 hours in a Beckmann SW41Ti rotor.

20-600 μl gradient fractions were collected. 100 μl of each fraction were directed to RNA isolation (7.3.1). 100 μl were used for RNA measurement at A254nm (7.1.2) and the remaining fractions were TCA-precipitated (7.4.3).

7.4.8 Dialysis of Protein

Dialysis is useful for exchange of buffer or removal of low-molecular weight solutes after protein purification. The process of dialysis is driven by the difference in concentration of solutes on the two sides of a dialysis membrane. A semi permeable membrane separating protein solution from dialysis buffer allows free passage of molecules below a certain molecular weight, the so called molecular weight cutoff MWCO, while molecules larger than MWCO of dialysis membrane cannot penetrate the membrane pores.

Membrane preparation: dialysis tubing/membrane (Spectra/Por Biotech) was soaked in a large volume of deionized water for 30 min at RT.

Dialysis: protein solution to be dialyzed was loaded into a tubing of an appropriate length. The filled tubing was placed in 1x isotonic buffer contained in a beaker. Volume of dialysis buffer used was equal to 1000x of total sample volume. The dialysis buffer was mixed using a magnetic stirrer and dialysis was run overnight in the cold room.

7.4.9 Purification Using GST-Fusion Protein as Affinity Matrix (GST Pull-Down)

GST fusion protein is commonly applied to study protein-protein interactions and to identify proteins interacting with a protein of interest. In this study, GST pull-down was used to search for proteins in cellular extracts which potentially associates with IGHMBP2. 100 µg GST-IGHMBP2-6His or 100 µg GST alone were immobilized on glutathione sepharose beads. The beads were washed three times with ice-cold wash buffer by centrifugation at 100xg for 3 min at 4°C and were then incubated with 10 ml FM3A cytosolic extract (10 mg/ml) for 1 hour at 4°C. Unbound proteins were removed by washing with 2x 10 ml ice-cold wash buffer and centrifugation at 100xg for 3 min at 4°C. The beads were transferred to a new 1.5 ml tube and washed with 4x 1.5 ml ice-cold wash buffer by centrifugation at 100xg for 2 min at 4°C. GST recombinant protein and its bound proteins were eluted twice with 300µl ice-cold glutathione elution buffer, each with 10 min incubation at 4°C on a rocker. Proteins eluted were TCA-precipitated (7.4.3) and analyzed by SDS PAGE.

Wash buffer: 10 mM Hepes pH 7.4-7.5, 150 mM NaCl, 10% glycerol

Elution buffer: 50 mM glutathione SH, 10 mM Hepes pH 8.0, 150 mM NaCl

7.4.10 ATPase Assay

Radioactively-labeled ATP ($[\alpha\text{-}^{32}\text{P}]\text{-ATP}$) was incubated with 0.9 pmol protein (100 ng recombinant IGHMBP2) in 50 µl of a standard ATPase reaction mixture for 1 h at 37°C. ATPase reaction was stimulated by addition of single-stranded homopolymer RNA (poly (A), poly (G), poly (U), poly (G), Sigma-Aldrich) and double-stranded DNA (GE Healthcare) with the end concentration of 0.1 mg/ml. The reaction was stopped by addition of 1x volume of stop buffer. 0.8 µl of the reaction mixture was analyzed on PEI (poly-(ethylenimin)) cellulose thin-layer chromatography plates (Merck) and visualized by autoradiography and Bas200-phosphoImager/Fujifilm Europe GmbH (7.1.3.3). To identify the position of the hydrolysis product, $[\alpha\text{-}^{32}\text{P}]\text{-ATP}$ was incubated with 0.1U calf intestine phosphatase for 6 min at 37°C and loaded on PEI cellulose thin-layer chromatography plates parallel with the ATPase reaction mixture. Quantification of the hydrolysis product was done using TINA v2.0-Software (Raytest Isotop Messgeräte GmbH).

ATPase reaction mixture: 50 mM triethanolamine pH 8.2, 75 mM KCl, 1.5 mM MgCl_2 , 1.25 mM DTT, 10% glycerol and 20µM $[\alpha\text{-}^{32}\text{P}]\text{-ATP}$ (Amersham; specific activity 0.4 Ci/mmol).

Stop buffer: 0.5 M Na₂EDTA pH 8.0

7.5 Immunological and Immunobiochemical Analysis

7.5.1 Production of Polyclonal Antibody

Polyclonal antibodies were generated by immunizing rabbits with bacterially-expressed antigen. In this study, different anti mouse Ighmbp2 antibodies were produced: anti GST-flIghmbp2 antibody; anti GST-NT Ighmbp2; anti N-terminal Ighmbp2-6his (see Materials). The recombinant Ighmbp2 tagged with 6his or GST was expressed and purified as described in 7.4.6.2.1 and 7.4.6.2.2. Injection of antigen to rabbit was done by Immunoglobine GmbH Himmelstadt.

7.5.2 Antibody Purification using Affinity Chromatography

Antibodies are purified from serum by immunoaffinity chromatography. In this technique, antigen is covalently coupled to an affinity matrix and antibodies from the polyclonal pool are allowed to bind the antigen.

Preparation of an affinity column: see 7.4.5

Purification of antibody from serum: Eight ml of serum were incubated in an affinity column containing an appropriate antigen (~ 1 mg/ml) at 4°C overnight. The column was then washed three times with 10x ice-cold 1xPBS and subsequently eluted by pH shock with 10x 900 µl 100 mM glycine pH. 2.7. To neutralize the antibody solution, each eluted fraction was mixed with 100µl 1 M Tris pH 8.0. Antibody eluted was analyzed on SDS polyacrylamide gel. The fractions containing high amount of antibody was pooled and dialyzed against 1x PBS overnight. Protein concentration was determined as described in 7.4.1 and antibody was stored at -80°C.

7.5.3 Immunaffinity purification

Immunaffinity purification is a common biochemical approach to search for novel proteins that interact with a known protein of interest. This method takes advantage of the fact that protein-protein interactions in the living cell are conserved when a cell is lysed under non-denaturing condition. Protein of interest, in this case Ighmbp2, is immunoprecipitated with an antibody directed against Ighmbp2. If some proteins are physically associated with Ighmbp2 *in vivo*, they can be immunoprecipitated with Ighmbp2.

Preparation of an immunaffinity column: 500 µg antibodies were incubated to 250 µl (bed volume) protein A sepharose beads overnight at 4°C. The beads were then washed three times with 10V of 1xPBS at RT and subjected to covalent coupling by DMP (7.4.5). Prior to incubation with cell extracts, the column was washed with 3xV 100 mM glycine pH 2.7 to remove antibody molecules non-covalently bound to the matrix.

Binding and purification of antibody-antigen complex: FM3A cytosolic extracts or gradient fractions were incubated with anti polyclonal Ighmbp2 antibody immobilized on protein A-sepharose beads (see above) for 1 hour at 4°C. The beads were washed with an ice-cold appropriate buffer containing 0.01% NP-40. This wash step was repeated 4 times and the beads were then transferred to a new tube and washed once with an ice-cold appropriate buffer. Proteins were eluted by incubation in 100 mM glycine pH 2.7 for 10 min at 4°C. The eluate was subsequently concentrated using TCA or acetone (7.4.3).

7.5.4 Western Blot Analysis

Western blot was used to transfer proteins separated on SDS gel to a nitrocellulose membrane. In this work, Western blot was performed using semi-dry technique.

Gel preparation: see SDS PAGE 7.4.2

Western transfer of proteins: all Whatman papers and nitrocellulose membrane were previously placed in blot buffer. The blot apparatus was set up as following: katode-3 Whatman papers-a nitrocellulose membrane-the protein gel-3 Whatman membrane-anode. Protein transfer on the membrane was carried out for 3 hours at 200 mA and evaluated by staining with Ponceau S solution for several minutes. For destaining, the membrane was rinsed with ddH₂O.

Protein detection: The membrane was incubated with the blocking solution for 30 min at RT or overnight at 4°C and subsequently incubated with the primary antibody for 1 hour at RT. The blot was then washed for 4x 5min with 1x TBT. Following incubation with the appropriate secondary antibody for 1 hour, the blot was washed for 4x5 min with 1x TBT, incubated with ECL developing solution and exposed to film in the dark room.

Transfer buffer: 70% 10x Laemmli buffer, 30% Methanol

Ponceau S solution: 0.1% ponceau S in 1% acetic acid (w/v)

Blocking solution: 10% Milk in 1x wash buffer

ECL (enhanced chemoluminescence): Solution 1: 6.8mM coumaric acid in DMSO; solution 2: 1.25mM Luminol, 100mM Tris pH 8.5; solution 3: 30% H₂O₂ (these solutions were mixed shortly before used)

7.6 Methods in Cell Culture

7.6.1 Cell Cultivation

FM3A cells were cultivated *in vitro* in RPMI medium+ L-Glutamine supplemented with 50 µg/ml penicillin, 50 µg/ml streptomycin, 10% (v/v) heat-inactivated fetal calf serum (FCS). The culture was incubated at 37°C with 5% CO₂ under mild shaking.

HeLa, 293, COS7 and 3T3 cells were cultured in DMEM plus 10% fetal calf serum, 2 mM glutamine, in the presence of 50 µg/ml streptomycin and 50 µg/ml penicillin at 37° C with 5% CO₂.

7.6.2 Determination of Cell Density

Cell density was quantified using a hemacytometer “Neubauer”. A hemacytometer Neubauer consists of two chambers, each with a volume of 0.1 mm³. The grid is divided by triple lines into 9 large squares each with 1mm x 1mm. Each large square is divided into 25 medium squares and each medium square is further divided into 16 smaller squares. The number of cells is counted from one large square consisting of 25 medium squared. The cell density is determined according to an equation: cell density= $N \times 10^4$ /ml (N is number of counted cells; 10⁴ is chamber conversion factor for Neubauer).

7.6.3 Cell Transfection

7.6.3.1 Transfection using Nanofectin

24 hours prior to transfection, HeLa cells were seeded in 6-wells plates at the density of 2.4×10^5 per well. The medium was changed 2-4 hours before transfection. A transfection mixture for a 3.5 cm^3 culture dish was prepared as following:

Solution A: 3 μg DNA + 100 μl NaCl mixed briefly using vortex

Solution B: 9.6 μl Nanofectin + 100 μl NaCl, mixed briefly using vortex

Solution B was added to solution A and incubated for 20-30 min at RT. The transfection mix was drop wise added to cells. 48 hours after transfection, cells were harvested and directed to subsequent analysis.

7.6.3.2 siRNA transfection using Oligofectamine

For RNAi experiment, siRNAs were transfected into HeLa cells using a transfection agent Oligofectamine.

Cell preparation: 24 hours before transfection, HeLa cells were trypsinized and resuspended in DMEM medium supplemented with 10% FCS without antibiotics. The cells were seeded on 6 wells-plates at the density of 1.3×10^5 per well. Short prior to transfection, the cells were washed with medium without antibiotic and 800 μl Opti-MEM without antibiotics and FCS were added into the culture.

Transfection using Oligofectamine:

Transfection mix for one reaction:

Solution A: 11 μl Opti-MEM

4 μl Oligofectamine

Solution B: 10 μl 20 μM dsRNA

175 μl Opti-MEM

Solution A and B were incubated for 10 min at RT, mixed and incubated for an additional 20 min at RT. The transfection mix was drop wise added to the cells and mixed thoroughly. After incubation of the cells for 4 hours at 37°C and 5% CO_2 , 500 μl m Opti-MEM supplemented with 30% FCS. The cells were grown at 37°C and harvested at 24 hours, 48 hours, and 72 hours after siRNA transfection.

Cell extract preparation: The cells were washed twice with 1x PBS. 250 μl lysis buffers were added to each well. The cells were collected using cell scraper. Cell extraction was done as described 7.4.4.2. Cell extract concentration was determined using Bradford reagent (7.4.1) and proteins were analyzed by Western blot (7.5.4).

7.6.4 Metabolic Protein Labeling using ^{35}S

Proteins synthesis was traced by incorporating ^{35}S -methionine into polypeptide during translation. 72 hours after siRNA transfection, cells were washed with methionine-free DMEM supplemented with 10% FCS and 50 $\mu\text{g}/\text{ml}$ penicillin-streptomycin. The medium was discharged and replaced with fresh methionine-free DMEM. The cells were then incubated with ^{35}S methionine –containing DMEM medium for 1-3 hours at 37°C and washed with 1x PBS. Cell extract was prepared by adding hepes-lysis buffer in the cell culture (250 μl per 35 mm^2 dish). The cells were detached using a sterile cell scraper. Cell lysis was done by passing the lysate through a pipette several times or by three cycles of freezing and thawing the cells.

7.6.5 β -globin mRNA Reporter-Based Tethering Assay

Transfection: For this assay, transfection was performed using BBS/CaCl₂ method. One day prior to transfection, HeLa cells were grown at the density of 2.4×10^5 . Two hours before transfection, the medium was changed. Transfection mixture was prepared as following:

Plasmid DNAs: 1 μ g expression plasmid
 0.2 μ g reporter plasmid
 0.2 μ g GFP expression vector
 0.6 μ g translation efficiency control plasmid (internal control)
 Ad sterile ddH₂O to 90 μ l

Plasmid DNAs were mixed with 8 μ l 2.5 M CaCl₂ (final concentration 200 mM). 100 μ l 2x BBS was added to this DNA-CaCl₂ solution was thoroughly mixed and incubated at RT for 30 min. The transfection mix was added to the cell culture dishes and mixed gently. For the first 20 hours, the cells were grown at 37°C in the presence of 3 % CO₂. The precipitate was formed during this incubation step. The cells were then washed with TBS to remove precipitate and fresh medium was added. The cells were incubated for an additional 24 hours for optimal expression.

Cell extract preparation: 250 μ l of lysis buffer was added to each well of 6-wells plate. Cells were detached from the plate using scraper, and cell lysis was achieved by passing the cell suspension through a pipette several times. The homogenized lysate was transferred to a fresh tube and incubated on ice for 5 min. To remove nuclei and cell debris, the lysate was centrifuged at 10,000 rpm at 4°C for 10 min. 30 μ l of lysate was used for western blot analysis and the remaining was directed to RNA analysis.

RNA was isolated according to 7.3.2 and analyzed by Northern blot (7.3.7).

Data quantification: level of β -globin mRNA was described as a percentage of the radioactivity of reporter mRNA in relation with that of the corresponding internal control.

2x BES-buffered saline (BBS): 50 mM BES (*N,N*-bis[2-hydroxyethyl]-2-aminoethanesulfonic acid), 280 mM NaCl, 1.5 mM Na₂HPO₄·2H₂O, pH 6.96.

TBS (Tris-buffered saline): 8 g NaCl, 0.2 g KCl, 3 g Tris base, pH 7.4.

Lysis buffer: 10 mM Tris-HCl pH 7.2, 8 mM MgCl₂, 10 mM NaCl, 1 mM DTT, 5 mM Vanadyl-Ribosyl-Complex (VRC), 0.5% NP-40, 1.5 mM PMSF.

MS2-based tethering system: expression plasmid: pCI-MS2, pCI-MS2-IGHMBP2, pCI-MS2-hUpf2, pCI-MS2-hUpf1
 mRNA reporter plasmid: pCI-WT β globin-6MS2

λ N-based tethering system: expression plasmid: pCI- λ N, pCI- λ N-IGHMBP2, pCI- λ N-hUpf3b
 mRNA reporter plasmid: pCI-WT β globin-4BoxB

Translation efficiency control plasmid: pCI-WT β globin+e300

7.6.6 Immunofluorescence Microscopy

Cells grown on glass coverslips were rinsed with 1xPBS, fixed with 4% formaldehyde for 30-45 min at 4°C. The cells were washed with 1xPBS pH 7.4 for 3x 5 min, permeabilized and blocked with 0.3% triton X-100 in blocking buffer for 1h at RT. After 3x 5 min washing, the cells were stained with the primary antibody diluted in wash buffer for 2 hours at RT. The cells were then washed three times with wash buffer for 5 min and incubated with the corresponding fluorescent-conjugated secondary antibody made in wash buffer for 1 h at RT, followed by three 5-min washes in wash buffer containing DAPI. Cells were mounted in fluorescent mounting medium (Daco) and viewed using Carl Zeiss.

For double staining immunolocalization studies, two rounds of immunodetection were performed: the cells were first incubated with the first primary antibody for 2 hours at RT and the appropriate rabbit secondary antibody followed by the second round with the second primary and its appropriate secondary antibodies.

Blocking buffer: 10% BSA in PBS pH 7.4

Wash buffer: 1% BSA in PBS pH 7.4

8. ABBREVIATIONS

A	Adenosine	min	minute
ATP	Adenosine 5'-triphosphate	ml	Milliliter
C	Cytosine	mRNA	messenger RNA
cDNA	Copy DNA	MS	Mass spectrometry
Ci	Curie	N-terminus	Amino-terminus
C-terminus	Carboxyl-terminus	NTP	Nucleoside-5'-triphosphate
dATP	2',3'deoxyadenosine 5' triphosphate	pH	A measure of the acidity or alkalinity of a solution
ddH ₂ O	double distilled water		
Da	Dalton	pmol	Pico mole
DMSO	Dimethyl sulfoxide	RNA	Ribonucleic acid
DNA	Deoxyribonucleic acid	RNase	Ribonuclease
DNase	Deoxyribonuclease	RNP	Ribonucleoprotein
dNTP	2',3'deoxy nucleoside 5' triphosphate	Rpm	Rotation per minute
<i>E. coli</i>	<i>Escherichia coli</i>	rRNA	Ribosomal RNA
<i>et al.</i>	And others (Lat.: <i>Et alterae</i>)	RT	Room temperature
G	Guanosine	S	Svedberg
<i>In vitro</i>	within the reagent glass	Sec	Second
<i>In vivo</i>	in living organism	U	Uracyl
L	Liter	UTR	Untranslated region
kDa	Kilo Dalton	UV	Ultraviolet light
M	Molar (mol/L)	v/v	volume per volume
mA	Milliampere	w/v	weight per volume
MIM	Mendelian Inheritance in Man		

The single letter amino acid code

G	Glycine	P	Proline
A	Alanine	V	Valine
L	Leucine	I	Isoleucine
M	Methionine	C	Cysteine
F	Phenylalanine	Y	Tyrosine
W	Tryptophan	H	Histidine
K	Lysine	R	Arginine
Q	Glutamine	N	Asparagine
E	Glutamic Acid	D	Aspartic Acid
S	Serine	T	Threonine

9. REFERENCES

- Anderson JS and Parker RP. 1998. The 3' to 5' degradation of yeast mRNAs is a general mechanism for mRNA turnover that requires the SKI2 DEVH box protein and 3' to 5' exonucleases of the exosome complex. *EMBO J.* 17(5):1497-506.
- Atkin AL, Altamura N, Leeds P, Culbertson MR. 1995. The majority of yeast UPF1 co-localizes with polyribosomes in the cytoplasm. *Mol Biol Cell* 6(5):611-25.
- Birnboim HC and Doly J. 1979. A rapid alkaline extraction procedure for screening recombinant plasmid DNA. *Nucleic Acids Res.* 7(6):1513-23.
- Biswas EE, Nagele RG, Biswas S. 2001. A novel human hexameric DNA helicase: expression, purification and characterization. *Nucleic Acids Res.* 29(8):1733-40.
- Biswas EE, Fricke WM, Chen PH, Biswas SB. 1997. Yeast DNA helicase A: cloning, expression, purification, and enzymatic characterization. *Biochemistry* 36(43):13277-84.
- Bhattacharya A, Czaplinski K, Trifillis P, He F, Jacobson A, Peltz SW. 2000. Characterization of the biochemical properties of the human Upf1 gene product that is involved in nonsense-mediated mRNA decay. *RNA* 6(9):1226-35.
- Brown V, Small K, Lakkis L, Feng Y, Gunter C, Wilkinson KD, Warren ST. 1998. Purified recombinant Fmrp exhibits selective RNA binding as an intrinsic property of the fragile X mental retardation protein. *J Biol Chem.* 273(25):15521-7.
- Chang YF, Imam JS, Wilkinson MF. 2007. The nonsense-mediated decay RNA surveillance pathway. *Annu Rev Biochem.* 76:51-74.
- Chen NN, Kerr D, Chang CF, Honjo T, Khalili K. 1997. Evidence for regulation of transcription and replication of the human neurotropic virus JCV genome by the human S(mu)bp-2 protein in glial cells. *Gene* 185(1):55-62.
- Chen YZ, Hashemi SH, Anderson SK, Huang Y, Moreira MC, Lynch DR, Glass IA, Chance PF, Bennett CL. 2006 Senataxin, the yeast Sen1p orthologue: characterization of a unique protein in which recessive mutations cause ataxia and dominant mutations cause motor neuron disease. *Neurobiol Dis.* 23(1):97-108.
- Cheng Z, Muhlrud D, Lim MK, Parker R, Song H. 2007. Structural and functional insights into the human Upf1 helicase core. *EMBO J.* 26(1):253-64.
- Cook SA, Johnson KR, Bronson RT, Davisson MT. 1995. Neuromuscular degeneration (nmd): a mutation on mouse chromosome 19 that causes motor neuron degeneration. *Mamm Genome* 6(3):187-91.
- Cordin O, Banroques J, Tanner NK, Linder P. 2006. The DEAD-box protein family of RNA helicases. *Gene* 367: 17-37. Review.
- Cox GA, Mahaffey CL, Frankel WN. 1998. Identification of the mouse neuromuscular degeneration gene and mapping of a second site suppressor allele. *Neuron* 21(6):1327-37.
- Czaplinski K, Majlesi N, Banerjee T, Peltz SW. 2000. Mtt1 is a Upf1-like helicase that interacts with the translation termination factors and whose over expression can modulate termination efficiency. *RNA* 6(5):730-43.

- Czaplinski K, Weng Y, Hagan KW, Peltz SW. 1995. Purification and characterization of the Upf1 protein: a factor involved in translation and mRNA degradation. *RNA* 1(6):610-23.
- de la Cruz J, Kressler D, Linder P. 1999. Unwinding RNA in *Saccharomyces cerevisiae*: DEAD-box proteins and related families. *Trends Biochem Sci.* 24(5):192-8. Review.
- Diers A, Kaczinski M, Grohmann K, Hübner C, Stoltenburg-Didinger G. 2005. The ultra structure of peripheral nerve, motor end-plate and skeletal muscle in patients suffering from spinal muscular atrophy with respiratory distress type 1 (SMARD1). *Acta Neuropathol (Berl)* 110(3):289-97.
- Feng Y, Absher D, Eberhart DE, Brown V, Malter HE, Warren ST. 1997. FMRP associates with polyribosomes as an mRNP, and the I304N mutation of severe fragile X syndrome abolishes this association. *Mol Cell.* 1(1):109-18.
- Fukita Y, Mizuta TR, Shirozu M, Ozawa K, Shimizu A, Honjo T. 1993. The human S mu bp-2, a DNA-binding protein specific to the single-stranded guanine-rich sequence related to the immunoglobulin mu chain switch region. *J Biol Chem.* 268(23):17463-70.
- Gamsjaeger R, Liew CK, Loughlin FE, Crossley M, Mackay JP. 2007. Sticky fingers: zinc-fingers as protein-recognition motifs. *Trends Biochem Sci.* 32(2):63-70. Review.
- Gehring NH, Neu-Yilik G, Schell T, Hentze MW, Kulozik AE. 2003. Y14 and hUpf3b form an NMD-activating complex. *Mol Cell* 11(4):939-49
- Giannini A, Pinto AM, Rossetti G, Prandi E, Tiziano D, Brahe C, Nardocci N. 2006. Respiratory failure in infants due to spinal muscular atrophy with respiratory distress type 1. *Intensive Care Med.* 32(11):1851-5. Review.
- Gorbalenya, A. E. and Koonin, E. V. 1993. Helicases: amino acid sequence comparisons and structure-function relationships. *Curr Opin Struct Biol.* 3(4): 419-429.
- Graves-Woodward KL, Gottlieb J, Challberg MD, Weller SK. 1997. Biochemical analyses of mutations in the HSV-1 helicase-primase that alter ATP hydrolysis, DNA unwinding, and coupling between hydrolysis and unwinding. *J Biol Chem.* 272(7):4623-30.
- Grishin NV. 1998. The R3H motif: a domain that binds single-stranded nucleic acids. *Trends Biochem Sci.* 23(9):329-30.
- Grohmann K, Rossoll W, Kobsar I, Holtmann B, Jablonka S, Wessig C, Stoltenburg-Didinger G, Fischer U, Hübner C, Martini R, Sendtner M. 2004. Characterization of Ighmbp2 in motor neurons and implications for the pathomechanism in a mouse model of human spinal muscular atrophy with respiratory distress type 1 (SMARD1). *Hum Mol Genet.* 13(18):2031-42. Epub 2004 Jul 21.
- Grohmann K, Varon R, Stolz P, Schuelke M, Janetzki C, Bertini E, Bushby K, Muntoni F, Ouvrier R, Van Maldergem L, Goemans NM, Lochmüller H, Eichholz S, Adams C, Bosch F, Grattan-Smith P, Navarro C, Neitzel H, Polster T, Topaloglu H, Steglich C, Guenther UP, Zerres K, Rudnik-Schöneborn S, Hübner C. 2003. Infantile spinal muscular atrophy with respiratory distress type 1 (SMARD1). *Ann Neurol.* 54(6):719-24.
- Grohmann K, Schuelke M, Diers A, Hoffmann K, Lucke B, Adams C, Bertini E, Leonhardt-Horti H, Muntoni F, Ouvrier R, Pfeufer A, Rossi R, Van Maldergem L, Wilmschurst JM, Wienker TF, Sendtner M, Rudnik-Schöneborn S, Zerres K, Hübner C. 2001. Mutations in the gene encoding immunoglobulin mu-binding protein 2 cause spinal muscular atrophy with respiratory distress type 1. *Nat Genet.* 29(1):75-7.
- Gross T, Siepmann A, Sturm D, Windgassen M, Scarcelli JJ, Seedorf M, Cole CN, Krebber H. 2007. The DEAD-box RNA helicase Dbp5 functions in translation termination. *Science* 315(5812):646-9.

- Guenther UP, Varon R, Schlicke M, Dutrannoy V, Volk A, Hubner C, von Au K, Schuelke M. 2007a. Clinical and mutational profile in spinal muscular atrophy with respiratory distress (SMARD): defining novel phenotypes through hierarchical cluster analysis. *Hum Mutat.* 28(8):808-815.
- Guenther UP, Varon R, Handoko L, Stephani U, Tsao C-Y, Mendell JR, Hübner C, von Au K, Schuelke M. 2007b. Clinical variability in Spinal Muscular Atrophy with Respiratory Distress Type 1 (SMARD1): Determination of steady stage protein level in patients with infantile and juvenile disease onset (submitted in *J. Mol. Med.*).
- Guenther UP, Schuelke M, Bertini E, D'Amico A, Goemans N, Grohmann K, Hübner C, Varon R. 2004. Genomic rearrangements at the IGHMBP2 gene locus in two patients with SMARD1. *Hum Genet.* 115(4):319-26.
- Ho JH, Kallstrom G, Johnson AW. 2000. Nmd3p is a Crm1p-dependent adapter protein for nuclear export of the large ribosomal subunit. *J Cell Biol.* 151(5):1057-66.
- Ho JH, Kallstrom G, Johnson AW. 2000. Nascent 60S ribosomal subunits enter the free pool bound by Nmd3p. *RNA* 6(11):1625-34.
- Kerr D, Khalili K. 1991. A recombinant cDNA derived from human brain encodes a DNA binding protein that stimulates transcription of the human neurotropic virus JCV. *J Biol Chem.* 266(24):15876-81.
- Kolb SJ, Battle DJ, Dreyfuss G. 2007. Molecular Functions of the SMN Complex. *J Child Neurol.* 2007 22(8):990-4.
- Koonin EV. 1992. A new group of putative RNA helicases. *Trends Biochem Sci.* 17(12):495-7. Review.
- Lehner B, Sanderson CM. 2004. A protein interaction framework for human mRNA degradation. *Genome Res.* 14(7):1315-23.
- Liepinsh E, Genereux C, Dehareng D, Joris B, Otting G. 2003. Solution structure of the R3H domain from human Smubp-2. *J Mol Biol.* 326(1):217-23.
- Lorsch JR and Herschlag D. 1998. The DEAD box protein eIF4A. 2. A cycle of nucleotide and RNA-dependent conformational changes. *Biochemistry* 37. 2194-2206.
- Lykke-Andersen, M. Shu, J. Steitz. 2000. Human Upf Proteins Target an mRNA for Nonsense-Mediated Decay When Bound Downstream of a Termination Codon. *Cell.* 103(7):1121-31
- Maddatu TP, Garvey SM, Schroeder DG, Hampton TG, Cox GA. 2004. Transgenic rescue of neurogenic atrophy in the nmd mouse reveals a role for Ighmbp2 in dilated cardiomyopathy. *Hum Mol Genet.* 13(11):1105-15.
- Maystadt I, Zarhrate M, Landrieu P, Boespflug-Tanguy O, Sukno S, Collignon P, Melki J, Verellen-Dumoulin C, Munnich A, Viollet L. 2004. Allelic heterogeneity of SMARD1 at the IGHMBP2 locus. *Hum Mutat.* 23(5):525-6.
- Milligan & Uhlenbeck. 1989. Synthesis of small RNAs using T7 RNA polymerase. *Methods Enzymol.* 180:51-62.
- Mellins RB, Hays AP, Gold AP, Berdon WE, Bowdler JD. 1974. Respiratory distress as the initial manifestation of Werdnig-Hoffmann disease. *Pediatrics*; 53: 33-40.
- Mitchell P, Tollervey D. 2000. mRNA stability in eukaryotes. *Curr Opin Genet Dev.* 10(2):193-8. Review.

- Mizuta TR, Fukita Y, Miyoshi T, Shimizu A, Honjo T. 1993. Isolation of cDNA encoding a binding protein specific to 5'-phosphorylated single-stranded DNA with G-rich sequences. *Nucleic Acids Res.* 21(8):1761-6.
- Mohan WS, Chen ZQ, Zhang X, Khalili K, Honjo T, Deeley RG, Tam SP. 1998. Human S mu binding protein-2 binds to the drug response element and transactivates the human apoA-I promoter: role of gemfibrozil. *J Lipid Res.* 39(2):255-67.
- Mohan U, Misra VP, Britto J, Muntoni F, King RH, Thomas PK. 2001. Inherited early onset severe axonal polyneuropathy with respiratory failure and autonomic involvement. *Neuromuscul Disord.* 11(4):395-9.
- Molnar GM, Crozat A, Kraeft SK, Dou QP, Chen LB, Pardee AB. Association of the mammalian helicase MAH with the pre-mRNA splicing complex. 1997. *Proc Natl Acad Sci U S A.* 94(15):7831-6.
- Moreira MC, Klur S, Watanabe M, Nemeth AH, Le Ber I, Moniz JC, Tranchant C, Aubourg P, Tazir M, Schols L, Pandolfo M, Schulz JB, Pouget J, Calvas P, Shizuka-Ikeda M, Shoji M, Tanaka M, Izatt L, Shaw CE, M'Zahem A, Dunne E, Bomont P, Benhassine T, Bouslam N, Stevanin G, Brice A, Guimaraes J, Mendonca P, Barbot C, Coutinho P, Sequeiros J, Durr A, Warter JM, Koenig M. 2004. Senataxin, the ortholog of a yeast RNA helicase, is mutant in ataxia-ocular apraxia 2. *Nat Genet.* 36(3):225-7.
- Oguro A, Takashi Ohtsu T, Svitkin YV, Sonenberg N, Nakamura Y. 2003. RNA aptamers to initiation factor 4A helicase hinder cap-dependent translation by blocking ATP hydrolysis. *RNA* 9:394-407.
- Pitt M, Houlden H, Jacobs J, Mok Q, Harding B, Reilly M, Surtees R. 2003. Severe infantile neuropathy with diaphragmatic weakness and its relationship to SMARD1. *Ann Neurol.* 54(6):719-24.
- Ramirez M, Wek RC, Hinnebusch AG. 1991. Ribosome association of GCN2 protein kinase, a translational activator of the GCN4 gene of *Saccharomyces cerevisiae*. *Mol Cell Biol.* 11(6):3027-36.
- Risebrough RW, Tissieres A, Watson JD. 1962. Messenger-RNA attachment to active ribosomes. *Proc Natl Acad Sci U S A.* 48:430-6.
- Rogers GW, Richter NJ, Lima WF, Merrick WC. 2001. Modulation of the helicase activity of eIF4A by eIF4B, eIF4H, and eIF4F. *J Biol Chem.* 276(33):30914-22.
- Rogers GW, Richter NJ, Merrick WC. 1999. Biochemical and kinetic characterization of the RNA helicase activity of eukaryotic initiation factor 4A. *J Biol Chem.* 274(18):12236-44.
- Rudnik-Schöneborn S, Stolz P, Varon R, Grohmann K, Schächtele M, Ketelsen UP, Stavrou D, Kurz H, Hübner C, Zerres K. 2004. Long-term observations of patients with infantile spinal muscular atrophy with respiratory distress type 1 (SMARD1). *Neuropediatrics* 35(3):174-82.
- Rudnik-Schöneborn S, Forkert R, Hahnen E, Wirth B, Zerres K. 1996. Clinical spectrum and diagnostic criteria of infantile spinal muscular atrophy: further delineation on the basis of SMN gene deletion findings. *Neuropediatrics*; 27: 8-15.
- Sebastiani G, Durocher D, Gros P, Nemer M, Malo D. 1995. Localization of the Catf1 transcription factor gene to mouse chromosome 19. *Mamm Genome* 6(2):147-8.
- Shieh SY, Stellrecht CM, Tsai MJ. 1995. Molecular characterization of the rat insulin enhancer-binding complex 3b2. Cloning of a binding factor with putative helicase motifs. *J Biol Chem.* 270(37):21503-8.

- Schrier M, Severijnen LA, Reis S, Rife M, van't Padje S, van Cappellen G, Oostra BA, Willemsen R. 2004. Transport kinetics of FMRP containing the I304N mutation of severe fragile X syndrome in neurites of living rat PC12 cells. *Exp Neurol*. 189(2):343-53.
- Singh R and Valcárcel J. 2005. Building specificity with nonspecific RNA-binding proteins. *Nat Struct Mol Biol*. 12(8): 645-53.
- Soultanas P, Dillingham MS, Wiley P, Webb MR, 2000. Wigley DB. Uncoupling DNA translocation and helicase activity in PcrA: direct evidence for an active mechanism. *EMBO J*. 19(14):3799-810.
- Tanner NK, Linder P. 2001. DExD/H box RNA helicases: from generic motors to specific dissociation functions. *Mol Cell*. 8(2):251-62. Review.
- Uchiumi F, Komuro M, Mizuta R, Tanuma S. 2004. Characterization of Smubp-2 as a mouse mammary tumor virus promoter-binding protein. *Biochem Biophys Res Commun*. 321(2):355-63.
- Ursic D, Chinchilla K, Finkel JS, Culbertson MR. 2004. Multiple protein/protein and protein/RNA interactions suggest roles for yeast DNA/RNA helicase Sen1p in transcription, transcription-coupled DNA repair and RNA processing. *Nucleic Acids Res*. 32(8):2441-52.
- Wang Y, Guthrie C. 1998. PRP16, a DEAH-box RNA helicase, is recruited to the spliceosome primarily via its nonconserved N-terminal domain. *RNA* 4(10):1216-29.
- Wang D, Xu M, Liu J, Wan Y, Deng H, Dou F, Xie W. 2006. Drosophila Ecp is a novel ribosome associated protein interacting with dRPL5. *Biochim Biophys Acta*. Sep;1760(9):1428-33.
- Weng Y, Czaplinski K, Peltz SW. 1996. Identification and characterization of mutations in the UPF1 gene that affect nonsense suppression and the formation of the Upf protein complex but not mRNA turnover. *Mol Cell Biol*. 16(10):5491-506.
- Wilmshurst JM, Bye A, Rittey C, Adams C, Hahn AF, Ramsay D, Pamphlett R, Pollard JD, Ouvrier R. 2001. Severe infantile axonal neuropathy with respiratory failure. *Muscle Nerve*. 24(6):760-8.
- Wong VC, Chung BH, Li S, Goh W, Lee SL. 2006. Mutation of gene in spinal muscular atrophy respiratory distress type I. *Pediatr Neurol*. 34(6):474-7.
- Young and Dong. 2004. Two-step total gene synthesis method. *Nucleic Acids Res*. 32(7):e59
- Zalfa F, Eleuteri B, Dickson KS, Mercaldo V, De Rubeis S, di Penta A, Tabolacci E, Chiurazzi P, Neri G, Grant SG, Bagni C. 2007. A new function for the fragile X mental retardation protein in regulation of PSD-95 mRNA stability. *Nat Neurosci*. 10(5):578-87.
- Zhang M, Wang Q, Huang Y. 2007. Fragile X mental retardation protein FMRP and the RNA export factor NXF2 associate with and destabilize Nxf1 mRNA in neuronal cells. *Proc Natl Acad Sci U SA* 104(24):10057-62.
- Zhang Q, Wang YC, Montalvo EA. 1999. Smubp-2 represses the Epstein-Barr virus lytic switch promoter. *Virology* 255(1):160-70.

Acknowledgements

Mein besonderer Dank gilt Prof. Dr. Utz Fischer für die Vergabe des Themas und die Betreuung der Arbeit.

Prof. Dr. F. Grummt möchte ich für die Bereitschaft danken, als Gutachter für diese Arbeit zu fungieren.

Prof. Dr. M. Gessler danke ich für die Bereitschaft, als dritter Prüfer meine Prüfungskommission zu vervollständigen.

Dr. med. Katja Grohmann von Au und Ulf Guenther möchte ich mich herzlich für die nette Zusammenarbeit in diesem Projekt bedanken.

Für das nette Arbeitsklima, die ständige Bereitschaft zu fachlichen und persönlichen Gesprächen, und die wissenschaftlichen Anleitungen möchte ich B116 (Bernhard Laggebauer, Bastian Linder und Lissy Kunkel), Simon Otter, Andreas Markert, Michael Klingenhäger, Ashwin Chari, Christian Eggert, Michael Grimm, Matthias Grimmer, Matthias Kroiss, Niels Neuenkirchen, Herrn Ohmer, Erika Dinkl, Emilia Gärtner, Hans D. Sickinger, Gudrun Grimmer, Annelie Kießling, Farah Badbanchi danken.

Für die Korrekturen dieser Arbeit möchte ich an Katja von Au, Ashwin Chari und Betti danken..auch an Niels + Andreas für die Kleinigkeit

Niels Gehring möchte ich mich für die nette Betreuung von Tethering assay bedanken. Vielen Dank auch an die NMD-Leute der AG Kulozik für die nette Arbeitsatmosphäre.

Meinen Freunden möchte ich dafür danken, dass sie über das Fachliche hinaus und jeder auf seine Art zu dieser Arbeit entscheidend beitrugen...Danke vielmals....

Buat temen temen indo dimanapun berada, Sendai, Darmstadt, Würzburg, München, Zürich, Jakarta and Bandung, makasih buuanget lo buat dukungannya baek moral (lewat doa doanya, telefon jarak jauh, jadinya tetep inget sama Yang di Atas) en material (yang suka traktir traktir, jadi gak kelaparan ☺). Semoga Tuhan memberkati kita semua and membalas jasa2 kalian.

Der größte Dank gilt meinen Eltern, die uns die Kinder immer unterstützen. Im Besonderen möchte ich mich bei meinen Geschwistern, our beloved Liem Swie Nio und N. Kels bedanken. „Thanks for your support and advice in many ways“.

Lebenslauf

Persönliche Daten

Name : Handoko
Vorname : Lusy Lusiana
Adresse : Kolpingstrasse 20, 97070 Wuerzburg
Geburtstag : Tuban, 9 April 1976
Familienstand : Ledig

Schulische Ausbildung

1987 Grundschule : SDN1 Tambakboyo, Tuban, Indonesien
1989 Mittelschule : SMPN 1 Surakarta, Indonesien
1993 Oberschule : SMAN 3 Surakarta, Indonesien

Akademische Laufbahn

8/1993-4/1998 Bachelor of Science, Biologie, Bandung Institute of Technology, Indonesien
4/1998-3/1999 wissenschaftliche Mitarbeiter am Institute für Genetik, Bandung Institute of Technology, Indonesien
4/1999-2/2000 Deutschkurs an der Technischen Universität Darmstadt
4/2000-12/2002 Studium der Biologie an der Technischen Universität Darmstadt
4/2002-12/2002 Diplomarbeit unter Anleitung von Prof. Dr. H.U. Göringer am Institut für Mikrobiologie und Genetik der Technischen Universität Darmstadt
5/2003-9/2007 Anfertigen der vorliegenden Dissertation unter der Anleitung von Prof. Dr. Utz Fischer am Max-Planck-Institut für Biochemie, Martinsried und der Universität Würzburg

Erklärung

Hiermit erkläre ich an Eides statt, dass ich die Dissertation „Functional Characterization of IGHMBP2, the Disease Gene Product of SMARD1 (Spinal Muscular Atrophy with Respiratory Distress Type 1)“ selbständig angefertigt und keine anderen als die von mir angegebenen Quellen und Hilfsmittel benutzt habe.

Ich erkläre außerdem, dass diese Dissertation weder in gleicher oder anderer Form bereits in einem anderen Prüfungsverfahren vorgelegen hat.

Ich habe früher außer den mit dem Zulassungsgesuch urkundlich vorgelegten Graden keine weiteren akademischen Grade erworben oder zu erwerben versucht.

Würzburg im September 2007

Lusy Lusiana Handoko